

**W-Pos83** A 210 Kd PROTEIN PURIFIED FROM THE SPERM PLASMA MEMBRANE INDUCES ANIONIC CHANNEL ACTIVITY IN PLANAR BILAYERS. E. Morales, L. de la Torre, V. Vacquier\* and A. Darszon, Dept. of Biochemistry, CINVESTAV-IPN, Apdo. Postal 14-740, 07000 México City and \*Scripps Institution of Oceanography, La Jolla, CA 92093, USA.

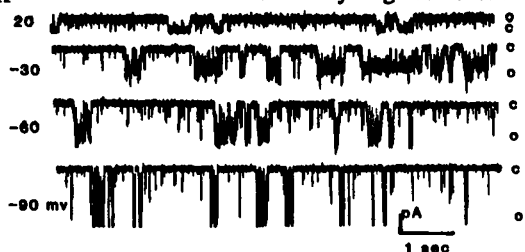
Ionic fluxes across the sea urchin sperm play a crucial role during its activation and in the acrosome reaction (AR). This latter reaction triggered by the egg jelly, has to occur before sperm can fertilize eggs. The egg jelly induces the uptake of  $\text{Ca}^{2+}$  and  $\text{Na}^+$  and the efflux of  $\text{K}^+$  and  $\text{H}^+$ . There is evidence which indicates that ionic channels participate in the sperm  $\text{Ca}^{2+}$  and  $\text{K}^+$  movements. To gain further insight into the molecular transport mechanisms involved in the AR a reconstitution approach is being used. A sperm plasma membrane protein of 210 Kd, most likely the receptor of jelly, has been purified, and antibodies raised against it inhibit the jelly induced  $\text{Ca}^{2+}$  uptake and the AR (J.B.C.260:2715). The fusion of liposomes containing this purified protein into diphyanoyl phosphatidyl choline planar lipid bilayers (BLMs) resulted in single channel activity selective for anions. The main unitary conductance in  $\text{NaCl}$  300 mM *cis* and  $\text{NaCl}$  100 mM *trans* was 118 pS. Other smaller transitions indicated the presence of subconductance states or of different channels. This anionic channel was blocked by 250-500  $\mu\text{M}$  DIDS or 250  $\mu\text{M}$   $\text{ZnCl}_2$  in *cis*. In contrast, the addition of the antibody, both in *cis* and in *trans* did not produce a significant effect. The anionic channel has been recorded from native sperm plasma membranes. Interestingly DIDS and  $\text{Zn}^{2+}$ , which block some anionic channels, also inhibit the AR (95 %, n=5 at 300  $\mu\text{M}$  DIDS, also Dev.Growth Differ.27:461), suggesting that  $\text{Cl}^-$  channels may be involved in sea urchin sperm AR. Occasionally a cationic channel with a unitary conductance of 76 pS has been observed. Help from A. Liévano is acknowledged. This work was supported by grants from CONACYT and WHO.

**W-Pos84** TIME-RESOLVED FLUORESCENCE OF THE THREE TRYPTOPHANS IN A CHANNEL-FORMING PEPTIDE OF COLICIN E1. A.R. Merrill<sup>1</sup>, H.Y. Song<sup>1</sup>, W.A. Cramer<sup>1</sup>, D.T. Krajarski<sup>2</sup>, and A.G. Szabo<sup>2</sup>, (Intr. by C. V. Stauffacher), Dept. of Biol. Sciences<sup>1</sup>, Purdue University, W. Lafayette, IN, 47907, U.S.A.; Dept. of Biol. Sciences<sup>2</sup>, Natl. Res. Coun., Ottawa, Ont., K1A OR6, Canada.

The three tryptophan residues (W-424, W-460, and W-495) of the thermolytic M<sub>18,000</sub> channel-forming peptide of colicin E1 are intrinsic fluorescence probes for the study of its structure and segmental dynamics. Preliminary studies have been done on site-directed mutants at positions 460 and 495. W-460 is conserved in the family of 5 channel-forming colicins and W-495 is located in the 35 residue hydrophobic domain of the channel. The fluorescence intensity of a W-495 → F mutant, with activity similar to wild type, is much reduced, indicating that W-495 is a major contributor to the fluorescence. The fluorescence decay of the channel peptide from wild-type colicin and of a W-460 → L mutant with lower *in vitro* and *in vivo* activities, was measured at pH 4 (optimum for *in vitro* activity) in solution and in Lubrol-PX detergent micelles. The decay times found for major emission components of wild-type peptide in solution and Lubrol-PX micelles were [4.6 ns ( $\lambda = 330 \text{ nm}$ ), 2.3 ns ( $\lambda = 320 \text{ nm}$ ), and 0.3 ns] and [6.4 ns ( $\lambda = 335 \text{ nm}$ ), 3.8 ns ( $\lambda = 325 \text{ nm}$ ) and 0.8 ns], respectively. In contrast to the wild type, for the W-460 → L mutant, the decay times in solution and Lubrol were the same: 5.6, 2.5, and 0.8 ns. The data indicate that interaction of the wild-type colicin channel peptide with a non-polar environment can be reported by changes in tryptophan fluorescence. [Supported by NIH GM-18457 (WAC), Natl. Res. Council of Canada (AGS), and a Canadian NSERC Fellowship (ARM).]

**W-Pos85** A VOLTAGE-REGULATED, CALCIUM-PERMEABLE CATION CHANNEL IN MYOBLASTS AND MYOTUBES FROM THE MOUSE C2 CELL LINE. Alfredo Franco Jr. and Jeffry B. Lansman, Graduate Program in the Neurosciences and Dept. of Pharmacology, School of Medicine University of California at San Francisco, CA 94143.

A role for calcium influx in myoblast differentiation and fusion to form myotubes has been postulated, however, a pathway for  $\text{Ca}^{2+}$  entry into myoblasts has not been reported. We have identified a cation-specific channel that first appears in aligned (pre-fusion stage) myoblasts after ~24 hrs in culture and which persists in mature myotubes following myoblast fusion. Recordings of single channel activity from cell-attached patches with 110 mM  $\text{BaCl}_2$  in the patch electrode reveal unitary currents with a slope conductance of ~20 pS and which reverse at ~+22 mV. With 110 mM  $\text{CaCl}_2$  in the electrode, the slope conductance is ~15 pS and current reverses at ~+34 mV. The relative selectivity of divalent over monovalent cations estimated from reversal potential measurements suggests that the channel is more selective for  $\text{Ca}^{2+}$  than for  $\text{K}^+$  with  $\text{P}_{\text{Ca}^{2+}}/\text{P}_{\text{K}^+} > 10$ . Monovalent cations carry large currents through the channel as shown in the figure in which the pipet con-



tained 150 mM  $\text{CsCl}$ . The slope conductance with either 150 mM  $\text{CsCl}$  or  $\text{KCl}$  in the patch electrode is ~40 pS and current reverses at ~0 mV. Channel activity does not depend on cytoplasmic  $\text{Ca}^{2+}$  or cAMP. Channel gating depends strongly on membrane potential with burst duration increasing with depolarization. This channel appears to be the only channel open at the cell's resting potential that is capable of allowing  $\text{Ca}^{2+}$  entry into developing myoblasts and myotubes.

**W-Pos86 PROPERTIES OF NEURONAL STRETCH-ACTIVATED K<sup>+</sup> (SAK) CHANNELS.** W.J. Sigurdson and C.E. Morris, Dept. of Biology, University of Ottawa, Ottawa, Canada, K1N 6N5.

Hyposmotic shock (HOS) swells *Lymnaea* neurons, and should, if sufficiently intense activate SAK channels. Because of the compliance-mismatch (patch vs cell), single channel recording is not necessarily an ideal technique to quantitate such activation. Nevertheless in 35% of patches examined during 50% HOS-induced cell swelling, a reversible increase in open probability ( $P(O)$ ) was observed. In impaled cells, perfusion with normal saline induced a 4+1 mV (n=16) hyperpolarization whereas perfusion with 50% saline (which caused swelling) produced a 14+4 mV (n=13) hyperpolarization.

SAK channel activity shows almost no voltage-dependence in the physiological range. Between the resting potential and  $V_m = +30$  mV,  $P(O)$  changes not more than e-fold per  $143 \pm 26$  mV (n=4). At greater depolarizations, voltage sensitivity does increase (e-fold per  $19 \pm 9$  mV, n=3), but this should be irrelevant for normal channel function. A minor effect of voltage that we note in cell-attached patches is the flickery appearance of inward (but not outward) channel currents with high external K<sup>+</sup> (100 mM). Kinetic analysis indicates that under these conditions, brief closings are voltage-independent, but that the longer of two open times decreases with hyperpolarization.

The neuronal SAK channel is insensitive to intracellular Ca<sup>2+</sup>. To illustrate: when an inside-out patch with Ca<sup>2+</sup>-activated K<sup>+</sup> and SAK channels is exposed to EGTA, the former become inactive, whereas SAK channels remain activatable by suction. (Supported by NSERC and Muscular Dystrophy Association of Canada.)

**W-Pos87 MULTIPLE EFFECTS OF Ca<sup>2+</sup> ON CYCLIC AMP-GATED Na<sup>+</sup> CURRENT.** R.-C. Huang and R. Gillette, Depart. of Physiology & Biophysics, Univ. of Ill., Urbana, IL 61801.

Intracellular injection of cAMP induces depolarization and spiking of identified neurons of the mollusc, *Pleurobranchaea californica*. cAMP stimulates a Na<sup>+</sup> current resisted to kinase inhibitors, and thus probably mediated by direct binding at the channel. The  $I_{Na,cAMP}$  response to pulsed injection of cAMP decreases with more positive potentials between -70 and -30 mV. A depolarizing prepulse from -50 mV to a more positive potential suppresses the  $I_{Na,cAMP}$  response. Both voltage-sensitivity and depolarizing pulse suppression of  $I_{Na,cAMP}$  are abolished in low-Ca<sup>2+</sup> saline and with intracellular BAPTA injection. In contrast, increasing intracellular cAMP levels reduces both voltage-sensitivity and the extent of depolarizing pulse. This mutual antagonism between intracellular Ca<sup>2+</sup> and cAMP is not mediated via a possible alteration of phosphodiesterase activity, but is more likely a result of direct interaction of Ca<sup>2+</sup> with the cAMP-activated Na<sup>+</sup> channels at the binding sites.

A model of competition between Ca<sup>2+</sup> and cAMP binding to the channel receptors successfully unifies the results. For this model, the Hill Plot indicates there is a stoichiometric ratio of one for cAMP binding; one-to-one binding for Ca<sup>2+</sup> is assumed. The intracellular Ca<sup>2+</sup> effect on  $I_{Na,cAMP}$  response is exerted by decreasing cAMP binding. The reverse is true for the antagonizing effect of increasing intracellular cAMP levels. Extracellular Ca<sup>2+</sup>, independent of and opposite to intracellular Ca<sup>2+</sup>, enhances the apparent binding affinity.

**W-Pos88 STRUCTURAL STUDIES OF MODEL ION CHANNELS (ALAMETHICIN, MELITTIN, GRAMICIDIN) BY USING PERFECTLY ALIGNED MULTILAYER SAMPLES\***

Huey W. Huang, Mark Lesmeister, Glenn Allen Olah, and Yili Wu, Physics Department, Rice University, Houston, TX 77251

Because of the difficulty in making single crystals of membrane ion channels in their native states (suitable for diffraction studies), there is a lack of structural information for understanding their molecular mechanisms. One dimension ordered multilayers, in which the channels are uniformly oriented within the membranes, can be exploited to obtain valuable structural data. We have developed 1) the technique for preparing such multilayer samples, and 2) the spectroscopic methods (circular dichroism and x-ray diffraction) for extracting structural information from these samples. The sample variables include electric field, water content, lipid type, ion concentration, etc. Angular dependent circular dichroism is used to determine the orientation of  $\alpha$ -helical sections. X-ray diffraction is used to determine the location of ion binding sites within the channel. Preliminary results of the alamethicin channel agree with the barrel model, rather than the flip-flop model.

\* Supported in part by ONR, NIH, and Welch Foundation.

**W-Pos89** CHARACTERIZATION OF A LARGE CONDUCTANCE, CATION SELECTIVE CHANNEL, ISOLATED FROM SEA URCHIN EGGS AND INCORPORATED INTO PLANAR BILAYERS. Ture Li Lu and David G. Levitt, Department of Physiology, University of Minnesota, Minneapolis, MN 55455.

Vesicles isolated from sea urchin eggs contain a large conductance cation selective channel that can be easily studied in planar bilayers. Only one channel type appears when the vesicles are squirted directly on the bilayer and channel number (from 1 to 100's) can be easily controlled by varying the vesicle concentration. Although the channel number tends to decay within minutes, this can be prevented by the addition of a sulfhydryl reagent (e.g. dithiothreitol, glutathione) to the cis side. In asymmetrical KCl/TEACl, the current is carried entirely by  $K^+$ , indicating that  $Cl^-$  and TEA $^+$  are impermeable. In symmetrical 500 mM the  $K^+$  conductance is 600 pS and the relative selectivity is  $K$  (1) > Cs (0.54) > Na (0.5) > Li (0.2). The  $K^+$  conductance reaches a maximum at about 250 mM. The Li/K permeability ratio is 6.0 at 1M indicating that a high affinity site produces the low Li $^+$  conductance. The Li/K permeability ratio is concentration dependent, decreasing to 1.4 at 200 mM, suggesting that the channel is multiply occupied. The addition of 1 mM Ca $^{2+}$  reduces the conductance of 500 mM  $K^+$  by a factor of three. Every cation tested (choline, TEA, lysine, histidine, arginine, divalent cations, etc.) produced a significant channel block in the mM range. A number of cations ( $La^{3+}$ , gallamine, quinidine) produce a flickering block, indicating a relatively long lived blocked state.  $La^{3+}$  has the highest affinity, producing a 50% block in 500 mM  $K^+$  at 4  $\mu$ M. This channel resembles a sperm activated channel found in ascidian eggs (DeFelice and Kell, Dev. Biol. 119:123, 1987).

**W-Pos90** CHARACTERIZATION OF A CALCIUM-ACTIVATED NONSELECTIVE CATIONIC CHANNEL IN A RENAL CELL LINE. Manuel Kukuljan, Nancy Araya, Raul Caviedes and Andres Stutzin. Dept. of Physiology and Biophysics and Dept. of Experimental Medicine, Fac. of Medicine, Universidad de Chile. P.O. Box 70055, Santiago, Chile.

The presence of calcium-activated nonselective (CAN) cationic channels has been documented in a number of cell types, i.e. neurones, cardiac cells, neutrophils, pancreatic acinar cells, etc. However, the physiological role of this kind of channel is unclear. It has been proposed that it could participate in stimulus secretion coupling events and in the control of the firing rate of excitable cells. Here we report the existence of a CAN channel in a rat distal tubule cell line which displays epithelial markers and retains the ability to synthesize kallicrein.

Cells were kept in F-12 Dulbecco's modified medium and plated twice a week for electrophysiological records. Patch clamp technique, in its inside-out configuration, was used. In symmetrical ionic conditions (130 NaCl, 10 NaHEPES, 1 CaCl<sub>2</sub>, pH 7.40), the measured conductance of the channel was 18 pS. The substitution of chloride by aspartate did not modify this conductance. Studied in bi-ionic condition, the permeability ratio for  $Na^+$  :  $K^+$  was 1 : 0.97. The mean open time distribution can be described by a double exponential ( $\tau_{\alpha_1} = 3.7$  msec.,  $\tau_{\alpha_2} = 31.2$  msec.). The channel exhibited at least two closed states ( $\tau_{\alpha_1} = 11.2$  msec.,  $\tau_{\alpha_2} = 82.4$  msec.). The kinetics of the channel displayed no evident voltage dependence in the range of -70 mV to +70 mV. No channel activity was observed at low "intracellular" calcium (pCa 6.5); activity appeared by rising the free concentration of  $Ca^{2+}$  to the millimolar range. The modulation of gating of this channel and its physiological significance remain to be elucidated.

Supported by Cystic Fibrosis Foundation and FONDECYT.

**W-Pos91** ANGIOTENSIN II (ANG) AND OTHER CALCIUM MOBILIZING HORMONES ACTIVATE A CHLORIDE CHANNEL IN VASCULAR SMOOTH MUSCLE CELLS. Lucinda Smith and Jeffrey Bingham Smith. Dept. Pharmacology, University of Alabama at Birmingham, UAB Station, Birmingham, AL 35294.

Smooth muscle cells were cultured from rat aorta and labelled with 77Br. Rapid 77Br efflux (10 sec intervals for 3 min) was used to assay Cl transport. The addition of ANG 60 s after starting the efflux assay strikingly increased 77Br efflux. Two other neurohormones, arginine vasopressin and ATP, increased 77Br efflux similarly to ANG. ANG and ATP stimulated 77Br efflux similarly in the presence or absence of external Ca. ANG stimulated 36Cl, but not [35S]sulfate, efflux. Replacing external Cl with gluconate almost abolished [35S]sulfate efflux indicating that it occurs almost entirely by Cl/sulfate exchange. ANG stimulated 77Br efflux in a Cl-free medium indicating that the anion exchanger is not responsible for ANG-stimulated 77Br efflux. Additionally bumetanide, which inhibits the Na/KCl cotransporter, had no effect on basal or ANG-stimulated efflux in the absence of external Cl indicating that the cotransporter makes no contribution to 77Br efflux under these conditions. The removal of external Na (Na<sub>o</sub>) stimulated 77Br and 36Cl efflux similarly to the Ca mobilizing hormones. The stimulation of 77Br and 36Cl efflux by Na<sub>o</sub> removal was absolutely dependent on the presence of external Ca and loading the cells with Na. Previously we reported that Na<sub>o</sub> removal causes Ca influx via the Na/Ca exchanger only if intracellular Na is raised above the basal level. Because an increase in Ca influx stimulated 77Br efflux similarly to the Ca mobilizing hormones, it is likely that Ca itself is the intracellular messenger that activates the Cl efflux pathway. Cell Cl was measured after equilibration with medium containing 36Cl and divided by cell water space which was measured with [14C]urea. Cell Cl was  $38.3 \pm 1.4$  mM in Medium 199 which contained 124 mM Cl and  $63.3 \pm 2.6$  mM in physiological salts solution which contained 147 mM Cl ( $p < 0.01$  for unpaired t test, n=3 experiments in duplicate or triplicate), indicating that the cells actively accumulate Cl in both media. In conclusion, a rise in cytosolic free Ca, produced either by the release of stored Ca or an increase in Ca influx, activates a Cl uniporter which is probably a plasma membrane Cl channel. (Supported by Grants DK39258 and HL01671 from the National Institutes of Health and a Grant-in-Aid from the American Association.)

**W-Pos92** PATCH-CLAMP STUDIES OF BACTERIAL MEMBRANES IN A RECONSTITUTED SYSTEM, A.H. Delcour, B. Martinac, J. Adler, C. Kung, Dept. of Biochemistry, Lab. of Molecular Biology, Dept. of Genetics, University of Wisconsin, Madison, WI 53706.

Bacterial membranes were fused with exogenous lipids (azolectin) to form giant liposomes according to a procedure involving a dehydration-rehydration cycle of the lipid film (Criado M. and Keller B.U., *FEBS Letters*, 224, 172-176, 1987). The liposomes were not patch-clamped directly but collapsed in the patch-clamp chamber by exposure to a "magnesium solution" (150 mM KCl, 0.1 mM EDTA, 5 mM Hepes pH 7.2, 20 to 50 mM MgCl<sub>2</sub>). Within 10 minutes, faint blisters, probably unilamellar or paucilamellar, emerge from the collapsed liposomes. High resistance seals (10-50 GΩ) are easily and frequently obtained by gentle touch of the electrode to the blister surface. In our hands, the rate of success for obtaining high seals was greater with these blisters than the intact liposomes. Experiments were performed on excised patches. Ion channels have been routinely observed with liposomes fused with *Escherichia coli* membranes. The most frequent channel is a voltage-dependent cation channel, which appears mostly open at low voltages, but displays an increased frequency of transition to the closed state with increased voltages (negative pipette). In the open state, the channel exhibits fast transitions to a sub-conducting state, which also appear to be voltage-dependent. The mechanosensitive ion channel described in *E. coli* spheroplasts (Martinac et al., *Proc. Natl. Acad. Sci. USA*, 84, 2297-2301, 1987) was observed in this reconstituted system as well. Similar experiments were also performed with *Bacillus subtilis* membranes, and their ion channels are presently being characterized. Supported by NIH GM 37926, DK 39121 and Muscular Dystrophy Association.

**W-Pos93** IONIC CURRENTS IN SEPTAL NEURONS AND INHIBITION OF SODIUM CURRENT BY THYROTROPHIN-RELEASING HORMONE (TRH). A. CASTELLANO, H. SANTOS-ROSA, C. CAPUTO and J. LOPEZ-BARNEO. Dpto. de Fisiología y Biofísica. Universidad de Sevilla. SEVILLA, SPAIN.

The ionic currents of dispersed septal neurons were studied using the "whole-cell" variant of the "patch-clamp" technique. The action of TRH on these currents was also tested. On depolarization all septal neurons generate Na, Ca, and K currents. The Na current activates rapidly and inactivates in 3 to 4 ms. At -10 mV half-activation time is 0.25 ms and inactivation time constant is 0.6 ms. The Ca current is due to the activity of two types of calcium channels with properties similar to fast (FD) and slowly (SD) deactivating channels of other cells. The K current is mediated by at least three different K channels. There is a fast transient current which is inactivated at potentials more positive than -65 mV. At +40 mV this current inactivates almost totally in 20 ms. In addition, there are two more components of slowly activating outward current, one of them with a clear dependence on the intracellular Ca<sup>2+</sup> concentration. The density of Na channels and the contribution of the different Ca and K channels to the total current varied from cell to cell, which indicates that there are several neuronal types in the septal nucleus. In some cells exposure to external TRH (0.5 to 2 μM) produces a reversible decrease of the Na current amplitude without affecting neither the activation and inactivation time courses nor the shape of the I-V curve. The action of TRH on septal Na channels seems to be specific since the K currents remain unaltered. These results indicate that neuropeptides, which are known modulate the activity of voltage-dependent Ca and K channels, can also regulate neuronal activity by acting on voltage-dependent Na channels.

**W-Pos94** PRESSURE-INDUCED MEMBRANE TENSION ACTIVATES A MECHANOSENSITIVE ION CHANNEL IN THE OUTER MEMBRANE OF THE BACTERIUM *ESCHERICHIA COLI*. B. Martinac\*, Anne H. Delcour<sup>a</sup>, M. Buechner<sup>a</sup>, J. Adler<sup>a†</sup>, and C. KUNG<sup>\*\*</sup>, <sup>a</sup>Lab. of Molecular Biology\*, Department of Biochemistry<sup>a</sup>, Department of Genetics<sup>b</sup>, University of Wisconsin, Madison, WI 53706.

We have used patch-clamp recording technique to characterize further a mechanosensitive ion channel in the cell envelope of the Gram-negative bacterium *E. coli* (Martinac et al., *Proc. Natl. Acad. Sci. USA*, 84, 2297-2301, 1987). The channel was studied in giant spheroplasts of wild-type cells and in giant cells of a *lpp-ompA*- double mutant. The results obtained with mutant cells suggest that the channel is located in the outer membrane of the bacterial cell envelope. The steady-state opening probability of a single channel shows sigmoidal dependence on membrane tension, as predicted by a model for displacement-sensitive channels (Howard, Roberts, and Hudspeth, *Ann. Rev. Biophys. Biophys. Chem.* 17, 99-124, 1988). Assuming a hemispherical patch of 2 μm in diameter, we calculate that between 7 and 14 nm<sup>2</sup> membrane area is displaced by opening of the channel, which is comparable to the dimensions of known ion channels. The treatment of inside-out excised patches with lysozyme causes an increase in channel pressure sensitivity. This result suggests that peptidoglycan (the bacterial cell wall) may play the role of an elastic element to restrain channel activation. Supported by NIH DK 39121.

W-Pos95 NMR STUDIES OF A CHANNEL-FORMING COOH-TERMINAL PEPTIDE OF COLICIN E1. R.J.P. Williams<sup>1</sup>, M.R. Wormald<sup>1</sup>, and W.A. Cramer<sup>2</sup>, (Intr. by M.G. Rossmann), Inorganic Chemistry Dept.<sup>1</sup>, Oxford University, Oxford OX1 3QR, United Kingdom; Dept. of Biological Sciences<sup>2</sup>, Purdue University, West Lafayette, IN, 47907, U.S.A.

The bactericidal protein colicin E1 forms a voltage-dependent channel in the *E. coli* cytoplasmic membrane that depolarizes the cell. The solution and membrane structures of the channel domain are of fundamental interest. Initial studies have been carried out on the solution, structure of the M<sub>r</sub> 18,000 thermolytic COOH-terminal peptide of colicin E1 using one- and two-dimensional <sup>1</sup>H NMR spectroscopy. The spectra obtained show that the protein has at least two different structural regions in aqueous solution, one with a very stable and well-defined tertiary fold and the other showing far less structure and much greater mobility. The structured region contains very little  $\beta$ -structure, the spectra being consistent with a mostly  $\alpha$ -helical fold. The rate of exchange of backbone -NH protons with deuterium shows that water has almost no access to the centre of the structured region, the hydrophobic core of the protein. From the variation of the spectra between pH 5 and 8, the protein retains its tertiary structure over the whole pH range but there is a rearrangement in the hydrophobic core between pH 5 and 6. Using 2D COSY and NOESY spectra, we have started to identify, by type, the amino acids in the structured region(s) and to determine their spatial arrangement. [We acknowledge the essential technical contribution of Xiaoqing Yu and support from NIH GM-18457.]

W-Pos96 FRACTAL AND MARKOV MODELS OF KINETIC BEHAVIOR IN SINGLE ION CHANNELS.

Andrew S. French, Lisa L. Stockbridge, Marek Duszyk and S.F. Paul Man, Departments of Physiology and Medicine, University of Alberta, Edmonton, Alberta, Canada T6G 2H7.

The kinetic behavior of ion channel gating has traditionally been analysed by assuming the existence of a finite number of open and closed states, where each state has a lifetime which is independent of previous channel history but possibly dependent on gating factors such as voltage or calcium concentration. This kind of model produces a Markov process, whose probability density is a sum of simple exponential components. In contrast, the fractal model of channel gating proposes an infinite number of channel states, with transition rates between states distributed continuously. This model can also approximate some other alternative non-Markov models of channel gating. We have now used recordings of several types of ion channels from chick and human fibroblasts and from human airway epithelia to try to discriminate between Markov models and fractal models of single ion channel kinetic behavior. Data were analysed using the data transformation technique of Sigworth and Sine (*Biophys. J.*, 52:1047-1054), with each model being fitted to the transformed data using the maximum likelihood method. To provide an objective discrimination between different models, the Akaike asymptotic information criterion was calculated from the log likelihood ratio and the number of free parameters. Preliminary results indicate that multiple exponential models are favored over simple fractal models in each case. Supported by the Canadian Medical Research Council and the Alberta Heritage Foundation for Medical Research.

W-Pos97 NON-SELECTIVE CATION CHANNELS IN THE SURFACE MEMBRANE OF RAT SKELETAL MUSCLE. M. Chua & W. J. Betz. Dept. of Physiology, University of Colorado Health Sciences Center, Denver, CO 80262.

The tight seal patch clamp technique was used to study the ionic channels present on the surface membrane of mammalian skeletal muscle. Chloride, potassium and non-selective cation channels were observed. The last type is described in this study.

Isolated fibers were prepared from rat flexor digitorum brevis muscles by the collagenase treatment (Bekoff & Betz, 1977 *J. Physiol.* 271, 25-40). Electrodes were filled with 141 mM NaCl and 2.0 mM TES (pH 7.4), 0.5 mM EGTA and 0.4 mM CaCl<sub>2</sub>. For inside-out patches, the bathing solutions had the same composition as the electrode solution except that the major cation was changed during the recording. Reversal potential and conductance were measured using voltage ramps. Long silent periods were punctuated by fast flickering openings lasting several seconds. Sub-conductance states were observed and ranged from 33 pS to 320 pS in approximately 30 pS steps. The I-V relationship for the channel in the cell attached mode was almost linear. The selectivity sequence was Na<sup>+</sup> = K<sup>+</sup> = Cs<sup>+</sup> (1.0) > Ca<sup>2+</sup> = Mg<sup>2+</sup> (0.5) > N-Methyl-D-Glucamine<sup>+</sup> (0.3). In NaCl solutions reducing the ionic strength at the intracellular face while maintaining osmolarity with sucrose made the reversal potential more positive. The changes in reversal potential were consistent with a cation selective channel with a Cl<sup>-</sup> to Na<sup>+</sup> permeability ratio of less than 0.03. Calcium concentration, tetrodotoxin, 10 mM CoCl<sub>2</sub>, 10 mM CdCl<sub>2</sub> or suction had little or no effect on the channel activity. The macroscopic action of the non-selective cation channel is to depolarize the cell, and produces a leakage current. (M.C. was supported by a Muscular Dystrophy Association fellowship)

**W-Pos98** CONTROL OF IONIC CHANNELS IN RABBIT CORNEAL ENDOTHELIUM. James L. Rae, Jerry Dewey, and Kim Cooper, Departments of Physiology and Biophysics and Ophthalmology, Mayo Foundation, Rochester, MN 55905.

The apical membrane of the rabbit corneal endothelium contains a K<sup>+</sup> selective channel ( $P_K/P_{Na} \approx 40/1$ ) whose gating depends on both extracellular Cl<sup>-</sup> and HCO<sub>3</sub><sup>-</sup>. In a bath containing a methane sulfonate Ringer, the open probability ( $P_o$ ) is less than .05 over the entire physiological voltage range in cell attached patches.  $P_o$  increases when extracellular HCO<sub>3</sub><sup>-</sup> is increased in the 1-20 mM range and also shows increased dependence on voltage, i.e.  $P_o$  increases with depolarization. Extracellular Cl<sup>-</sup> also increases  $P_o$  but has a smaller effect than does HCO<sub>3</sub><sup>-</sup>. Both ions have a greater effect when 100 μM DIDS is included in the pipette filling solution. Patch excision (inside-out patches) results in rapid loss of channel activity. The activity cannot be restored by bath pH changes in the range of 6.8-7.9, c-AMP or GTP.

This membrane also contains a non-selective cation channel which is activated by intracellular Ca<sup>++</sup> in the 1 μM to 1 mM range. The channel is also inhibited by internal ATP in the 10 μM to 1 mM range. Ba<sup>++</sup> and Ca<sup>++</sup> are unable to carry inward current and so the channel appears selective for monovalent cations. Its open probability depends on voltage but not on pipette suction.

Supported by NIH grants EY03282 and EY06005.

**W-Pos99** EXTRACELLULAR AND INTRACELLULAR CALCIUM BUFFERS AFFECT THE CELLULAR VOLUME OF ASTROCYTES FROM PRIMARY CULTURE. James E. Olson and W. Bruce Murray, Department of Emergency Medicine, Wright State University School of Medicine, Dayton, Ohio 45401

Cerebral astrocytes play a major role in the homeostasis of extracellular ion concentrations and water content of the brain. Astrocyte swelling accompanied by alterations in the extracellular concentration of Ca<sup>++</sup> is observed in many pathological states. To investigate the influence of calcium on astrocyte volume we exposed these cells to decreased extracellular free calcium in the presence and absence of intracellular calcium buffers.

Astrocyte cultures were prepared from the cerebral cortices of 2-4 day-old rat pups and grown for 2-4 weeks at 37°C. Cells were removed from the culture dish and incubated for 30 min at 37°C in normal PBS or in PBS containing 2 mM EDTA. Some cell suspensions also contained 50 μM BAPTA-AM (B-AM) or 5-5',dimethyl-BAPTA-AM (DM-B-AM). Following this incubation period, cells were resuspended in normal PBS. Cell volumes then were measured for 30 min using a Coulter Counter. Cellular BAPTA content was measured spectrophotometrically after lysing the cells with 0.1% triton.

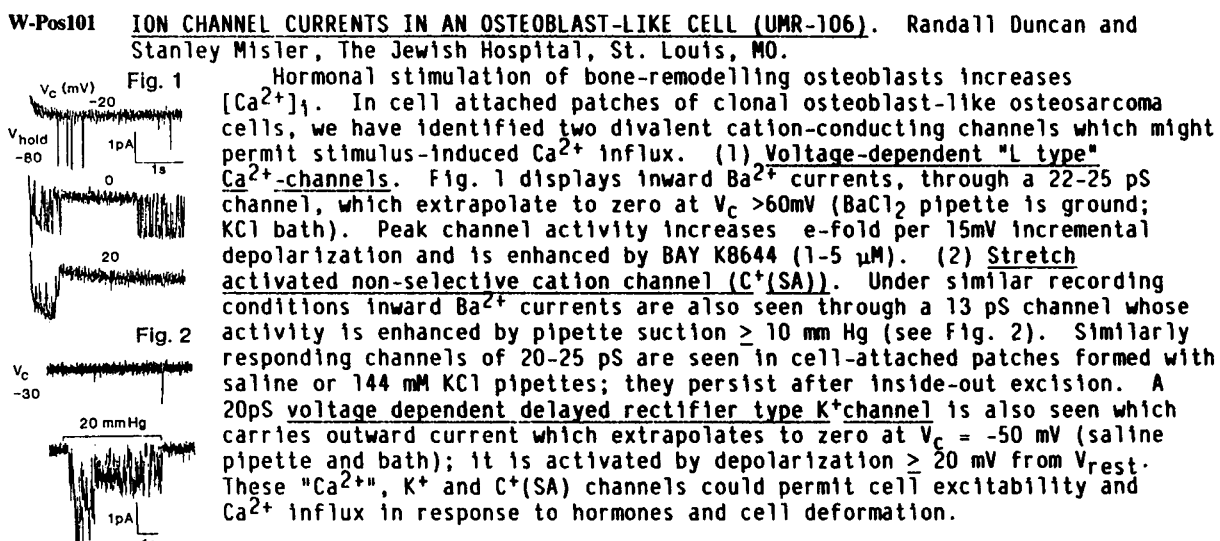
After incubation in PBS plus EDTA, astrocytes were 43±5% larger than cells incubated in PBS alone (mean+SEM). Thirty min after resuspension in normal PBS, the volume of these cells was only 27±3% greater than that of cells incubated in PBS without EDTA. This volume recovery could be hastened by the addition of 10 μM A23187. Intracellular BAPTA concentrations were 9-17 mM after incubation in B-AM. Cells incubated in B-AM or DM-B-AM had volumes which were 55±9% or 20±4% greater than the volume of cells incubated in normal PBS, respectively. The volume of these cells was constant during the 30 min following resuspension in normal PBS. Cells incubated in EDTA plus B-AM or DM-B-AM had volumes which were 35% larger than cells incubated in B-AM or DM-B-AM alone. Within 30 min, these cells shrank to the volume of B-AM and DM-B-AM loaded cells incubated without EDTA.

Our data suggest that both extracellular and intracellular calcium concentrations can alter astrocyte volume. Supported by NIH grant NS23218 and the WSU Dept. of Emerg. Med. Develop. Fund.

**W-Pos100** IS ATP PERMEABILIZATION MEDIATED BY CHANNELS OF DEFINED SIZE?

Peter E.R. Tatham<sup>1</sup> and Manfred Lindau.<sup>2</sup> <sup>1</sup>Dept. of Experimental Pathology, University College London, London WC1E 6JJ, UK. <sup>2</sup>Biophysics Group, Dept. of Physics, Freie Universität Berlin, D-1000 Berlin 33, FRG. (Intr. by W. Almers.)

We have characterized the ATP-induced permeabilization of rat peritoneal mast cells by measuring uptake of fluorescent dyes and by voltage clamp measurements using the patch-clamp technique. In the absence of divalent cations cells are permeabilized by ATP at concentrations as low as 3 μM. In normal saline containing 1 mM MgCl<sub>2</sub> and 2 mM CaCl<sub>2</sub> dye uptake and electric conductance are detectable at 100 μM ATP corresponding to 5 μM ATP<sup>-4</sup>. The permeabilization is half maximal at an ATP concentration of 10-20 μM with a Hill coefficient of about 2. The ATP-induced whole-cell conductance at saturating ATP concentrations was 35-70 nS exhibiting only weak cation selectivity. In whole cells as well as outside-out patches discrete openings and closings of channels could not be observed. The single channel conductance obtained from noise analysis is below 10 pS. Pores which are large enough to allow for permeation of substances up to 1000 dalton m.w. are expected to have a unit conductance of about 300 pS suggesting that the pores are of variable size which can increase or decrease by very small units. Experiments on ATP-induced exocytosis support a concentration dependence of the pore size. Supported by DFG within SFB 312/B6.



**W-Pos102 Automated Tracking Of LDL Receptors On Cell Surfaces With Nanometer Precision.**

*Richik N. Ghosh and Watt W. Webb, Applied and Engineering Physics, Cornell University, Ithaca, N.Y. 14853.*

We are measuring the lateral motion of individual low density lipoprotein receptor molecules (LDL-R) on cell surfaces. The LDL-Rs are labeled with the bright fluorescent ligand dil-LDL (Barak and Webb, *J. Cell Biol.* 90, 595, 1981) and time lapse fluorescence images of the cell are collected using digital video fluorescence microscopy. We have previously described software and methods to automatically identify and track receptors and have reported diffusion and concerted motion on the living cell's surface (Ghosh and Webb, *Biophys. J.* 53, 352a, 1988). This technique has now been further automated to facilitate simultaneous real time tracking of the complete population of a few thousand LDL-Rs on a cell's surface. Image analysis allows relative location of each receptor to about 5 nanometer precision. The digitized diffraction limited fluorescence image of each dil-LDL labeled receptor covers an area equivalent to about  $1 \mu\text{m}^2$  and is spread over about 100 pixels. This image is non-linear least squares fit by a two dimensional Gaussian to localize its center. Details of our technique and its limitations will be presented along with the latest results of high precision tracking of LDL-Rs on cells where the nanometer scale molecular motions can be compared with supra-micrometer scale movements.

Supported by grants from the NSF (DMB-8609084), ONR (N00014-84-K-0390), NIH (GM33028-02) and the Cornell Biotechnology Program.

**W-Pos103 IN AQUEOUS BUFFER NEWLY DISSOLVED  $\alpha$ -BUNGAROTOXIN BECOMES MONOMERIC VERY SLOWLY. Wilson Radding, Department of Physiology and Biophysics, UAB, Birmingham, AL 35294.**

In the crystalline form  $\alpha$ -bungarotoxin is arrayed as dimers. Fluorescence spectra of  $\alpha$ -bungarotoxin dissolved in water and then quickly diluted in PBS are almost completely quenched. A small peak appears in the vicinity of 325nm. Both quenching and peak position of the tryptophan fluorescence imply that  $\alpha$ -bungarotoxin is at least dimeric when first dissolved this way. Over a period of days the fluorescence spectrum gradually comes to resemble that of  $\alpha$ -cobratoxin with a peak in the hydrophilic range 350-354nm and with similar magnitude. These results imply that  $\alpha$ -bungarotoxin in aqueous solutions without detergent takes a long time to become monomeric, and that both kinetic and equilibrium experiments performed with freshly dissolved  $\alpha$ -bungarotoxin may be misleading.

**W-Pos104 MECHANISMS OF RELEASE AND RELOADING OF CALCIUM INTERNAL STORES IN BAE CELLS AFTER BRADYKININ STIMULATION: A SINGLE-CHANNEL STUDY. M. Chahine, R. Sauvé and J. Verdetti\*. Groupe de recherche en transport membranaire, Université de Montréal, Montréal Canada and \*Dépt de physiologie cellulaire cardiaque (CNRS) U.A. no 632, Université de Grenoble, Grenoble, France.**

Recently, Sauvé et al. (1988) has demonstrated in endothelial cells the presence of  $\text{Ca}^{++}$ -activated  $\text{K}^+$  channels, the activity of which could be induced by ATP via  $\text{P}_2$ -receptor stimulation. From these results it was suggested that endothelial cells respond to ATP (the agonist) stimulation by a biphasic increase in  $\text{Ca}^{++}$  concentration, namely an initial phase related to internal stores mobilization and the second phase requiring external  $\text{Ca}^{++}$ . The present experiments performed in the cell-attached configuration show that bradykinin (10 nM) in BAE cells induce a  $\text{gK},\text{Ca}$  activation by the same mechanism. In this regard, our results indicate: 1) that bradykinin is able to trigger a  $\text{gK},\text{Ca}$  activity in presence of  $\text{Ca}^{++}$  free external medium and 2) that bradykinin induces a secondary  $\text{Ca}^{++}$  influx which requires external  $\text{Ca}^{++}$  and which could be blocked by  $\text{Co}^{++}$  or  $\text{La}^{++}$ . In addition, we could also show that bradykinin does not lead to a  $\text{gK},\text{Ca}$  channel activation if the cells were maintained in a  $\text{Ca}^{++}$  free medium after bradykinin stimulation in a normal  $\text{Ca}^{++}$  medium. These results lead to the hypothesis 1) that external  $\text{Ca}^{++}$  is required to reload the cell internal stores and 2) that the internal stores cannot be refilled in presence of the agonist. Finally, in experiments in which the cells were stimulated by bradykinin in presence or in absence of external  $\text{Ca}^{++}$ , a return to a normal  $\text{Ca}^{++}$  concentration after a  $\text{Ca}^{++}$  free period without the agonist could induce an increase of  $\text{gK},\text{Ca}$  activity. This effect was more pronounced when the internal stores were full, suggesting a  $\text{Ca}^{++}$  induced  $\text{Ca}^{++}$  release mechanism and also that the refilling of  $\text{Ca}^{++}$  internal stores occurs via the cytosolic space.

**W-Pos105** SINGLE-CHANNEL ANALYSIS OF THE OSCILLATORY ACTIVATION PROCESS OF A  $\text{Ca}^{++}$ -DEPENDENT  $\text{K}^+$  CHANNEL CAUSED BY INTERNAL CALCIUM FLUCTUATIONS IN RESPONSE TO  $\text{H}_1$  RECEPTOR STIMULATION IN HELA CELLS. R. Sauvé, C. Simoneau, A. Diarra and G. Roy. Membrane Transport Research Group, University of Montreal, Montreal, Quebec, Canada H3C 3J7

Patch-clamp and fluorescence experiments were undertaken in order to determine the molecular mechanism underlying the cyclic activation of a  $\text{Ca}^{++}$ -dependent  $\text{K}^+$  channel ( $\text{K}^+-\text{Ca}^{++}$ ) following  $\text{H}_1$  receptor stimulation in HeLa cells. The results obtained indicate essentially: 1) that the histamine induced internal  $\text{Ca}^{++}$  fluctuations measured using the  $\text{Ca}^{++}$  indicator Fura-2 correspond well to the cyclic activation of the  $\text{K}^+-\text{Ca}^{++}$  channel following  $\text{H}_1$  receptors stimulation; 2) that the  $\text{K}^+-\text{Ca}^{++}$  cyclic activation process is a biphasic phenomenon with an initial phase related to the release of  $\text{Ca}^{++}$  from internal stores and a second phase requiring the presence of external  $\text{Ca}^{++}$ ; 3) that the second phase can be blocked by calcium channel blockers such as  $\text{Co}^{++}$  (4 mM),  $\text{La}^{++}$  (25  $\mu\text{M}$ ) or abolished by depolarizing the cells using high  $\text{K}^+$  external solutions; 4) that removing the agonist during the second phase results in a complete abolition of the  $\text{K}^+-\text{Ca}^{++}$  oscillatory process; 5) that a sudden increase of the agonist concentration (100 fold) produces an augmentation of the oscillatory frequency coupled to a substantial increase of the time period over which oscillations can be maintained; 6) that the amplitude of the  $\text{K}^+-\text{Ca}^{++}$  channel bursts during the oscillation process is not function of the frequency at which the bursts appear. It is concluded from these results that internal  $\text{Ca}^{++}$  oscillations induced by histamine depend on a dynamic intracellular  $\text{Ca}^{++}$  release- $\text{Ca}^{+}$  sequestration mechanism maintained by the activation of  $\text{Ca}^{++}$  channels operated by internal messengers. (Work supported by MRC of Canada)

Sauvé et al. (1987) J. Membr. Biol. 96: 119-208.

**W-Pos106** EFFECTS OF HISTAMINE ON INTRACELLULAR CALCIUM AND INOSITOLPHOSPHATE FORMATION IN HUMAN SKIN FIBROBLASTS. C.L. Johnson, C.G. Johnson, A. Ahluwalia, E. Bazan, D. Garver and E. Gruenstein (Intr. by A. Martin), Departments of Pharmacology & Cell Biophysics, Molecular Genetics, Biochemistry & Microbiology, and Psychiatry, Univ. Cincinnati, Cincinnati, OH 45267.

Histamine (HA) has been reported to stimulate cell growth and collagen production in fibroblasts. We examined the influence of HA on intracellular free calcium ( $\text{Ca}_i$ ) and formation of inositol phosphates (IP), responses often associated with the action of growth factors such as bradykinin (BK).  $\text{Ca}_i$  was measured by video imaging microscopy of fura-2 loaded cells. Microscope fields of 15-30 cells were analyzed, providing time course measurements within single cells as well as average responses for the entire field. HA caused a transient increase in  $\text{Ca}_i$  within 5-10 secs.  $\text{Ca}_i$  then decreased but remained elevated above baseline for up to 10 min. These effects were independent of external calcium. HA stimulated IP formation within 5 secs in cells labeled with [ $^3\text{H}$ ]-inositol. HA responses were blocked by mepyramine indicating that  $\text{H}_1$  receptors were involved. Phorbol esters completely blocked the effects of HA indicating that the  $\text{H}_1$  receptor is regulated by protein kinase C. Forskolin or isoproterenol partially blocked the HA effects, suggesting that protein kinase A may also regulate  $\text{H}_1$  receptor responses. BK caused much larger increases in both  $\text{Ca}_i$  and IP formation compared to HA. Our results suggest that HA-induced IP formation and mobilization of  $\text{Ca}_i$  could be associated with the reported effects on growth and collagen production. In addition our single cell  $\text{Ca}_i$  measurements demonstrate marked variation between cells within the same field in the kinetics and maximal responses for both HA and BK. This cell heterogeneity is seldom recognized due to the common use of cuvette type fluorescence measurements on cell populations. Supported by HL22619, NS21663, and HL40113.

**W-Pos107** BILAYER PARTITIONING RATES FOR DIHYDROPIRIDINES AND AMIODARONE. David W. Chester and Yvonne Vant Erve. Department of Medicine, University of Connecticut Health Center, Farmington, CT. 06032

Highly lipophilic drugs, such as amiodarone and dihydropyridines (DHP) appear to mediate their effects by partitioning into the bilayer and diffusing laterally to some specific site of action. While the functional significance of bilayer partition remains unproven, we have used the bilayer pathway model supported by membrane partition coefficient, critical micellar concentration, and drug location data as a starting assumption. Determination of the microscopic rate constants associated with drug-membrane binding has involved the measurement of DHP diffusional dynamics and now bilayer partition rates for amiodarone and DHP's in a variety of unilamellar membrane systems. Rates for amiodarone partitioning were determined by following amiodarone quenching of diphenyl-hexatriene (DPH) fluorescence. Stern-Volmer plots of integrated fluorescence intensity versus drug concentration clearly demonstrate quenching via changes in DPH quantum yield as a function of added amiodarone with no change in ground state DPH absorbance. DHP partition rates were assessed as increases in relative PN 200,110 fluorescence intensity since it's quantum yield increases significantly upon bilayer partitioning. Despite the large disparity in membrane partition coefficients for amiodarone and DHP, we have determined that these drugs partition into native bilayers with similar half-times and first order rate constants of approximately 7 seconds and 0.1 ( $\text{sec})^{-1}$ . As such, we are currently able to ascertain microscopic rate constants for bilayer partition, lateral diffusion and hope to evaluate the receptor binding event such that we can gain further insight into the mechanism of lipophilic drug action. Research Supported by NIH-HL33026.

**W-Pos108 Fluorescence Resonance Energy Transfer on Single Living Cells: Application to Oligomerization and Ring Closure of IgE by DNP-Haptens.**

*Ulrich Kubitscheck<sup>1</sup>, Martin Kircheis<sup>1</sup>, Reinhard Schweitzer-Stenner<sup>1</sup>, Wolfgang Dreybrodt<sup>1</sup>, Thomas M. Jovin<sup>2</sup>, Donna Arndt-Jovin<sup>2</sup> and Israel Pecht<sup>3</sup>*

<sup>1</sup>*University of Bremen, Fachbereich 1 - Physics Department, D-2800 Bremen 33, FRG*

<sup>2</sup>*Max Planck Institute for Biophysical Chemistry, Department of Molecular Biology, D-3400 Goettingen, FRG*

<sup>3</sup>*Weizmann Institute of Science, Department of Chemical Immunology, Rehovot 76100, Israel*

A recently developed technique (T.M.Jovin, D.Arndt-Jovin in press. In *Microspectrofluorometry of Single Living Cells*, eds. E.Kohen, J.S.Ploem, J.G.Hirschberg. Orlando, FL: Academic Press) permits the quantitative determination of fluorescence resonance energy transfer on single living cells by photobleaching the donor fluorescence in a microscope. In order to compare the new method with already established techniques we measured the FITC quenching upon binding of a DNP-hapten to anti-DNP IgE from hybridoma HI 26.82 (J.Erickson et al, Mol.Immunol.23(7), 769-781 (1986)) that is bound to cell surface receptors by the photobleaching method. The energy transfer efficiencies obtained by the photobleaching experiments were in very good agreement with those determined by fluorescence quenching measurements. Thus we applied the technique to study the specific binding of mono- and bivalent haptens to surface bound IgE on live RBL cells attached to cover slides. We analysed the binding curves in terms of a thermodynamic model describing different steps of oligomerization of IgE-Receptor complexes. Finally we compared the results to fluorescence quenching experiments on the same IgE molecules in solution.

**W-Pos109 Possible configurational constraints determine the efficiency of transmembraneal signals caused by receptor aggregation: The mast cell case.**

*Enrique Ortega<sup>1</sup>, Reinhard Schweitzer-Stenner<sup>2</sup> and Israel Pecht<sup>1</sup>*

<sup>1</sup>*Weizmann Institute of Science, Department of Chemical Immunology, Rehovot 76100, Israel*

<sup>2</sup>*University of Bremen, Fachbereich 1 - Physics Department, 2800 Bremen 33, Fed. Rep. of Germany*

Three different, IgG class monoclonal antibodies(mAbs) specific for the monovalent high-affinity membrane receptor for IgE( $F_{c\epsilon}R$ ) were used to analyse the response of mast cells of the RBL-2H3 line to crosslinking of their  $F_{c\epsilon}R$ . All three mAbs (designated F4,H10,J17) compete with each other and with IgE for binding to the  $F_{c\epsilon}R$ . Their stoichiometry of binding is 1 Fab: $F_{c\epsilon}R$ . Therefore the intact mAbs aggregate the  $F_{c\epsilon}R$ s to dimers. Since all three mAbs cause secretion, we conclude that  $F_{c\epsilon}R$  dimers serve as signal element for mediators secretion from RBL-2H3 cells. The secretory dose response of the cells to these mAbs, however, are significantly different: F4 cause rather high secretion (max. 80% of the cells content), whereas J17 and H10 cause release of 30-40%. We calculated the extent of  $F_{c\epsilon}R$  dimerization caused as a function of each of the mAb concentration and compared it with the secretory dose response. For this end we used binding data obtained for each mAb and its respective Fab fragment as well as parallel measurements of IgE binding. Results of the analysis showed that F4, J17 and H10 cause maximal dimerization of 20%, 60% and 100% respectively. The secretory response to the three different mAbs cannot be correlated simply with the extent of  $F_{c\epsilon}R$ -dimerization which they produce. This is interpreted as indicating that the triggering efficiency of dimers depends on the relative orientation of the crosslinked receptors.

**W-Pos110 CLUSTERED vs NON-CLUSTERED AChR ROTATIONAL MOBILITY ON RAT MYOTUBES.**

*Marisela Velez and Daniel Axelrod, Biophysics Research Division and Dept. of Physics, University of Michigan, Ann Arbor, MI 48109*

Acetylcholine receptors (AChR) on rat myotubes in primary culture occur in two coexisting states of aggregation: scattered clusters of several hundred microns, and non-clustered regions elsewhere. In an attempt to understand the molecular mechanism of the aggregating process, we have used polarized fluorescence photobleaching recovery (PFPR) to measure the rotational mobility of the receptor (labeled by rhodamine bungarotoxin) in living cells under different aggregating conditions. Care must be taken to subtract from the polarized photobleaching recovery of the total fluorescence the recovery curves due to autofluorescence (up to 60% of the total in diffuse areas) obtained from cells pretreated with unlabeled bungarotoxin. Statistically significant results can be obtained in diffuse areas by signal averaging 200,000 runs, each one collected from a different spot on the myotube surface. The use of a computer controlled motorized stage allows us to collect these data in an experimental time of approximately 20 hours. Clustered receptors show a rotational diffusion coefficient slower than  $\approx .2 \text{ sec}^{-1}$ , whereas diffuse receptors show two components: one with a diffusion coefficient of  $\approx 1000 \text{ sec}^{-1}$  and a slower component with a coefficient slower than  $\approx 200 \text{ sec}^{-1}$ . The effect on the AChR rotational motion of carbachol, a receptor agonist known to disaggregate clusters, and of spinal cord explants, known to aggregate AChR, will be discussed. Supported by NIH grant #NS14565.

**W-Pos111** FLUCTUATIONS IN LATENCY OF THE ANTIGEN-INDUCED  $[Ca^{2+}]_i$  RISE IN TUMOUR MAST CELLS. T. A. Ryan,\* P. J. Millard,\*\* C. M. S. Fewtrell,\*\* and W. W. Webb.\*\*\* Departments of Physics\*, Applied and Engineering Physics\*\*\*, and Pharmacology\*\*, Cornell University, Ithaca, NY 14853.

We have followed the time course of the changes in free cytoplasmic calcium ( $[Ca^{2+}]_i$ ) in individual rat basophilic leukemia (RBL) cells as they are induced by crosslinking cell surface IgE-receptor complexes with multivalent antigen. Our previous results have shown protracted lag times or latencies between the addition of antigen to the bulk solution surrounding the cells and the initial relatively fast rise in  $[Ca^{2+}]_i$ . [PNAS, 85, 1854 (1988)]. We have now characterized the distribution of these lag times using quantitative digital imaging of the fluorescent indicator fura-2 by following simultaneously the time course in large numbers of cells (50-70 cells). The most probable lag times ( $T_L$ ) and the widths of their distributions ( $\sigma$ ) have been measured over a six decade range in antigen concentration and a 2 decade range in cell surface receptor density. These measurements reveal strong systematic increases in both  $T_L$  and  $\sigma$  for both decreasing receptor density and decreasing antigen concentration and weaker dependence upon antigen concentration in the range at which secretion is already fully stimulated. We hope that systematic analysis of the variations in the activation times of the initial rise in  $[Ca^{2+}]_i$  in antigen-stimulated cells (primarily due to release of calcium from intracellular stores) will lead to an understanding of the mechanisms involved in the early events in IgE-R-mediated stimulus-secretion coupling.

Supported by ONR (N00014-84-K-0390), NSF (DMB-8609084) (T.A.R. and W.W.W.), NSF (DCB-8702584) (P.J.M. and C.M.S.F.) and the Cornell Biotechnology Program.

**W-Pos112** ANTIGEN STIMULATED DEGRANULATION OF RAT BASOPHILIC LEUKEMIA CELLS MAY BE LIMITED BY THE RATE OF IMMUNOGLOBULIN E RECEPTOR CROSSLINKING. Jon W. Erickson, David Holowka, and Barbara Baird, Department of Chemistry, Cornell University, Ithaca, NY 14853

We have measured multivalent antigen binding to immunoglobulin E (IgE)-sensitized rat basophilic leukemia cells simultaneously with serotonin secretion that is due to the crosslinking of IgE-receptor complexes, and the results indicate that the stimulatory signal provided by an individual crosslink is relatively shortlived with a lifetime of less than two minutes. Less than 10% of the bound antigen is dissociated by the addition of monovalent hapten under conditions where serotonin release is immediately halted. This implies that receptors remain crosslinked but become deactivated after a period of time and that the continued formation of new crosslinks is necessary to maintain the secretory response. We have also measured binding and crosslink formation by a bivalent ligand, and we find that the crosslinks are extensive and long lived compared to the timecourse of the secretory process and intermediate second messenger responses even though this ligand stimulates poor serotonin secretion. We suggest that the rate of crosslinking by this bivalent ligand is too slow to overcome a concurrent deactivation process. A kinetic model for crosslink-mediated signal transduction is proposed to account for these results.

**W-Pos113 GRAMICIDIN SINGLE CHANNELS IN PLANAR BILAYERS SHOW NO SOLVENT HISTORY DEPENDENCE.** D.B. Sawyer, R.E. Koepppe II\*, and O.S. Andersen., Dept. Physiol. Biophys., Cornell Univ. Med. Coll., New York, NY 10021, and \*Dept. Chem. Biochem., Univ. Arkansas, Fayetteville, AR 72701.

It has recently been shown that the membrane conformation of the linear gramicidins may depend on the solvent in which they were dissolved before incorporation into lipid vesicles at peptide/lipid ratios of 1/10 (P.V. LoGrasso et al., *Biophys. J.* **54**: 259, 1988; J.A. Killian et al., *Biochemistry* **27**: 4848, 1988), and it was suggested that the solvent history could affect the functional characteristics of gramicidin channels. This question was examined using single channel recordings in planar lipid bilayers. HPLC-purified gramicidin A was first dissolved into eight separate solvents: benzene, chloroform, dimethylsulfoxide, dioxane, ethanol, ethylacetate, methanol, or trifluoroethanol and equilibrated for at least 1 hour. Each gramicidin dilution was then added separately to a 1.0 M NaCl solution at both sides of a diphyanoylphosphatidylcholine bilayer, and single channel currents were recorded at 100 mV applied potential. The channel behavior was independent of the solvent. It is possible that brief exposures to the electrolyte solution make the peptides "forget" their solvent history. To test this, gramicidin was co-solubilized with lipid in four solvents (benzene, chloroform, ethanol and trifluoroethanol) at peptide:lipid ratios of  $10^{-6}$ . The solvents were evaporated and the lipid/peptide mixtures were suspended in decane, planar bilayers were formed, and single channel currents were recorded. Again, channels from all solvents behaved identically, with no obvious dependence of single channel behavior on solvent history of the peptides.

**W-Pos114 ON THE SUPRAMOLECULAR ORGANIZATION OF GRAMICIDIN CHANNELS.** A.S. Cifu, R.E. Koepppe II\*, and O.S. Andersen, Dept. Physiol. Biophys., Cornell Univ. Med. Coll., New York, NY 10021, and Dept. Chem. Biochem., Univ. Arkansas, Fayetteville, AR 72701.

The linear gramicidins form membrane-spanning NH<sub>2</sub>-to-NH<sub>2</sub>-terminal  $\beta^{6,7}$ -helical dimers that generally are believed to be the elementary conducting units. It has been proposed, however, that the elementary conducting unit is some higher oligomer (Stark et al., *J. Membrane Biol.* **89**:23, 1986). This question was examined using channels formed by mixtures of gramicidin A (GA) and O-pyromellityl gramicidin A (OPGA), peptides that have comparable channel formation kinetics (Stark et al., op cit). The experiments exploit that the pyromellityl moiety at the channel entrances should produce quite asymmetric hybrid channels, which facilitates identification of different hybrid channel types. In addition, the negative charges on OPGA enables us to detect lateral associations among membrane-spanning dimers, or among monomers and dimers. Only two hybrid channel types were observed in symmetrical mixtures of GA and OPGA. In amplitude histograms, the four peaks had similar standard deviations, corresponding to that of the standard channel peak for either of the pure channels. It is thus unlikely that hybrid channel types were missed, and the presence of only two hybrid peaks strongly suggests that the channels are dimers. The hybrid channels were further identified in experiments where one or both peptides were added asymmetrically, and there was no evidence for channel formation by lateral association of a GA and an OPGA dimer. In 0.05 M CsCl the Debye length is comparable to the center-to-center distance between two  $\beta^{6,7}$ -helices in an oligomer, but the peak corresponding to the uncharged GA channels was unaffected by addition of OPGA. There cannot be any significant association between uncharged dimers and charged monomers. The elementary conducting unit is a dimer.

**W-Pos115 GRAMICIDIN CHANNELS THAT HAVE NO TRYPTOPHAN RESIDUES.** V. Fonseca, P. Daumas, L. Ranjala-hay-Rasoloarijao, F. Heitz, R. Lazaro, Y. Trudelle, and O. Andersen, Cornell Univ. Med. Coll., New York, NY, USA, and CNRS, Montpellier and Orleans, France.

The aromatic residues in gramicidin channels are important for their function, as replacement of the four tryptophans in gramicidin A (GA) with phenylalanines in the optically reversed gramicidin M' (GM) decreases the small-signal single-channel conductance (in 1.0 M CsCl) some 20-fold (Heitz et al., *Biophys. J.* **40**:87, 1982). These conductance changes could result from altered ion-dipole interactions between permeating ions and the aromatic side chains (Tredgold and Hole, *BBA* **471**:189, 1977), as the indole and phenyl rings have dipole moments of 2.1 and 0 D, respectively. To study this question further, we examined channels formed by gramicidins where the aromatic residues were either tyrosine (GT), O-benzyl-tyrosine (GT'), or naphtylalanine (GN). The aromatic rings in the side chains have dipole moments of 1.6, 1.2, and 0 D, respectively. Except for GM, these peptides form channels that are structurally equivalent to GA channels, as they form hybrid channels with GA. The sequence substitutions induce large alterations in the average duration and conductance of gramicidin channels in diphyanoylphosphatidylcholine membranes. In 1.0 M CsCl, the average durations (at 200 mV) were: GA, 0.6 s; GT, 0.1 s; GT', 0.7 s; GM, 0.3 s; and GN, 0.9 s. There is no obvious relation between average duration and the characteristics of the aromatic side chain. The small-signal single-channel conductances were: GA, 48 pS; GT, 27 pS; GT', 6 pS; GM, 3.4 pS; and GN, 3 pS. The conductance decreases as the dipole moment of the aromatic ring decreases. The quite different conductances of GT and GT' channels suggests further that the average orientations of the dipolar residues are important - as would be expected if ion-dipole interactions were important in altering the energy barrier for ion movement through the channels.

**W-Pos116 SINGLE TRYPTOPHAN-TO-PHENYLALANINE SUBSTITUTIONS IN GRAMICIDIN CHANNELS.** M.D. Becker, D.B. Sawyer, A.K. Maddock, R.E. Koeppel II\*, and O.S. Andersen. Cornell Univ. Med. Coll., New York, N.Y. 10021, and Univ. Arkansas, Fayetteville, AR 72701.

The aromatic side chains in the COOH-terminal half of Gramicidin A play an important role in modulating channel function (Heitz et al., *Biophys. J.* 40:87, 1982; see also accompanying Abstract by Fonseca et al.). In order to examine the differential effects of the four Trp side chains, we have studied the behavior of gramicidin channels formed by peptides with single Trp → Phe substitutions at position #9, #11, or #15. These peptides form channels that are structurally equivalent to gramicidin A channels, because each peptide forms hybrid channels with gramicidin A, with hybrid channel appearance rates that can be predicted from the pure channel appearance rates using the binomial distribution. In 1.0 M NaCl, the small-signal single channel conductances were 5.0, 7.1, or 9.3 pS for channels with Phe at position #9, #11, or #15, which should be compared to 12.6 pS for gramicidin A channels. A Trp → Phe substitution decreases the conductance independently of where the substitution is made. The average channel durations (at 200 mV) were 0.5, 2.4, or 0.5 s for channels with substitutions at positions #9, #11, or #15, which should be compared to 0.6 s for gramicidin A channels. The ratio of the small-signal conductances in 1.0 M and 0.1 M NaCl was 2.3 in Gramicidin A channels and 2.8, 2.5, or 3.5 in channels with position #9, #11, or #15 substitutions. Trp → Phe substitutions near the COOH-terminal end of gramicidin channels decrease the single-channel conductance, but they appear to do so through differential effects on the maximal conductance and ion affinity, which together with the variable effects on channel stability suggests that Trp #9, #11 and #15 are functionally distinct.

**W-Pos117 THE GRAMICIDIN CHANNEL SELECTIVITY FILTER: GUANIDINIUM PERMEATION.** Brian Turano, Ingfei Chen, and David Busath. Sect. of Physiology and Biophysics. Brown Univ. Providence, RI 02912.

To further elucidate the "selectivity filter" concept, we have performed experimental and theoretical studies of the permeability of gramicidin A channels to guanidinium and similar organic cations. We measured gramicidin A single channel currents in GMO/hexadecane bilayers bathed on one side with electrically grounded 1.0 M KCl and on the other with 1.0 M guanidinium Cl to which a 4 Hz, +/-100 mV potential was applied. 17 channels were selected for their standard potassium conductances during negative cycles and their average currents during positive cycles were determined. The net current from the guanidinium compartment averaged -92.0 fA (+/- 7.8 fA, S.E.M.), a backflux appropriate, according to the Ussing flux ratio equation, for potassium backflux in the absence of guanidinium, ammonium, chloride, hydrogen, or contaminant potassium flux from the guanidinium compartment. From the level of error in the measurement, we place a limit of 0.004 x g(K) on the guanidinium conductance of gramicidin. In contrast, the channel conductance in 1.0 M formamidinium Cl is similar to that in 1.0 M KCl. From these results, we hypothesized that formamidinium fits through the channel "selectivity filter" but that guanidinium does not. We then used CHARMm to calculate the minimum energy positions along the channel axis for formamidinium and guanidinium. The channel model was based on dihedral angles given by Venkatachalam and Urry (*J. Comp. Chem.* 4:461, 1983). Energy minimization of this structure *in vacuo* produced a constriction in the pore entrances. The constriction gave rise to a large Van der Waals barrier which was much higher for guanidinium than for formamidinium. However, when the channel was free to move within the constraints imposed by the empirical bond energies, the Van der Waals barrier was eliminated with only minor gramicidin motion. A video animation of the computed coordinates suggests that gramicidin's selectivity for formamidinium over guanidinium must be due NOT to the enthalpic Van der Waals barrier (ie., fitting through the filter), but rather to kinetic factors related to gramicidin motions and/or to a greater decrease in guanidinium entropy in the channel. (Supported by NIH GM33361).

**W-Pos118 THE NON-SPECIFIC ERYTHROCYTE MEMBRANE PERMEABILITY INDUCED BY HIGH CONCENTRATIONS OF GRAMICIDIN IS INHIBITED BY STILBENE BLOCKERS OF BAND 3.** John P. Pooler, Physiology Dept., Emory University School of Medicine, Atlanta, GA 30322.

It has been shown recently that high concentrations of gramicidin induce a non-specific permeability in erythrocyte membranes that allows passage of relatively large anions and even oligosaccharides (Classen et al. [1987] *Biochemistry* 26:6604). This permeability may be assessed as rates of hemolysis in buffered monovalent salt solutions. Below a certain threshold gramicidin concentration (= 40 µg/ml packed cells), lysis occurs at a rate limited by the native monovalent anion permeability. Above the threshold, lysis rate is greatly increased. The present work shows both the native anion permeability at low gramicidin concentrations and the gramicidin-induced anion permeability at high concentrations are blocked more than 50% by irreversible (H<sub>2</sub>DIDS) and reversible (DNDS) stilbene inhibitors of band 3 anion exchange. Furthermore, both the native and gramicidin-induced permeabilities show a similar temperature dependence ( $E_a = 18 \text{ kcal/mole}$ ).

**W-Pos119** CONFORMATION AND ORDER OF GRAMICIDIN A IN PHOSPHOLIPID DISPERSIONS. B.A Cornell and F. Separovic, CSIRO, P.O.Box 52, North Ryde, NSW 2113, and R. Smith and D.E. Thomas, University of Queensland, St Lucia, Australia.

Aligned hydrated dispersions of DMPC and labelled analogs of the ionophore gramicidin A, (15:1) have been studied by solid state carbon-13 NMR. Individual analogs have been synthesised in which carbon-13 labels have been incorporated into most of the backbone carbonyl sites of gramicidin A and in the C2 position of Trp-9, Trp-11, Trp-13, and Trp-15. Based on measurements of the reduced carbon-13 chemical shift anisotropy and the reduced dipolar interaction of carbon-13 with neighbouring spins, these data have been analysed to yield information on the conformation and order of the gramicidin. Issues that will be addressed include refinements of the helical geometry and the handedness of the  $\beta$  helix. The conformation and order of the tryptophan residues was found to depend on their location within the gramicidin A molecule and the phase of the lipid. Measurements will also be reported on the effect of varying the chainlength and class of the surrounding lipid.

**W-Pos120** PHOTOCHEMICAL AND ELECTRICAL STUDIES OF Tl(I) ION PERMEATION

AND BINDING FOR FUNCTIONAL GRAMICIDIN CHANNELS

Michael E. Starzak, Department of Chemistry, State University of New York at Binghamton, Binghamton, New York 13901

Tl(I) ion permeation, binding and channel blockage in gramicidin channels in lipid bilayers are studied by a combination of electrical and photochemical techniques which permit determination of the net Tl(I) ion flux through the channels when this ion competes with Na(I) or K(I) for channel sites. The fraction of net current carried by Tl(I) ion at a series of transmembrane potentials is monitored using Tl(I) ion quenching of the probe ANTS. The population of intrachannel Tl(I) ions produced by this current flow is monitored with Tl(I) ion fluorescence resulting from the enhanced absorption of Tl(I) ion at 265 nm when this ion interacts with gramicidin. A two pulse potential regimen is used to displace all Tl(I) from the channel to provide an accurate calibration of intrachannel Tl(I) populations at a series of transmembrane potentials including zero potential. These data are used to test an ion displacement model which suggests a consistent explanation for the role of Tl(I) as a permeant ion when present as the majority cation and a blocking ion at low mole fractions plus a consistent explanation for the non-saturation of Tl(I) ion currents at large transmembrane potentials. Supported by the Office of Naval Research - RR04108

**W-Pos121** MOLECULAR DYNAMICS STUDIES OF WATER STRUCTURE AND WATER AND ION MOVEMENT WITHIN THE GRAMICIDIN CHANNEL. Chiu, S. W., Subramanian, S.,

Jakobsson, E. and J. A. McCammon, Department of Physiology and Biophysics and Program in Bioengineering, University of Illinois, Urbana, IL 61801, and Department of Chemistry, University of Houston, Houston, TX 77004. We have used the GROMOS molecular modeling program as described in our companion paper at this meeting to simulate the gramicidin A channel with water and ions in the lumen. We observe one type of persistent water structure that is similar to that described previously by Mackay et al (1) in which the waters all align with their dipole moments oriented in the same direction along the channel axis. However we also observe, both from energy minimization and also molecular dynamics simulations, another type of structure, in which regions of waters with similarly aligned dipoles as described above are "bridged" by waters with their dipoles oriented roughly normal to the channel axis. A transition between the two types of structure has been observed, which appears to involve a coordinated motion of several parts of the channel-water complex. Because the movement of the channel contents is so coordinated, we have begun time-correlation analysis on the center-of-mass motion of the channel contents, to the end of determining water and ion transport properties across the channel. 1. Mackay et al. 1984. *Biophys. J.* 46, 229. Support from the Bioengineering Program and NIH (University of Illinois), National Center for Supercomputing Applications (Champaign, Illinois), and NSF (University of Houston).

**W-Pos122 MOLECULAR DYNAMICS STUDIES OF GRAMICIDIN CHANNEL STRUCTURE.** Chiu, S. W., Subramanian, S., Jakobsson, E. and J. A. McCammon, Department of Physiology and Biophysics and Program in Bioengineering, University of Illinois, Urbana, IL 61801, and Department of Chemistry, University of Houston, Houston, TX 77004. We have used a modified version of the GROMOS molecular modeling program to explore via molecular dynamics simulation the structure of the gramicidin A channel. Our modification is to impose an all-atom restraint in which the atomic positions relax to a postulated original structure (1) with a time constant of 10 picoseconds. (We find that some artificial restraint is necessary to preserve the overall helical structure in the absence of the lipid environment of the channel protein.) We find that even in the absence of water or ions in the channel, the helix flexes and the amide planes tilt so as to move carbonyl oxygens towards the channel lumen. The presence of water in the channel only slightly increases this tendency. This inward "leaning" of the carbonyl oxygens seems likely to be a contributor to the channel's ability to solvate waters and cations. We find an alternating pattern in the angles that different backbone N-H's make with the channel axis. This pattern is in good semi-quantitative agreement with NMR data. (2) In further work we will explore the sensitivity of the precise computed channel structure to the type of restraints imposed on the molecule. 1. Koepp et al 1984. Biopolymers, 23, 23. 2. Fields et al. 1988. PNAS 85, 1384. Support from the Bioengineering Program and NIH (University of Illinois), the National Center for Supercomputing Applications (Champaign, Illinois), and NSF (University of Houston).

**W-Pos123 CATION CONDUCTANCE OF TRUNCATED GRAMICIDINS.** H. ROTTENBERG\* AND R.E. KOEPPE, II<sup>1</sup>  
 \*PATHOLOGY DEPARTMENT, HAHNEMANN UNIVERSITY, PHILADELPHIA, PA AND <sup>1</sup>DEPARTMENT OF  
 CHEMISTRY AND BIOCHEMISTRY, UNIVERSITY OF ARKANSAS, FAYETTEVILLE, ARKANSAS.

Gramicidin and the truncated derivatives: desformyl gramicidin (desfor) and des(formylvalyl) gramicidin (desval) stimulate monovalent cation transport in rat liver mitochondria. Cation fluxes were compared indirectly from the effect of cations on the membrane potential at steady-state (State 4) or from the associated stimulation of electron transport. Rb<sup>+</sup> transport was measured directly from the uptake of <sup>86</sup>Rb. The truncated gramicidins show enhanced selectivity for K<sup>+</sup> and Rb<sup>+</sup> when compared to gramicidin. Moreover, the pattern of selectivity within the alkali-cation series is altered, i.e. Rb<sup>+</sup> > K<sup>+</sup> > Cs<sup>+</sup> > Na<sup>+</sup> > Li<sup>+</sup> for desfor and desval, as compared to Cs<sup>+</sup> > Rb<sup>+</sup> > K<sup>+</sup> = Na<sup>+</sup> > Li<sup>+</sup> for gramicidin. The cation fluxes through the truncated derivatives are more strongly dependent on the cation concentration. The presence of high concentrations of permeating cation enhances the transport of other cations through the truncated derivative channels, suggesting that cations are required for stabilizing the channel structure. In high concentrations of KC1, desfor and desval are nearly as effective as gramicidin in collapsing the mitochondrial membrane potential, and consequently, in the uncoupling of oxidative phosphorylation and enhancement of ATP hydrolysis. Preliminary experiments with liposomes show that <sup>86</sup>Rb exchange is stimulated by desfor and desval almost to the same extent as gramicidin. These results strongly suggest that the truncated gramicidins form a novel conducting channel which differs from the gramicidin head-to-head, single-stranded  $\beta$ -helical dimer ("channel") in its conductance characteristic and its structure. We suggest that the antiparallel double-stranded helix dimer ("pore") is a likely alternative structure for this novel channel. Supported by NIH Grants #GM-28172 (H.R.) and #GM-34968 (R.E.K.)

**W-Pos124 STRUCTURAL FLUCTUATIONS IN THE HEAD-TO-HEAD JUNCTION CAUSE RAPID GATING OF THE GRAMICIDIN A CHANNEL**

S.H. Heinemann, C.J. Stankovic\*, J.M. Delfino#, S.L. Schreiber\*, and F.J. Sigworth. Dept. of Cellular and Molecular Physiology, Yale School of Medicine, New Haven, CT 06510. \* Dept. of Chemistry, Yale University, New Haven, CT 06511. # Dept. of Mol. Biophys. and Biochem., Yale University, New Haven, CT 06511.

Gramicidin A (GA) channels incorporated into artificial bilayers exhibit fast gating features as shown earlier (Sigworth and Shenkel, 1988. Curr. Top. Membranes and Transport 13, 113-130). Specifically, in glycerol-monooleate/squalene membranes, at 300mV membrane potential, in symmetrical 640mM KCl solutions, and at room temperature a closed state of ~10μs duration (frequency of occurrence ~2-5/s) and a subconductance state of ~500μs duration (frequency ~1/s, 75% reduction of amplitude) are observed. The question of the molecular cause of these events was addressed by the investigation of covalently linked GA dimers. Desformyl GA monomers were linked by C<sub>2</sub>-symmetric dicarboxylic acids derived from S,S- and R,R-tartaric acids. The SS-linkage, which is expected to maintain an undistorted  $\beta$ <sup>6,3</sup>-helix, results in ion channels with a 15% smaller conductance than regular GA. The frequency of brief gaps and sublevels is reduced by more than an order of magnitude. This result implicates the head-to-head junction as the cause of the fast gating events. The RR-linked dimers form channels of considerably smaller conductance, presumably due to structural distortion at the head-to-head junction. In addition, these channels show closing events of ~90μs duration (frequency ~20/s). A possible explanation of this behavior is a flipping of the dicarboxylic ring between the outside (open) and the inside (closed) of the pore. We expect that tests of GAs covalently linked by other agents will provide further insight into the structural basis of the rapid gating events.

**W-Pos125** PARTICLE MORPHOLOGY IN THE PHASE MAP OF MIXED BILE SALT-LECITHIN COLLOIDS BY SMALL ANGLE NEUTRON SCATTERING. R.P. Hjelm<sup>1</sup>, M.H. Alkan<sup>2</sup>, and P. Thiagarajan<sup>3</sup>, Los Alamos Neutron Scattering Center, Physics Division, Los Alamos National Lab., Los Alamos, NM; Department of Pharmaceutics, University of Illinois at Chicago, Chicago, IL; and IPNS and Chemistry Divisions, Argonne National Laboratory, Argonne IL.

Small-angle neutron scattering has been used to construct a morphological phase map of mixed glycocholate-lecithin colloids. At high total lipid concentrations mixed micelles are present which are globular in shape. As the total lipid concentration is reduced at lipid to bile salt ratios between 0.3 and 0.9 the mixed micelles are seen to elongate, eventually forming very long rods. The elongated and rod like particles appear to have radii of 27 Å, but are heterogeneous in length. At lower total lipid concentrations the rods apparently raft together to form extended sheet-like structures or large vesicles. Single bilayer vesicle morphology becomes more apparent as the solution is diluted further. The vesicle size is smaller as the total lipid concentration is decreased further due to the removal of bile salt from the particles. Again, the population of vesicles is heterogeneous, and some aspects of this are characterized. The growth of mixed micelles into long rods and the mechanism of vesicle formation are not in accord with the predictions of the standard model of this system.

This work is supported by the United States Department of Energy.

**W-Pos126** BIOPHYSICAL ANALYSIS OF ATHEROSCLEROTIC VESSELS. Stefanella Bortini, Leonard J. Lis, Carl E. Arentzen, John W. Kauffman. Northwestern University, Evanston, IL.

Differential Scanning Calorimetry (DSC) and Fourier Transform Infrared Spectroscopy (FTIR) were used to detect phase transitions and delineate their molecular basis and other biophysical properties of the intact atherosclerotic plaque and of a lipid model in the range of 5°-50°C. Homozygous Watanabe rabbits (WHHL), which develop aortic atherosclerosis, provided the aorta from which the intima was scraped. Model systems containing appropriate amounts of cholesterol, cholesterol esters, lecithin, lysolecithin and sphingomyelin were also studied. Thermal events in the range of 29°-35°C and 41°-44°C are recorded by DSC and sudden (between 20°-25°C) and slow (between 28°-50°C) changes in frequency were observed by FTIR. Very slow changes in the CH<sub>2</sub> stretching band frequency over the temperature range of 5°-51°C and in the CO stretching band frequency over 30°-51°C were determined for the scraped thoracic aortic intima. FTIR spectra of the thoracic aorta at 39°C were also obtained from 12 WHHL and 5 NZW (control) rabbits. Vibrational bands and their corresponding spectra ( $\text{cm}^{-1}$ ) are listed below.

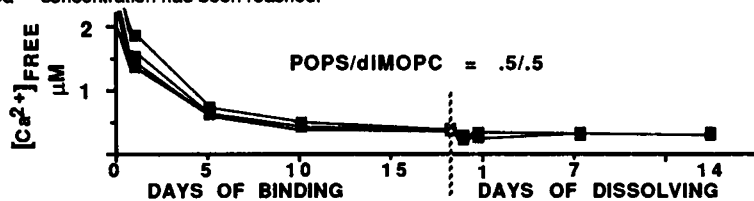
| Vibrational Bands          | WHHL rabbits  | NZW rabbits   |
|----------------------------|---------------|---------------|
| CH <sub>2</sub> Stretching | 2852.5±0.63sd | 2854.0±1.37sd |
| CH <sub>2</sub> Bending    | 1446.7±2.34sd | 1458.4±2.34sd |
| CO Stretching              | 1739.6±1.26sd | 1744.5±0.75sd |
| CO Stretching              | 1734.1±1.3sd  | 1733.8±0.75sd |

The difference in absorption spectra may be of practical importance in distinguishing between normal and atherosclerotic vessels.

**W-Pos127** THE MOLECULAR STRUCTURE OF LIPOSOMES CONTAINING THE ANTIARRHYTHMIC AGENT AMIODARONE. Gordon L. Jendrasik, Ph.D., East Carolina University and Medical School; Thomas J. McIntosh and Anthony Ribeiro, Duke University Medical School; Joseph M. Costello, University of North Carolina and R. Stephen Porter, Hahnemann University. Negatively charged liposomes, containing the antiarrhythmic drug amiodarone, have been studied by means of nuclear magnetic resonance (NMR). These liposomes, as characterized by electron microscopy and light scattering, are mainly unilamellar vesicles of less than 1000 Å in diameter. Proton spectra of liposomes containing amiodarone or cholesterol, respectively, at the same concentrations show that cholesterol has a greater effect on the hydrocarbon region of the liposomes than does amiodarone whereas amiodarone has a greater effect on the lipid head-group region. The effect of amiodarone on the head-group NMR signal resembles that of the fluorescent dye ANS which is known to be located in the polar head-group region of the liposomes. This effect on the head group NMR signal is thought to arise because of the amiodarone "ring currents." The amiodarone metabolite desethylamiodarone exhibits a NMR spectrum similar to that of amiodarone. When the cholesterol containing liposomes are exposed to the pseudohalide, thiocyanate, the splitting of the NMR head-group signal is clearly increased whereas for the amiodarone containing liposome it is decreased. X-ray diffraction experiments on oriented multilayers show that the lamellar repeat period and thickness of the lipid bilayer are reduced by the amiodarone some 4 to 5 Å; modelling studies indicate that the amiodarone iodine is within a few angstroms of the bilayer center. All of our studies thus indicate that at neutral or acidic pH values, the amiodarone is located near the lipid polar head-groups, and has different effects on lipid packing than does cholesterol.

**W-Pos128 MEASUREMENT OF HIGH-AFFINITY  $\text{Ca}^{2+}$  BINDING TO PHOSPHATIDYL SERINE/PHOSPHATIDYL CHOLINE MIXTURES IN SIMPLE MULTILAMELLAR DISPERSIONS.** J.E. Swanson and G.W. Feigenson, Section of Biochemistry, Molecular and Cell Biology, Cornell University, Ithaca, NY 14853.

We have obtained equilibrium measurements of high-affinity  $\text{Ca}^{2+}$  binding to PS/PC mixtures in simple multilamellar dispersions.  $\text{Ca}^{2+}$  concentration was controlled and measured by use of the chelator-indicators BAPTA or BrBAPTA. The central feature of this method is to allow sufficient time for significant  $\text{Ca}^{2+}$  binding to occur, and then, upon lowering the free  $\text{Ca}^{2+}$  concentration, to allow sufficient time for PS-bound  $\text{Ca}^{2+}$  to dissolve until a near-equilibrium  $\text{Ca}^{2+}$  concentration is reached.  $\text{Ca}^{2+}$  binding to POPS (1-palmitoyl-2-oleyl-sn-glycero-3-phosphoserine) was measured in mixtures with dIMOPC (1,2-dimyristoleoyl-sn-glycero-3-phosphocholine). The time course of  $\text{Ca}^{2+}$  binding was conveniently followed by absorbance measurements, thereby making possible the initiation of the " $\text{Ca}^{2+}$  dissolving period" after a suitably low free  $\text{Ca}^{2+}$  concentration had been reached.



The experimental finding is that the equilibrium  $\text{Ca}^{2+}$  concentration for  $\text{Ca}(\text{PS})_2$  formation varies as the inverse square of the POPS mole fraction, indicating apparent ideal mixing of POPS with dIMOPC at all mole fractions. This result contrasts with the behavior of POPS/POPC mixtures, wherein Henry's Law describes the data at low POPS mole fractions and Raoult's Law describes the data at high POPS mole fractions.

**W-Pos129 QUADRUPOLAR  $^{13}\text{C}$ - $^{14}\text{N}$  COUPLINGS AND  $^{14}\text{N}$  RELAXATIONS IN AGGREGATED AND NONAGGREGATED LYSOPHOSPHATIDYLCHOLINES.** V.V. Kumar and Wolfgang J. Baumann, The Hormel Institute, University of Minnesota, Austin, Minnesota 55912.

Earlier work from our laboratory had shown that nitrogen-14 spin-lattice relaxation times ( $^{14}\text{N}$   $T_1$ ) and quadrupolar  $^{13}\text{C}$ - $^{14}\text{N}$  couplings ( $J_{\text{CN}}$ ) of choline phospholipids are most sensitive to changes in the nitrogen environment. Hence, measuring of  $^{14}\text{N}$   $T_1$  and  $J_{\text{CN}}$  values was thought to be useful to monitor changes in phospholipid headgroup association and in the state of phospholipid aggregation (*J. Am. Chem. Soc.* 103, 1238, 1981). We now determined both parameters on lysophosphatidylcholines (lysoPC) of different chain length in aqueous dispersion (100 mM). We found that the  $^{13}\text{C}$  NMR spectra (20 MHz) of lysoPC with a carbon chain of up to  $\text{C}_{10}$  show well resolved triplets for the choline methyls ( $J_{\text{CN}} = 3.3 \pm 0.5$  Hz); however, the methyl triplets collapse to singlets for lysoPC with 12 or more carbons in the aliphatic chain. The  $^{14}\text{N}$   $T_1$  values (5.74 MHz) declined from 0.172 s for  $\text{C}_6$  lysoPC to 0.093 s for  $\text{C}_{12}$  lysoPC, but little change occurred for lysoPC with a chain length of  $\text{C}_{14}$  and longer (0.06 s). The data are consistent with our earlier calculations which predicted that triplet broadening would occur for  $^{14}\text{N}$   $T_1$  values shorter than 0.086 s with eventual collapse of the splittings. The data furthermore show that lysophosphatidylcholines (at 100 mM) with a chain length of  $\text{C}_{14}$  and longer form micelles, whereas shorter chain lysoPC tend to remain in the nonaggregated state. Carbon chemical shift measurements support these conclusions. The effect of lysoPC concentration on the spectral parameters was also investigated. (Supported by NIH Grant HL08214 and by the Hormel Foundation).

**W-Pos130 OPTICAL, INFRARED AND NMR STUDIES OF CATION-PHOSPHOLIPID COMPLEXES**  
Matthew Petersheim, Joanne Sun, Juris Blodnieks and Helen Nell Halladay, Chemistry Dept. Seton Hall University, South Orange, NJ 07079. Introduced by Ruth E. Stark, Chemistry Department, College at Staten Island-CUNY, Staten Island, NY 10301.

This work centers on the use of the luminescent lanthanide, Tb(III), as a probe of the cation binding sites on artificial phospholipid vesicles and micelles. Both the excitation and emission spectra of Tb(III) are sensitive to its' coordination sphere, which changes with the chemical and physical properties of the phospholipid membrane to which it is bound. Optical studies of Tb(III)-phospholipid complexes will be presented which reflect: homogeneous phase changes induced by the bound cation, cation competition for heterogeneous sites on single component and mixed lipid membranes, and slow phase changes in the lipid induced by binding of Tb(III) and other cations. Infrared was used to compare Tb(III) and Ca(II) binding to the phospholipids and NMR spectroscopy provided information about the lanthanide-phospholipid stoichiometry and some structural details.

These results demonstrate the potential for using the luminescent lanthanides to characterize transient or dilute cation-phospholipid states such as those expected during membrane fusion or in site-selective binding of cations in mixed lipid systems

**W-Po131 LEARNING ABOUT BILAYERS FROM MONOLAYERS: THEORETICAL AND PRACTICAL APPLICATIONS OF EQUILIBRIUM BETWEEN THE TWO STRUCTURES.** Robert C. MacDonald, Department of Biochemistry, Molecular Biology & Cell Biology, Northwestern University, Evanston, IL 60208.

Monolayers are potentially very useful for providing information on physical properties of bilayers. Since monolayers of membrane lipids collapse into bilayers, monolayers and bilayers are necessarily at equilibrium at the collapse pressure. The goal of this inquiry is to ascertain how this equilibrium can be exploited to obtain information on bilayers from monolayers. The device of equating the chemical potentials of a molecule at equilibrium between two phases is a powerful analytical tool for bulk phases; however, in the case of interfacial phases, particularly bilayers, this practice is less common, perhaps because there are several alternative forms for the chemical potential and the proper choice requires knowledge beyond the fact that two systems are at equilibrium. Thus, although the surface energy term for an isolated surface is (surface tension)  $\times$  (surface area), that for a monolayer is (surface pressure)  $\times$  (surface area). The difference in the two cases is the nature of the work required in transporting a molecule to the surface. Since the work of transporting a molecule to a monolayer is both easily defined and measured, the chemical potential may be formulated rigorously and in terms of easily accessible experimental parameters. In contrast, the work of transport into bilayers involves internal forces which are complex and not easily measured. It is therefore expedient to make use of equilibrium monolayers to experimentally establish the surface energy of bilayers. It is, in fact, a simple matter to demonstrate the higher surface energy (lower surface pressure) of sonicated liposomes by allowing them to equilibrate with monolayers. As expected, molecules migrate from a monolayer to sonicated vesicles when the former is at the higher equilibrium pressure for multilayers. Supported by NIH GM38244.

**W-Po132 A CENTRALIZED DATABASE FOR THERMODYNAMIC DATA ON LIPID MESOMORPHIC PHASE TRANSITIONS AND MISCELLIBILITY**

Martin Caffrey, Denis Moynihan, Saty Raghavachary. Department of Chemistry, 120 W. 18th Ave., The Ohio State University, Columbus, Ohio 43210.

The systematic study of the mesomorphic phase properties of synthetic and biologically-derived lipids began some 20 years ago. In the past decade, interest in this area has grown enormously. As a result, there exists a wealth of information on lipid phase behavior, but, unfortunately, this data is scattered throughout the literature in a variety of journals, books and proceedings both foreign and domestic. We are in the process of compiling and evaluating this data with a view to providing ready access to the data itself and to the appropriate literature. The intention is to compile evaluated data in a single, continuously revised computer file. The file will be accessed by means of an interactive computer program and hard copies of the data will be available on request and/or through a network system. The compilation is being prepared in two parts. The first is a tabulation of all known and of evaluated mesomorphic and polymorphic phase transition temperatures and enthalpies for synthetic and biologically-derived lipids in the dry and in the partially and fully hydrated states. The second part of the compilation concerns the miscibility properties of lipids. Here, data is being graphically presented in the form of evaluated isobaric and isothermal phase diagrams.

## W-Pos133 CHEY:PHOSPHATE INTERACTIONS &amp; THEIR POSSIBLE ROLE IN BACTERIAL CHEMOTAXIS

Leela Kar<sup>†</sup>, Philomen Z. de Croos<sup>†</sup>, Michael E. Johnson<sup>†</sup> and Philip Matsumura<sup>‡</sup>

Departments of <sup>†</sup>Medicinal Chemistry & Pharmacognosy and <sup>‡</sup>Biological Sciences  
University of Illinois at Chicago, Chicago, IL 60680.

Signal transduction in bacterial chemotaxis involves the products of the CheA, CheW, CheY and CheZ genes. It has been shown *in vitro* that the CheA protein is autophosphorylated in the presence of ATP and the phosphorylated product can, in turn, phosphorylate the CheY protein. The current biochemical model of signal transduction in bacteria suggests that the transfer of the phosphate group from CheA to CheY activates the CheY protein, allowing it to interact with the flagellar basal body and hence influence the sense of rotation of the motor. We have used <sup>1</sup>H- and <sup>31</sup>P-NMR to study the interaction of CheY with ATP and other related molecules. Our results indicate that CheY is capable of binding to a variety of phosphate containing compounds and will remove the terminal, ester linked phosphate group from the bound substrate. Neither the phosphate binding nor the phosphate cleavage by CheY is found to be specific for adenine. Spin label induced resonance suppression has been used in 2D-Double Quantum Filtered COSY experiments to identify amino acid residues close to the bound phosphate. This information is being used in conjunction with 2D-NOESY and TOCSY data to obtain sequential assignments for these residues and to define the stereochemistry of the phosphate binding site(s). Initial analysis of a number of CheY mutants with reduced levels of phosphorylation indicates that there are at least two possible phosphorylation sites. The phosphate binding interactions of one such mutant protein are being characterized in order to determine whether the phosphate binding and phosphate cleavage properties of the wild type protein are related to its activation by phosphorylation in bacterial chemotaxis. Supported in part by National Institute of Health Research Grant AI18985 and a Chicago Heart Association Senior Fellowship to L.K.

W-Pos134 ASSESSING LINKED EQUILIBRIA BETWEEN PHOSPHATE AND CATIONS BY <sup>31</sup>P NMR

Herbert Halvorson and Ana Q. Vande Linde, Department of Pathology and NIH Center for Cerebrovascular Disease Research, Department of Neurology, Henry Ford Hospital, Detroit MI 48202

Phosphates interact, with varying degrees of strength, with many different cations. Potassium, magnesium and the proton are particularly pertinent to the intracellular environment. The interactions are readily monitored by observing changes in the chemical shift of the phosphorus affected. The difficulty in interpreting these observations arises from disagreement as to the appropriate "apparent" binding constant. Our approach has been to consider explicitly all the known complexes involving the three principal identifiable phosphates of the *in vivo* <sup>31</sup>P NMR spectrum (orthophosphate, phosphocreatine and ATP) and to formulate complete mass action expressions. Analysis of *in vitro* spectra, representing a broad array of conditions, by singular value decomposition reveals the significant species and their characteristic chemical shifts. The resulting truncated mass action expressions permit construction of an interpolating function, valid within the domain of the original data. Standard nonlinear estimation procedures can then extract estimates of intracellular concentrations from measured chemical shifts. Our estimate for normal human brain [Mg<sup>2+</sup>] is 0.3 mM, +/- 10%. Additional results and some limitations will be discussed.

W-Pos135 NMR STUDIES OF THE BOHR EFFECT IN THE REGULATORY SUBUNIT OF *E. COLI* ASPARTATE TRANS-CARBOAMOYLASE. P. C. Harkins, I. M. Russu and N. M. Allewell, Wesleyan University, Middletown, Connecticut 06457.

The allosteric properties of ATCase are strongly pH dependent and both the catalytic trimers ( $c_3$ ) and regulatory dimers ( $r_2$ ) exhibit Bohr effects upon ligand binding. A variety of approaches including kinetic studies, reaction microcalorimetry, potentiometry and modified Tanford-Kirkwood theory have been used to derive pK values of residues whose ionization is linked to ligand binding. Changes in the environment of three His residues of  $r_2$  upon ATP binding have also been demonstrated by <sup>13</sup>C NMR [Moore, A. C., Browne, D. T. (1980) Biochemistry 19, 5768]. We have begun to study the effects of pH on  $r_2$  by <sup>1</sup>H NMR. Studies to date indicate that several aromatic resonances which are resolved over the spectral region 6-9 ppm from DDS are sensitive to titration of the four His residues of  $r_2$  and/or pH-induced conformational changes. ATP alters several of these resonances and also induces specific changes in the ring-current shifted region of the spectrum ( $\pm 0.5$  ppm from DDS). Experiments to determine His pK values and their role in the Bohr effect, to characterize ATP and CTP binding sites and to use <sup>31</sup>P NMR to analyze changes in the ionization properties of these allosteric effectors on binding are continuing. Supported by NIH grant AM-17335.

**W-Pos136 INTERACTION OF POTENTIAL ANTISICKLING AGENTS WITH HEMOGLOBIN.  
F-19 NMR MEASUREMENTS**

Kumudini M. Meepagala, Bruce L. Currie and Michael E. Johnson. Department of Medicinal Chemistry and Pharmacognosy, University of Illinois at Chicago, Chicago, IL, 60680.

Several analogs of Phe and Trp have shown antigelation activity with sickle cell hemoglobin (HbS).

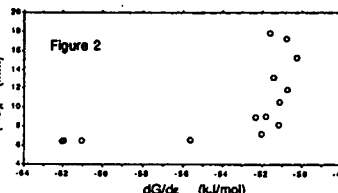
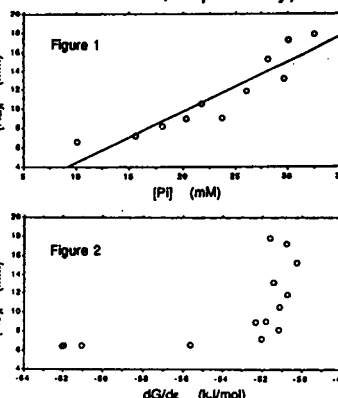
We have synthesized SL-Phe-tBu ester, SL-Trp-Trp, 5-F-Trp-Trp by standard procedures as probes for the investigation of mechanism and location of interaction of Phe and Trp derivatives with hemoglobin (Hb). We adopted F-19 NMR in our investigation to get conclusive evidence on the proximity of these compounds to the  $\beta$ -93 region. We F-19 labelled the hemoglobin at the  $\beta$ -93 position with a CF<sub>3</sub>COCH<sub>2</sub> group. In the presence of SL-Phe-tBu ester and SL-Trp-Trp, the F-19 resonance showed an enhancement of the transverse relaxation time compared to TEMPO, which suggests a specific interaction with Hb. The enhancement effects were more pronounced with deoxy HbA than with carbonmonoxy Hb. This indicates that these compounds bind in close proximity to the  $\beta$ -93 region.

(Supported in part by NIH grant HL23697.)

**W-Pos137 INHIBITION OF Na<sup>+</sup> PUMP IN ISCHEMIC GUINEA PIG MYOCARDIUM.** Laura C. Stewart, Luce Vander Elst and Joanne S. Ingwall; NMR Lab for Physiol. Chem., Brigham and Women's Hospital, Boston, MA.

Na<sup>+</sup>,K<sup>+</sup>-ATPase activity is the primary determinant of the transsarcolemmal Na<sup>+</sup> gradient. It has been shown *in vitro* that decreased pump activity can be attributed to a combination of decreased substrate (ATP) availability and/or direct inhibition by ADP or Pi (ADP and Pi are non-competitive inhibitors at ~0.1-2.0 mM and 10-20 mM, respectively).

To test whether ADP or Pi, or both, contribute to Na<sup>+</sup> pump inhibition in intact guinea pig hearts, we perturbed concentrations of intracellular sodium ([Na]<sub>i</sub>) and ATP hydrolysis products by imposing 56 min global ischemia. We used <sup>31</sup>P NMR to define changes in pH, [ATP], [CrP], [Pi] and <sup>23</sup>Na NMR in combination with the shift reagent Dy(TTHA)<sup>3-</sup> to define changes in [Na]<sub>i</sub>. There are concomitant changes in [ATP], [Pi] and [Na]<sub>i</sub>: 10 fold decrease in [ATP]; 30-fold increase in [Pi]; 3-fold increase in [Na]<sub>i</sub>. [Na]<sub>i</sub> increases linearly with increasing [Pi] (Fig 1). In contrast, [ADP], calculated from the creatine kinase equilibrium, shows only a transient, 5 fold increase and there is no correlation between [ADP] and [Na]<sub>i</sub>. The plot of the free energy change of ATP hydrolysis, dG/dc versus [Na]<sub>i</sub> (Fig 2) shows little variation in [Na]<sub>i</sub> until the dG/dc reaches a threshold value of -52 kJ/mol. We conclude that the energetic changes (as defined by dG/dc) are sufficient to explain the increase in [Na]<sub>i</sub>. These results also suggest that despite the high K<sub>i</sub> for Pi the Na<sup>+</sup> pump is inhibited primarily by Pi in ischemic myocardium.



**W-Pos138 PARVALBUMIN: METAL-ION INDUCED CONFORMATIONAL CHANGES AS PROBED BY NMR MONITORED LANTHANIDE EXCHANGE.** Thomas C. Williams\* and Brian D. Sykes, MRC Group in Protein Structure and Function, Department of Biochemistry, University of Alberta, Edmonton, Alberta, Canada T6G 2H7, and \*Department of Pharmacology, Medical University of South Carolina, Charleston, SC 29425.

Within the *helix-loop-helix* class of calcium-binding proteins, the correlation between structure and function is best understood for parvalbumins, 108-residue proteins having two high affinity calcium/magnesium sites. In order to evaluate the charge-density specificity of such sites, the largest lanthanide analogue of calcium, La(III), and the lanthanide analogue of magnesium, Lu(III), have been used to prepare two diamagnetic analogues of Ca-pike(III)parvalbumin. By using one- and two-dimensional proton NMR spectroscopy, we have assigned 66 of the 91 detectable mainchain HN-C( $\alpha$ H) correlations in Ca-pike(III)parvalbumin and both metal-binding sites of each lanthanide form. Local conformational perturbations arising from calcium to-lanthanide metal-ion exchange have been evaluated from the changes in the COSY and NOESY spectra. To better understand the global conformational changes associated with metal-ion exchange in parvalbumin and larger proteins of this class, site-selective exchange by paramagnetic lanthanides has also been used. Paramagnetic contributions to the chemical shift and relaxation of several assigned NMR resonances have been determined in order to begin to evaluate paramagnetically shifted spectra of parvalbumin in terms of its solution conformation.

**W-Pos139 INFLUENCE OF MOLECULAR GEOMETRY ON UNCERTAINTY IN NOE DETERMINED DISTANCES.**  
Steven B. Landy and B. D. Nageswara Rao, Physics Department, IUPUI, P.O. Box 647, Indianapolis, IN 46223

The initial-slope and full relaxation-matrix methods of extracting internuclear distances from NOE data are examined with special emphasis on the effect of the geometrical arrangement of the spins on the accuracy of the ratios of distances determined. The errors are influenced by molecular geometry because the elements of the dipolar relaxation matrix, which governs the NOE, are proportional to the sharply varying function  $r_{ij}^{-6}$  of the distance  $r_{ij}$  between the different pairs of spins  $i$  and  $j$  in the molecule. The source of geometric error may be understood in terms of the relationship of molecular conformation to the relative sizes of the eigenvalues of the NOE relaxation matrix. If these eigenvalues differ greatly in magnitude, large distance errors may result. It is shown that for certain molecular geometries the distance between spins may be accurately measured by either method, while some geometries require the full matrix analysis for accuracy. There are a few structures which cannot be resolved by either procedure. These distinctions are revealed by an analytical solution for the homonuclear NOE in an isotropically tumbling three-spin system in the limit of long correlation time. This solution was utilized to obtain computer simulation of the NOE for a variety of geometrical arrangements. Contour maps are presented to depict the errors in the distances as well as the distance ratios determined from NOE. These error contours indicate exactly which structures are resistant to NOE analysis.

Work supported by NSF DMB 8608185.

**W-Pos140 Conformational Analysis of Restricted Peptide Turn Mimetics by NMR and Molecular Modeling Techniques.** Y.-H. Lee<sup>1</sup>, M. Kahn<sup>2</sup>, and M.E. Johnson<sup>1</sup>. Department of Medicinal Chemistry & Pharmacognosy<sup>1</sup> and Chemistry<sup>2</sup>, University of Illinois at Chicago, Chicago, Illinois 60680

Peptides and proteins play critical roles in the regulation of virtually all biological processes, yet a detailed analysis of these events at the molecular level remains in its infancy. We have designed conformationally restricted nonpeptide mimetics of peptide beta and gamma turns, to investigate the relationship between peptide structure and function.

Two-dimensional nuclear magnetic resonance techniques were used to elucidate the solution conformations of the mimetics through the measurements of coupling constants and dihedral angles. Computer assisted molecular modeling with the molecular dynamics and energy minimization methods was used to compare the predicted low energy conformers of the turn mimetics with the X-ray structures of corresponding peptides and proteins. The high agreement shown between the conformations predicted from both NMR and molecular modeling studies indicates that the restricted ring structures will provide excellent foundations for the development of a variety of protein turn mimetics.

**W-Pos141 EFFECT OF TEMPERATURE AND BUFFER CONCENTRATION ON THE PRESERVATION OF HUMAN ATRIAL APPENDAGES:  $^{31}\text{P}$  AND  $^1\text{H}$  NMR STUDIES.**

S. Lareau, R. Deslauriers, M. Campredon, W. J. Keon<sup>+</sup> and G. W. Mainwood\*. Division of Biological Sciences, National Research Council of Canada, Ottawa, Ont. K1A OR6;

\*Department of Cardiothoracic Surgery, University of Ottawa Heart Institute, Ottawa, Ont. K1Y 4E9; \*Department of Physiology, University of Ottawa, Ottawa, Ont. K1H 8M5,

In order to determine optimal preservation conditions, we have measured changes in intracellular ATP and pH, together with lactate production, in isolated ischemic human atrial tissue. The measurements were made using  $^{31}\text{P}$  and  $^1\text{H}$  NMR. ATP preservation in NaCl 0.9% is improved as temperature is reduced from 20°C to 1°C due to a progressive decrease in energy demand. At 12°C, ATP preservation is improved by increasing the extracellular buffer capacity with PIPES buffer at concentrations up to 100 mM. At this temperature, energy demand is higher than at 1 or 4°C but the ATP level is kept relatively constant for periods of 10 hours or longer. This appears to be due to a tighter regulation between supply and demand in which glycolysis is driven faster at relatively lower ADP and Pi levels. This tight regulation may be attributed to the better maintenance of intracellular pH. Preliminary results indicate that decreasing of the temperature to 4°C interferes to some extent with ATP preservation at high buffer concentration. Work is in progress to explain these results.

**W-Pos142** 3-(TRIMETHYLSILYL)-1-PROPANE-SULFONIC ACID(TMSPS) AT OR BELOW 3mM DOES NOT IMPAIR HOG

CAROTID ARTERY MECHANICS OR PHOSPHORUS METABOLISM. J.F.Clark and P.F.Dillon, Departments of Physiology and Radiology, Michigan State University, East Lansing, MI 48824.

TMSPS is a molecule which has been used as an  $^1\text{H}$  and  $^{13}\text{C}$  NMR frequency marker in aqueous solutions. Because of its similar structure to TMS, TMSPS's 0.0 ppm peak is easily visible at relatively low concentrations. In this study we wished to determine if TMSPS can be used as a non-toxic frequency marker for hog carotid arteries. TMSPS is visible in  $^1\text{H}$  spectra of the isolated perfused carotid artery.  $^{31}\text{P}$  NMR was used to monitor the high energy phosphate metabolism. Separate muscle mechanics experiments monitored maximal force development of carotid strips at 37°C. The strips were stimulated with 75mM  $\text{K}^+$  PSS first to get maximal control tension, then stimulated in the presence of 0, 0.5, 1, 3, and 10mM TMSPS sequentially. NMR experiments were done on a Bruker 9.4 Tesla spectrometer.  $^{31}\text{P}$  NMR experiments consisted of 1800 1 second scans at 37°C. The results of the mechanics showed no significant change in force for TMSPS at 3mM or less. At a concentration of 10mM there was a significant decrease in percent maximal tension to  $0.94 \pm .02(\text{SD})$  of control(n=4).  $^{31}\text{P}$  NMR showed that 6mM TMSPS decreased the phosphocreatine(PCr) concentration to  $0.82 \pm .04(\text{SD})(n=3)$  of the control value at rest and decreased PCr to  $0.59 \pm .11(\text{SD})(n=3)$  of control during  $\text{K}^+$  contractures. The conclusions of this study are that below 3mM TMSPS does not significantly effect the maximal force of artery strips and that TMSPS is less useful above 6mM due to a reduction in both tension and PCr concentration. Supported by USPHS grant AM 34885.

**W-Pos143** COMPARISON OF THE 3 NITROGENASE ENZYMES SYNTHESIZED BY *AZOTOBACTER VINELANDII*. Brian J. Hales, Patricia L. Bounds and Kathleen A. Scorsone, Department of Chemistry, Louisiana State University, Baton Rouge, LA 70803

It is now well known that the bacterium, *Azotobacter vinelandii*, possesses the ability to synthesize three distinctly different nitrogenases. All of these enzymes are similar in that they are two protein enzymes with one of the proteins, called the Fe-protein or component 2, being highly conserved. The second protein, called component 1, is felt to contain the site of substrate reduction and is also the more different protein in the three enzyme systems. The best known and most studied of the three nitrogenases, sometimes referred to as the conventional enzyme, was first isolated over 20 years ago and shown to have a component 1 which contained both Mo and Fe. The subsequent isolation of nitrogenase from many diverse bacteria has shown that the enzyme is highly conserved and always contains Mo. This situation existed until 1986 when a second, or alternative, nitrogenase was isolated<sup>1</sup> and found to contain vanadium instead of Mo. It was recently shown<sup>2</sup> that there exists a third form of the enzyme which contains neither Mo nor V. We have observed that growing *A. vinelandii* in the presence of Mo, V, W and Re induces the three different enzymes each with a metal composition dependent on the metal in the growth medium. These different enzyme forms will be compared.

1. Robson, R.L., Eady, R.R., Richardson, T.H., Miller, R.W., Hawkins, M., and Postgate, J.R. (1986) *Nature (London)* **322**, 388; Hales, B.J., Case, E.E., Morningstar, J.E., Dzeda, M. F., and Mauterer, L.A. (1986) *Biochemistry* **25**, 7251.
2. Chisnell, J.R., Premakumar, R., and Bishop, P.E. (1988) *J. Bacteriol.* **170**, 27.

**W-Pos144** INVESTIGATION OF THE FREE SULPHYDRYL ENVIRONMENTS OF PLASMA FIBRONECTIN BY ESR SPECTROSCOPY. C. Narasimhan, J.-J. Yin and C.-S. Lai, National Biomedical ESR Center, Medical College of Wisconsin, 8701 Watertown Plank Road, Milwaukee, WI 53226.

Human plasma fibronectin (pFn) is a glycoprotein consisting of two subunits of about 250-kDa each. The subunits are linked together by two disulfide bridges near the carboxyl termini. pFn is a multi-functional protein that plays important roles in cell adhesion, wound healing, phagocytosis and aging. In this study, the free sulphydryl environments of pFn were investigated by both spin-probe - spin-label and saturation recovery pulse ESR methods.

The two free sulphydryl groups per chain of pFn were labeled with an  $^{15}\text{N}^2\text{H}$ -maleimide spin label. The conventional X-band ESR spectrum of the labeled protein revealed a single strongly immobilized component with an effective rotational correlation time of about 17 nanoseconds, suggesting that the two labeled sites per chain cannot be distinguished by line-shape analysis. We then used saturation recovery ESR to measure directly the spin-lattice relaxation time( $T_1$ ) of the labeled protein at 22°C. The time evolution of the signal was found to be biphasic, consisting of two  $T_1$  values, 1.4 and 4.5 usec. The results obtained using pFn fragments showed that the 1.4 usec component is associated with the label attached onto the sulphydryl near the cell-binding domain and the 4.5 usec component is associated with the label attached onto the sulphydryl near the carboxyl terminus. The data presented here suggest that the saturation recovery ESR is a sensitive technique for differentiating two labeled sites that undergo similar rates of rotational motion at least near the slow tumbling time regimes. The solvent accessibility as well as the relative hydrophobicity of the labeled sites that may account for the observed differences in  $T_1$  will be discussed.

**W-Po145 STUDIES OF THE MOLECULAR INTERACTION OF PHE AND TRP ANALOGS WITH HEMOGLOBIN USING  $^1\text{H}$ NMR AND EPR TECHNIQUES**

Chung Jeing Yuan, Philomen Z. de Croos, Bruce L. Currie and Michael E. Johnson. Department of Medicinal Chemistry and Pharmacognosy, University of Illinois at Chicago, Chicago, IL 60612.

Sickle cell anemia is a genetic disease resulting from a mutation that produces a substitution of a valine residue for a glutamic acid residue at position  $\beta$ 6. This change from a polar acidic side chain in normal adult hemoglobin (HbA) to a nonpolar side chain in sickle hemoglobin (HbS) leads to aggregation of deoxygenated HbS molecules to form long helical fibers, also known as gelation. Phenylalanine and tryptophan and some analogs are known antigelation compounds. Their mechanism of inhibition of gelation has been investigated. We have synthesized nitroxide spin-labeled- L-Phe, -Trp and -Trp-Trp as probes to monitor the interaction of Phe and Trp analogs with hemoglobin. We have used transverse relaxation NMR measurements on hemoglobin, in combination with distance calculations, to locate the position of the bound nitroxide of spin labeled compounds on the hemoglobin molecule. Using the relaxation data of the three assigned resonances,  $\beta$ 2,  $\beta$ 97 and  $\beta$ 146, we calculate the probable site of the bound nitroxide to be in a region near the N-terminal of the  $\beta$ -chain. The binding site of the aromatic moiety of the spin-labeled compound should be in the vicinity of this region. Competitive binding studies using EPR techniques indicate that SL-Trp-OH and SL-Trp-Trp-OH are quantitatively displaced by 5-Br-Trp and Trp-Trp, two relatively active antigelation compounds. Thus, both spin-labeled and non-spin-labeled compounds are inferred to bind at the same binding site.

**W-Po146 STUDIES OF THE ORIENTATION OF DOXYL-2-SPIRO-4'-PIMELATE COVALENTLY BOUND TO A SPECIFIC SITE IN THE EXTRACYTOPLASMIC DOMAIN OF THE ANION EXCHANGE CHANNEL (BAND 3) IN INTACT HUMAN ERYTHROCYTES.** J.E. Nieves, A.H. Beth, P.S.R. Anjencyulu, and J.V. Staros. Departments of Biochemistry and Molecular Physiology and Biophysics, Vanderbilt University School of Medicine, Nashville, TN 37232.

The Anion Exchange Channel (Band 3) is a dimeric integral protein in the erythrocyte membrane and is responsible for the transmembrane exchange of  $\text{CO}_2$  (as bicarbonate) for chloride. This transmembrane protein is also known to be a major point of attachment of the membrane with the cytoskeleton, and as such is implicated in the maintenance of erythrocyte shape and elastic deformability.

It is our intention to develop a rotational diffusion model to describe the motion of Band 3 in the erythrocyte membrane. Our laboratories have developed membrane impermeant bifunctional nitroxide spin labeling reagents which selectively react with Band 3 in intact erythrocytes allowing study of its motion by Linear and Saturation Transfer (ST) EPR. Fitting the ST-EPR data to a relevant rotational diffusion model requires knowledge of the orientation of the nitroxide principal axes relative to the membrane normal axis and ultimately to Band 3 itself. Orientation studies, in turn, require knowledge of cell shape. Since ATP depletion is known to be related to the loss of the biconcave shape of the erythrocyte,  $^{31}\text{P}$  NMR studies were employed to develop a buffer system where the intracellular ATP pool is maintained at a high level for up to 9 hrs. We are currently developing a method for the preparation of stacked monolayer samples of erythrocytes. Such fully oriented samples will allow the collection of orientation data necessary to model the intrinsic motion of the label. This model will be used to study the effects of physiological perturbations which alter the shape and deformability of the cell on the dynamics of Band 3 in an effort to better understand the molecular basis for the maintenance of shape and for the elastic deformability of the erythrocyte. Supported by: NIH DK31880 and HL34737.

**W-Pos147 HIGH PRESSURE-FLUORESCENCE STUDIES OF TRP REPRESSOR SUBUNIT INTERACTIONS.**

Terry Harrigan\*, Catherine A. Royer\* and Kathleen S. Matthews#. Dept. of Biochemistry and Laboratory for Fluorescence Dynamics, Dept. of Physics, University of Illinois at U-C, Urbana, IL 61801 and #Dept. of Biochemistry, Rice University, Houston, TX 77251.

A combination of high pressure and fluorescence techniques are being used to determine the role of subunit interactions in a DNA binding protein, trp repressor. The effects of corepressor and operator DNA on the subunit interactions are being examined. Polarization of dansylated trp repressor and average emission energy of intrinsic tryptophan fluorescence of trp repressor show large, reversible, concentration-dependent changes upon the application of hydrostatic pressure. These results indicate significant dissociation of the protein subunits below 2 kbar of pressure at micromolar concentrations of protein. The observed large decrease in intrinsic tryptophan average emission energy indicates increased solvation of the intrinsic tryptophans in the dissociated form of the protein. Addition of excess corepressor, tryptophan, appears to influence the subunit interactions as indicated by the observed changes in the dissociation profile. Operator binding measured using gel mobility shift assays shows negligible changes in affinity caused by pressurization of trp repressor. Addition of operator in the presence of excess tryptophan results in dissociation at higher pressures than observed when tryptophan is absent. This indicates that the anticipated stabilization of the trp repressor-operator complex in the presence of tryptophan occurs. Supported by NIH grants GM39969, RR03155 (TH, CR) and GM22441 (KSM).

**W-Pos148 MECHANISM OF TRYPTOPHAN FLUORESCENCE QUENCHING BY OXIDIZED DITHIOTHREITOL.** Enoch Kim,  
Faith M. Thompson and Gautam Sanyal. Department of Chemistry, Hamilton College, Clinton, NY 13323.

The quenching of tryptophan (W) fluorescence by oxidized dithiothreitol (DTT<sub>O</sub>) was studied by measuring fluorescence intensities (F), quantum yields and lifetimes ( $\tau$ ) of model compounds and peptides. N-acetyl-L-tryptophanamide (NATA) and mastoparan X, a 14-amino acid residue peptide containing a single W (W3), exhibited almost identical DTT<sub>O</sub> concentration dependence of quenching. Stern-Volmer plots of F<sub>0</sub>/F versus (DTT<sub>O</sub>) (where F<sub>0</sub> is the initial fluorescence in the absence of DTT<sub>O</sub>) were linear up to 4 mM DTT<sub>O</sub> and the inverse of the slope (1/K<sub>sv</sub>) was 2.4 mM in both cases at T=21° C and pH = 7.0. Multiple frequency phase-modulation fluorometry was used in the frequency range of 20–200 MHz to measure  $\tau$  of NATA and mastoparan X, with and without DTT<sub>O</sub> ( $\tau$  and  $\tau_0$  respectively) for each sample. DTT<sub>O</sub> did not have any effect on  $\tau$  for either sample when added up to concentrations that quenched 65% of the steady-state F<sub>0</sub>, i.e.  $\tau / \tau_0 = 1$  when F/F<sub>0</sub> = 0.35. This provided direct evidence that quenching of W fluorescence by DTT<sub>O</sub> was static, i.e., it involved ground-state complex formation as opposed to dynamic collision in the excited state. The 1/K<sub>sv</sub> value of 2.4 mM thus represented an apparent dissociation constant (K<sub>d</sub>) for the NATA-DTT<sub>O</sub> and mastoparan X-DTT<sub>O</sub> complexes. Similar evidence for static quenching by DTT<sub>O</sub> of tryptophan and tyrosine fluorescence of proteins will also be presented. (Supported by PRF Grant 18076-GB4 and NIH Grant GM 37471 to GS).

**W-Pos149 Correlations Between Protein Dynamics and Fluorescence in Single Tryptophan Proteins**

Axelsen, P. H., Nollet, K. E., and F. G. Prendergast. Department of Biochemistry and Molecular Biology, Mayo Clinic and Foundation, Rochester Minnesota, 55905.

Molecular Dynamics Simulations of porcine phospholipase-A2 (PLA2), mellitin tetramer, and azurin (from *P. aeruginosa*) have been conducted in order to correlate their structural features with fluorescence observables. These proteins have single tryptophan residues which span the complete range of solvent accessibility, yet in each case the simulation predicted fluorescence anisotropy decay agreed well with experimentally determined limiting anisotropy.

Other observations include: TRP-3 on the surface of PLA2 does not invert or "flip" in simulations due to interactions with adjacent residues; Mellitin tetramer tends to dissociate and unravel except under special conditions of dielectric and counterion placement; The electrostatic potential in the plane of TRP-47 in azurin is steeply graded and negative, despite the nonpolar character of residues adjacent to TRP-47. The latter observation suggests that the relatively blue-shifted emission of TRP-47 may be due, at least in part, to a blue shift of TRP-47 absorption. Supported by GM 34847.

**W-Pos150 FLUORESCENCE STUDIES OF PHOSPHOFRUCTOKINASE FROM BACILLUS STEAROTHERMOPHILUS.**

S. J. Kim<sup>1</sup>, B. C. Valdez<sup>2</sup>, S. H. Chang, E. S. Younathan<sup>2</sup>, and M. D. Barkley<sup>1</sup>, Depts of Chemistry<sup>1</sup> and Biochemistry<sup>2</sup>, Louisiana State University, Baton Rouge, LA 70803

Phosphofructokinase is an allosteric enzyme that catalyzes one of the key regulatory steps in glycolysis. The enzyme from B. stearothermophilus (Bs-PFK) has 4 identical subunits of 34 kD each with a single tryptophan. We examined the properties of the lone tryptophan by time-resolved and steady-state measurements. The emission had a quantum yield of  $0.35 \pm 0.04$  with an emission maximum at 328 nm indicating a hydrophobic environment. The Stern-Volmer rate constants for acrylamide and KI quenching,  $9.8 \times 10^8 M^{-1} s^{-1}$  and  $1.7 \times 10^7 M^{-1} s^{-1}$  respectively, indicate almost no accessibility of the fluorophore to iodide. The steady-state anisotropy at 295 nm excitation wavelength is 0.18 suggesting that the tryptophan environment is fairly rigid. The fluorescence decay is best represented by a double exponential decay of 0.4, and 4.7 ns lifetimes with amplitudes of 15% and 85%, respectively. The possible association of the two lifetimes with the R and T conformations of the protein was investigated using an Arg-252 mutated enzyme with altered allosteric properties. The Arg-252 mutation results in enzyme kinetic characteristics similar to those of the T-conformation of the wild-type enzyme. (Supported by N.I.H. grants GM35009 and AM 31676.)

**W-Pos151 FLUORESCENCE AND SOLID STATE  $^2H$ -NMR STUDIES OF INTERNAL MOTIONS OF A TRYPTOPHAN DERIVATIVE.**

L. Tilstra, W. Stryjewski, M. D. Barkley, M. Vela, M. McLaughlin, Intr. by J. Nelson

A derivative of tryptophan in which rotation about  $C^\alpha-C^\beta$  and  $C^\beta-C^\gamma$  bonds is constrained has an apparent single exponential fluorescence decay. However, solution  $^1H$ -NMR resolves two conformers. The reason that two lifetimes are not resolved could be: (1) the conformers interconvert rapidly compared to the fluorescence emission, or (2) the lifetimes of the two conformers are nearly the same.

We have investigated internal motions in the constrained tryptophan by solid state  $^2H$ -NMR spectra. Motional averaging present in these powder patterns is resolved by line-shape analysis to determine kinetic information about internal motions that may cause isomerization. Results are reported as a function of temperature and the energetics of the transition are estimated. The possibility of a tunneling mechanism for isomerization is discussed. Fluorescence studies done under similar conditions support the relationship between conformation and lifetime. (Supported by NIH GM 35009)

**W-Pos152 INFLUENCE OF TRP DYNAMICS AND PROTEIN CONFORMATION ON THE FLUORESCENCE DECAY CHARACTERISTICS OF SN3 AND RNASE T1. S. Sedarous, J. Hedstrom, P. Axelsen, C. Haydock, and F.G. Prendergast, Dept. of Biochemistry and Molecular Biology, Mayo Foundation, Rochester, MN 55905.**

Scorpion neurotoxin variant 3 (SN3) and ribonuclease T1 (RNase T1) are single tryptophan proteins which exhibit distinct spectral properties. For SN3 in aqueous solvents, the average fluorescence lifetime is short (~500 ps). Using discrete exponent model functions, the fluorescence decay was best fit by a triexponential process. Use of a triexponential model function for a single tryptophan protein implies the existence of three distinct states. In contrast, the fluorescence lifetime of RNase T1 is monoexponential (4ns) for solutions at pH 5.5, but apparently biexponential at higher pH - implying two pH induced conformational states. Binding of 2'Guanosine monophosphate (2'GMP) to the RNase T1 active site at pH 5.5 shortens the fluorescence lifetime and leads to heterogeneous fluorescence emission decay. Although the trp side chain in SN3 is largely solvent exposed and that of RNase T1 is protected from solvent access, it appears that the dominant determinant of the lifetimes is the protein matrix judging from the effects of temperature, solvent viscosity, pH and wavelength on the measured lifetimes. Traditional interpretations of intramolecular quenching in terms of the Stern-Volmer formalism does not appear, from molecular dynamics simulations and molecular graphics depictions, to provide a satisfactory explanation of the measured lifetimes (cf. the model of Tanaka & Matage--Biophys. J. 51:487, 1987) and in RNase T1 it is difficult to reconcile the existence of two unique conformations at pH greater than 5.5. It is apparent that other mechanisms for the intramolecular quenching must be proposed. Supported in part by GM 34847.

**W-Po153 THE DISTINCT EFFECTS OF CALCIUM AND MAGNESIUM ON THE CONFORMATIONAL PROPERTIES OF PARVALBUMIN: A SPECTROSCOPIC STUDY.** Cindy M.L. Hutnik. Dept. of Biochemistry, University of Ottawa and Division of Biological Sciences, National Research Council of Canada, Ottawa, Ontario, Canada K1A 0R6.

Cod III parvalbumin was purified by an extended procedure and was shown to be homogeneous by a number of biochemical techniques. Steady-state and time-resolved fluorescence spectroscopy, as well as circular dichroism studies of this single tryptophan containing protein revealed that calcium, but not magnesium induced conformational changes in the apo- ( $\text{Ca}^{2+}$ -free) form. Results also demonstrated that the commonly used method of EGTA treatment resulted in incomplete protein decalcification. Further, the addition of excess  $\text{Mg}^{2+}$  to EGTA-treated parvalbumin promoted spectral changes which were not due to  $\text{Mg}^{2+}$ -protein binding. In contrast to previous reports, the fluorescence decay of the various forms of this parvalbumin was best described by three lifetime components whose values were determined by global analysis. Both the emission (DAS) and excitation (IEDAS) spectra associated with each temporal component were obtained. These spectroscopic results argue against the generally accepted notion that  $\text{Ca}^{2+}$  and  $\text{Mg}^{2+}$  induce identical perturbations in parvalbumin.

I would like to acknowledge the financial support of NSERC and would also like to acknowledge my supervisor Dr. A.G. Szabo, whose expertise pervades the work being presented.

**W-Po154 TYROSYL AND TRYPTOPHYL EMISSION FROM SUBTILISINS.** K.J. Willis and A.G. Szabo. Division of Biological Sciences, National Research Council of Canada, Ottawa, Canada K1A 0R6.

Subtilisin Carlsberg is an exception to Teale's general rule [Teale, F.W.J. (1960) *Biochem. J.* 76, 381-388] that in proteins which contain both tyrosine and tryptophan residues, the predominant contribution to the emission is from tryptophan [Longworth, J.W. (1971) in *Excited States of Proteins and Nucleic Acids* (Steiner, R.F. & Weinryb, I., Eds.) pp. 319-484, Plenum Press, New York]. The tyrosyl and tryptophyl fluorescence contributions of underivatized subtilisin Carlsberg and the homologous enzyme subtilisin BPN' were resolved. Steady-state and picosecond time-resolved measurements over the whole emission spectrum were performed at different excitation wavelengths. Data were analysed using global techniques and associated spectra of the exponential decay components were derived (DAS). Samples purified by a novel HPLC method and free of autolysis products were found to emit from both tyrosine and tryptophan at an excitation wavelength of 295 nm. There is some evidence in the Carlsberg enzyme for a small tyrosine contribution even at an excitation wavelength of 300 nm. Disagreement with literature values of subtilisin fluorescence parameters results from rigorous elimination of autolysis products from the samples.

**W-Po155 MEASUREMENTS OF LIFETIMES OF TYROSINE AND TYROSINATE FLUORESCENCE IN PROTEINS.** Marvin D. Kempler<sup>†</sup>, Salah Sedarous<sup>††</sup>, and Franklyn G. Prendergast<sup>††</sup>, <sup>†</sup>Dept. of Physics, IUPUI and <sup>††</sup>Dept. of Biochemistry and Molecular Biology, Mayo Foundation, Rochester, MN 55905.

Time-correlated photon counting was used to measure the lifetimes of tyrosine and tyrosinate fluorescence in some small molecules (tyrosine, O-methyl tyrosine, and N-acetyl tyrosine ethyl ester) and in several proteins ( $\alpha$ - and  $\beta$ -purothionins, crambin, and an ovomucoid). Of the proteins at pH 7, only the purothionins evinced the characteristic tyrosinate emission ( $\lambda_{\text{em}} \sim 350$  nm) while the other proteins showed characteristic tyrosine emission ( $\lambda_{\text{em}} \sim 305$  nm). Tyrosine emission could be evoked in the purothionins by denaturation or by proteolytic cleavage. Tyrosinate emission was induced in N-acetyl tyrosine ethyl ester in solutions at pH 13. The fluorescence spectra and lifetimes were measured in various protonated and deuterated solvents. To adequately describe the fluorescence emission decays, two or three exponential terms were normally required. The average lifetimes of the decays in the small molecules were found to be shorter for tyrosinate emission than for tyrosine emission. The reverse situation was found for the proteins. In particular tyrosine emission occurred with shorter average lifetimes in the various proteins than did tyrosinate emission. The mechanistic basis for the tyrosinate emission in the purothionins and for the very short lifetimes of the tyrosine fluorescence in crambin and the ovomucoid is unclear but may relate to the relative rates of deprotonation-reprotonation reactions. Discussion of the results in terms of the protein structures will be given. Supported in part by NIH grant GM34847.

**W-Pos156 A FLUORESCENCE SPECTROSCOPIC METHOD FOR DETERMINING BINDING OF  $\alpha$ -BUNGAROTOXIN (BGTX) TO SYNTHETIC PEPTIDES CORRESPONDING TO THE LIGAND-BINDING SITE OF THE NICOTINIC ACETYLCHOLINE RECEPTOR (AChR).** S. Frieda Pearce and Edward Hawrot, Department of Pharmacology, Yale University School of Medicine, New Haven, CT 06510

The binding of BGTx to 12mer and 18mer peptides corresponding to residues 185-196 and 181-198 of the  $\alpha$ -subunit of the AChR from *Torpedo* was observed by fluorescence spectroscopy. Emission spectra showed a complex time course. The spectra ( $\lambda_{ex}$  280 nm) when acquired at early times were accompanied by a fluorescent enhancement ( $\lambda_{em}$  340 nm) which remained constant for approximately 24hr. Over a period of 4-7 days, however, the spectra showed a loss of enhancement and a shift of the  $\lambda_{max}$  to 335 nm. Both the 12mer and the 18mer give rise to identical spectra at equilibrium after binding to BGTx. The time dependent changes in fluorescence may suggest structural binding intermediates. Nevertheless, the enhancement in fluorescence was used as a means of monitoring binding and of determining dissociation constants. Varying amounts of the synthetic peptide (12mer or 18mer) with concentrations ranging from 0.1 $\mu$ M to 100  $\mu$ M were added to a constant concentration of BGTx. The difference in fluorescence on each addition was noted and the dissociation constants were calculated from a plot of the increasing fluorescence vs. increasing concentration. Experiments where the peptide concentration was held constant and BGTx varied produced similar results. The affinity constants obtained were 1.4  $\mu$ M and 0.33  $\mu$ M for the 12mer and 18mer at pH 7, respectively. In previous studies using solid phase binding assays, binding constants on the order of 10-20  $\mu$ M were obtained for the 12mer and 18mer (Wilson et al., *Molecular Pharm.*, *in press*). The fluorescence method provides a relatively easy means of determining the affinity constants in solution and at various pH values. The lower affinity seen with solid phase assays suggests that structural flexibility may be involved in the binding mechanism. This data is important for the interpretation of NMR studies of the 12mer and 18mer where solution conformations are being determined at different pH values depending on the solubility of the peptides. Supported by the AHA, NIH grant GM32629 and training grant CA-09085.

**W-Pos157 DISSOCIATION OF HUMAN SEX STEROID-BINDING PROTEIN SUBUNITS BY HIGH HYDROSTATIC PRESSURE.** J.B. Alexander Ross<sup>1</sup>, Catherine A. Royer<sup>2</sup>, Philip H. Petra<sup>3</sup>, <sup>1</sup>Department of Biochemistry, Mount Sinai School of Medicine, New York, NY 10029, <sup>2</sup>Laboratory for Fluorescence Dynamics, University of Illinois, Urbana-Champaign, IL 61801, <sup>3</sup>Department of OB/GYN, University of Washington, Seattle WA 98195.

Human Sex Steroid-Binding Protein (hSBP), a homodimeric glycoprotein from serum, binds the steroids dihydrotestosterone (DHT), testosterone and  $17\beta$ -estradiol with association constants of about  $3 \times 10^9$  M $^{-1}$ ,  $1 \times 10^9$  M $^{-1}$ , and  $3 \times 10^8$  M $^{-1}$  (4°C), respectively. The results of several laboratories suggest that there is one steroid-binding site per dimer, and that calcium stabilizes the hSBP. Recently, we have shown that there are four metal-binding sites. To investigate the role of calcium in the hSBP subunit interaction and the free energy linkage between steroid binding and the subunit interaction, we examined the dissociation of dansyl-labelled hSBP by high hydrostatic pressures. 1-2 dansyl groups were covalently bound per monomer. Their fluorescence emission spectrum and average lifetime suggest that the dansyl labels are not completely exposed to the bulk solvent; the emission is shifted to the blue and has a longer fluorescence decay time than do model compounds in water. The decrease in the steady-state anisotropy of the dansyl group up to 2.4 kbar was completely reversible on the return to 1 bar. The pressure-induced change in the anisotropy is consistent with a monomer-dimer equilibrium. Greater than stoichiometric amounts of DHT shifts the dissociation to higher pressures. Whether in the presence of excess steroid (10 $^{-6}$  M DHT, 10 $^{-7}$  M hSBP) or stoichiometric amounts of DHT, removal of calcium with EGTA shifts the dissociation to lower pressures. The effect of EGTA is reduced in the presence of excess steroid. These results indicate that calcium and DHT are functionally-linked ligands which both affect the self-association of hSBP.

**W-Pos158 COMPARTMENTAL ANALYSIS APPROACH TO FLUORESCENCE ANISOTROPY OF PERYLENE IN VISCOUS SOLVENTS.** David W. Piston, Timothy Bilash and Enrico Gratton. Dept. of Physics, Lab. for Fluorescence Dynamics, University of Illinois at U-C, 1110 W. Green St., Urbana, IL 61801.

The fluorescence intensity and anisotropy decays of perylene in viscous solvents are investigated at several temperatures between -20°C and 35°C using frequency domain fluorometry. The anisotropy decay data are globally analyzed over the temperatures studied using a compartmental model. We outline a generalized compartmental model that can be used to calculate anisotropy decay arising from any type of interconversion that introduces a change in the fluorescence polarization (Piston and Gratton, *Biophys. J.*, 51, 88a (1987)). These interconversions can be excited-state reactions, rotational diffusion, "jump" motions, or any combination of processes that can be treated in a compartmental form. We also present the application of this compartmental model to the perylene molecule undergoing only rotational diffusion motions, and use it to globally fit the anisotropy decay data at various temperatures and viscosities. We fit directly to the physical quantities needed to define the compartments; for perylene, we need only three fitting parameters, two rotational diffusion constants and the average angle between the absorption and emission dipoles. In previous studies, four parameters were used to fit the anisotropy decay of perylene, that is, two rotational correlation times and two pre-exponentials. The results of this study are shown to be in agreement with previous measurements. Supported by NIH RR03155 and NSF PCM8403107.

**W-Pos159 NANOSECOND FLUORESCENCE AND EMISSION ANISOTROPY KINETICS OF FURA-2 IN SINGLE CELLS.** Susan M. Keating, Theodore G. Wensell<sup>1</sup>, Tobias Meyer and Lubert Stryer, Department of Cell Biology, Sherman Fairchild Building, Stanford University School of Medicine, Stanford, California 94305.

A microscope-based time-correlated single photon counting instrument was used to measure nanosecond fluorescence and emission anisotropy decays of the  $\text{Ca}^{2+}$  indicator dye fura-2 in single adherent cells. The results were compared with decays obtained in solution, with and without added  $\text{Ca}^{2+}$  or protein, as well as with those of suspensions of fura-2-loaded cells. The decay of  $\text{Ca}^{2+}$ -free fura-2 fluorescence displayed two components:  $f_1 = 0.49$ ,  $\tau_1 = 0.77$  ns,  $f_2 = 0.51$  and  $\tau_2 = 1.5$  ns (where  $f_i$  is the relative amplitude and  $\tau_i$  is the excited state lifetime). When fura-2 was saturated with  $\text{Ca}^{2+}$ , the decay became essentially single-exponential with lifetime  $\tau = 1.77$  ns. Nanosecond depolarization measurements of both fura-2 and its  $\text{Ca}^{2+}$  complex displayed the subnanosecond anisotropy decay expected for a small molecule in aqueous solution. Fura-2 loaded into rat basophilic leukemia cells (using the ester) displayed altered fluorescence and anisotropy decays. A longer-lived component than either the  $\text{Ca}^{2+}$ -bound or  $\text{Ca}^{2+}$ -free forms of fura-2 ( $\tau_2 = 2.3$  ns,  $f_2 = 0.82$ ) appeared in the fluorescence decay. The anisotropy decay could be fit to two components, with a rapid correlation time,  $\theta_1$  of 166 ps and a much longer one,  $\theta_2 > 100$  ns. When the cells were permeabilized with saponin the anisotropy decays returned to those characteristic of the free dye. Results with single adherent cells were in agreement with those obtained with the cell suspensions, although the relative amplitudes and decay constants varied somewhat from cell to cell. These results indicate that fura-2 binds to macromolecular components in these cells, and that binding significantly alters its fluorescence properties. They also demonstrate that time-resolved pulsed-laser fluorescence microscopy can provide valuable information about the environment and mobility of fluorescent probes in single cells. Supported by NIH grants AR07803 to S.M.K., EY05815 to T.G.W. and GM24032.

1. Present address: Dept. of Biochemistry, Baylor College of Medicine, One Baylor Plaza, Houston, TX 77030.

**W-Pos160 Fluorescence Investigation of the Steroid-Binding Site of Human Sex Steroid-Binding Protein Using the Estrogen  $17\beta$ -Dihydroequilenin.** Lisa Galati<sup>1</sup>, Paul Brian Contino<sup>1</sup>, William R. Laws<sup>1</sup>, Philip H. Petra<sup>2</sup>, and J.B. Alexander Ross<sup>1</sup>, <sup>1</sup>Department of Biochemistry, Mount Sinai School of Medicine, New York, NY 10029, and <sup>2</sup>Department of OB/GYN, University of Washington, Seattle, WA 98195.

Human Sex Steroid-Binding Protein (hSBP) is a 90,000 M<sub>r</sub> protein comprised of two subunits with identical amino acid sequences. The homodimer appears to have a single steroid-binding site and four calcium-binding sites. Previous studies of the steroid-binding site using equilenin indicated that the environment was hydrophobic but contained a group(s) capable of hydrogen bonding with the 3'-hydroxyl of the estrogen.  $17\beta$ -Dihydroequilenin ( $17\beta$ -DHE) is a better steroid probe than equilenin because both its hydrogen-bonded and ionized forms have higher fluorescence quantum yields, and it has a higher affinity for hSBP. The maxima of the absorption and fluorescence excitation spectra of  $17\beta$ -DHE are shifted to the red in toluene (340 nm) compared to cyclohexane (338 nm); in water (pH 6), the maximum is the same as for hexane but the spectral envelope is broader. Upon addition of triethylamine (TEA) to  $17\beta$ -DHE in either cyclohexane or toluene, the spectra are shifted to 343 nm and they become essentially identical. Ionization of the 3'-hydroxyl group in water (pH 12) results in a broad absorption/excitation with a maximum at 360 nm. The protein-bound steroid has an excitation maximum near 346 nm. The emission maximum of the steroid in organic solvents and in water (pH 6) is near 360 nm. Addition of TEA to the steroid in cyclohexane shifts the emission to 370 nm. Basic pH (ionization) and TEA in toluene shifts the emission out to 420 nm. The emission of hSBP-bound  $17\beta$ -DHE is at 378 nm and resembles the TEA/cyclohexane environment. Thus, the shifted excitation spectrum indicates that the protein-complexed steroid is hydrogen bonded, and the emission spectrum indicates that this interaction is not changed in the excited state.

**W-Pos161 SPECTROSCOPIC STUDIES OF FLUORESCENT DERIVATIVES OF *E. coli* SINGLE-STRANDED DNA-BINDING (SSB) PROTEINS AND THEIR COMPLEXES WITH POLY(DEOXYTHYMIDYLIC) ACID.** Jose R. Casas-Finet<sup>1</sup>, Su-Yau Mao<sup>2</sup>, John W. Chase<sup>3</sup>, and August H. Maki<sup>1</sup>. (1) Department of Chemistry, University of California, Davis, CA 95616, (2) Department of Biophysics and Medical Physics, University of California, Berkeley, CA 94720, and (3) Department of Biochemistry, Case Western Reserve University, School of Medicine, Cleveland, OH 44106. (Intr. by Kenneth H. Downing)

The fluorescent probe, 6-acryloyl-2-(dimethylamino)naphthalene (acrylodan) was reacted with *E. coli* and F-plasmid SSB proteins. Acrylodan bound covalently to the single cysteinyl residue of FSSB, and to *E. coli* SSB mutants containing single Cys at positions 70 or 87. The labeled proteins all have about 1 fluorophore molecule per protein molecule and maintain high affinity for single-stranded polynucleotides. The emission spectra of conjugated proteins were blue-shifted relative to those of the 2-mercaptoethanol or cysteine adducts, indicating that acrylodan experiences a less polar environment in the proteins. This was accompanied with high quantum yields compared to cysteine adduct in aqueous buffer. Denaturation of protein-acrylodan conjugates resulted in a red shift of the emission spectrum, which means the Cys residue became exposed to the aqueous medium in the denatured proteins. Binding of poly(deoxythymidylic) acid [poly(dT)] to FSSB or *E. coli* SSB fluorescent derivatives led to the following modifications: (1) a blue shift (1 to 10 nm) of emission peak, (2) an increase of quantum yield by 30 to 50%, (3) a red shift (2 to 4 nm) and a narrowing of excitation peak, (4) lower sensitivity to collisional quenching caused by potassium iodide, and (5) a decrease of pseudo-first order reaction rate of acrylodan conjugation to Cys residue. These modifications were interpreted by shielding of Cys residue to a more hydrophobic environment when poly(dT) binds to these proteins. However, binding of the oligonucleotide (dT)<sub>8</sub> to FSSB or *E. coli* SSB(Cys70) resulted in an increase of the acrylodan conjugation rate and higher sensitivity to potassium iodide quenching. This suggests a protein conformational change induced by (dT)<sub>8</sub> binding which renders the fluorescent probe more accessible to the solvent.

This work was supported in part by NIH grants AI-19605, GM-11301, CA-13330, and ES-02662.

**W-Pos162 THE USE OF  $Gd^{+3}$  FLUORESCENCE AS A PROBE TO WATER COORDINATED TO BIOMOLECULES**  
 I. E. T. Iben,<sup>a</sup> R. B. MacGregor, E. Shyamsunder, M. Stavola, and J. M. Friedman<sup>a</sup>  
 a. AT&T Bell Laboratories, Murray Hill, NJ b. Princeton University, Princeton, NJ

Relatively little is known about the structure and dynamics of the interface between water and biological materials. A probe of the structure of water is the fluorescence of rare earth (RE) ions. In the fluorescence spectrum of the RE ion, weak vibronic bands have been observed that are due to interactions that couple the RE electronic transitions to the vibrational transitions of the ion's ligands. For aqueous solutions of Gd salts a hydration layer is formed about the  $Gd^{+3}$ . Excitation of the state  $Gd^{+3}({}^1P_1)$  with light at  $\sim 275\text{nm}$  is followed by non-radiative relaxation to the  $({}^3P_{1/2})$  state from which fluorescence to the  $({}^3S_{1/2})$  state occurs. In addition to the electronic emission, a vibronic band  $\sim 400$  times weaker is observed at the electronic transition energy less the OH stretch frequency  $\nu(\text{OH})$ , and is ascribed to the complexed water.\* Because the fluorescence lifetime of  $Gd^{+3}$  is relatively long,  $\sim 2\text{ms}$ , fast fluorescence and Raman signals can be gated away.

$Gd^{+3}$  is a promising probe for biological materials in that it binds to the same sites as does  $Ca^{+2}$ .  $Ca^{+2}$  binds to the head groups of many lipids, to proteins, and to DNA molecules. Measurements of  $\nu(\text{OH})$ , via the side band of  $Gd^{+3}({}^3P_1)\rightarrow Gd^{+3}({}^3S_{1/2})$  should yield valuable information on the coordination of water to the surface of these biological materials. In addition, the vibration of ligands other than water can be observed to give further information about the RE ion's binding sites. The application of this technique to proteins, lipids and nucleic acids will be addressed. \*Stavola, M., Friedman, J. M., Stepnoski, R. A., and Sceats, M. G., Chem. Phys. Letters, 80 (1981).

**W-Pos163 SITE-SPECIFIC VARIANTS OF ONCOMODULIN PROBED BY EUROPIUM LUMINESCENCE.** Edward R. Birnbaum, William A. Palmisano, Thomas W. Hurd, and Michael T. Henzl, Dept. of Chem., New Mexico State Univ., Las Cruces, NM

Although the aligned sequences of oncomodulin and parvalbumin from rat are identical at 55 of 108 positions, the two proteins exhibit significant structural and functional differences. For example, the CD site of parvalbumin displays affinity for both  $Ca^{2+}$  and  $Mg^{2+}$  under physiological conditions, whereas the CD site of oncomodulin is specific for  $Ca^{2+}$ . To explore the molecular basis for this difference in protein behavior, we have replaced the oncomodulin codon with the corresponding codon from parvalbumin at several points of nonidentity via oligonucleotide-directed mutagenesis. The luminescent lanthanide ion  $Eu^{3+}$  represents a potentially valuable probe of our site-specific variants, inasmuch as the  $Eu^{3+} 7F_0 \rightarrow 5D_0$  excitation spectra of oncomodulin and parvalbumin differ appreciably in appearance and pH-dependence (JBC 263, 10674-10680). Whereas the  $Eu^{3+}$  spectrum of rat parvalbumin at pH 5.0 displays features at  $5792\text{\AA}$  and  $5796\text{\AA}$ , the contributions of the CD and EF binding domains are unresolved in the oncomodulin spectrum at that pH. Moreover, the oncomodulin spectrum undergoes a pH-dependent transition with an apparent  $pK_a = 6.0$ , while the corresponding transition occurs with a  $pK_a$  of 8.2 in parvalbumin. We find that replacement of aspartate 59 of oncomodulin by glutamate, the residue present in parvalbumin, affords a protein (D59E) that more closely mimics the spectroscopic behavior of the latter -- exhibiting features at 5790 and 5796 at pH 5.0 and displaying a  $pK_a$  of 6.75 for the spectral interconversion. Simultaneous replacement of aspartate 59 and glycine 60 with glutamate residues yields a protein (D59E, G60E) having a spectroscopic signature even more reminiscent of parvalbumin.

**W-Pos164 BIOPHYSICAL APPLICATIONS OF PULSED-LASER PHOTOACOUSTIC CALORIMETRY.**

Jeanne Rudzki Small, Louis J. Libertini and Enoch W. Small  
 Department of Biochemistry & Biophysics, Oregon State University, Corvallis, OR 97331-6503.

Time-resolved photoacoustic calorimetry measures the heat released by photoexcited molecules as they relax back to the ground state. The technique is thus complementary to fluorescence in that it provides information on alternate, non-luminescent channels for the decay of excited states. We have shown how the Marquardt analysis method used in time-domain, fluorescence decay spectroscopy can be modified to allow rapid deconvolution of photoacoustic waveforms. This allows the determination of photoinduced enthalpic changes of a system, along with the kinetics of those changes. We are exploring the interface between fluorescence and photoacoustics to maximize the information extractable from spectroscopic studies of biological systems.

In addition to measuring enthalpic changes, the photoacoustic technique may be used to measure volumetric changes in proteins on fast (e.g. nsec) timescales. Applications of pulsed-laser photoacoustics to protein dynamics will be explored. The optimal methods for extracting volumetric information from waveform data will be discussed.

JRS acknowledges support from NIH (GM-10889), NSF (DMB-8707705), the Medical Research Foundation of Oregon and Tektronix, Inc. The work of EWS is supported by NIH (GM-25663).

**W-Pos165** SPECTRAL CHARACTERISTICS OF CADMIUM CONTAINING PEPTIDE COMPLEXES ISOLATED FROM THE FISSION YEAST SCHIZOSACCHAROMYCES POMBE. Donald J. Plocke, Biology Department, Boston College, Chestnut Hill, MA 02167 and Jeremias H.R. Kägi, Biochemisches Institut der Universität Zürich, CH-8057 Zürich, Switzerland

Phytochelatins, heavy metal containing peptides with the structures  $(\gamma\text{-Gly-Cys})_n\text{Gly}$ , where  $n=2-8$ , have been previously identified in higher plants and Schizosaccharomyces pombe. We have isolated several complexes of these peptides from S. pombe cells treated with 1 mM CdCl<sub>2</sub>. A lower molecular weight fraction from a Sephadex G-50 column yielded at least three distinct species when fractionated using DE52 cellulose. HPLC chromatography of three fractions revealed them to be composed of complexes of glutathione and PC<sub>1</sub> (phytochelatin with  $n=2$ ) in Fraction I, PC<sub>2</sub> and PC<sub>3</sub> in Fraction II, and PC<sub>2</sub>, PC<sub>3</sub> and PC<sub>4</sub> in Fraction III. Tentative stoichiometries are proposed for each of these complexes, based on analyses for Cd, -SH, inorganic sulfide, and amino acid content of the complexes and component peptides. All three complexes contain Cd, while Fractions II and III but not Fraction I contain inorganic sulfide. Although the UV absorption and MCD spectra of fractions II and III were nearly identical, the CD spectra of these two fractions were strikingly different. The CD spectrum of Fraction III resembled CD spectra previously reported for cadmium containing phytochelatins, with a positive band at 279nm and two negative bands at 259nm and 234nm, while the CD spectrum of Fraction II displayed a single negative CD band at 272nm and a positive band at 255nm. Compared to both Fractions II and III, the CD and MCD bands exhibited by Fraction I were extremely weak. Preliminary analyses of a higher molecular weight fraction from Sephadex G-50 indicated the presence of peptides with  $n$  values up to 7. These await further study.

**W-Pos166** INTERFACIAL STRUCTURE AND ACYL CHAIN ORIENTATION OF PHOSPHOLIPID MONOLAYER FILMS AT THE AIR/WATER INTERFACE. AN INFRARED REFLECTANCE STUDY

Melody L. Mitchell, Rodney D. Hunt and Richard A. Dluhy,  
The National Center for Biomedical Infrared Spectroscopy  
Battelle Columbus Division, 505 King Avenue, Columbus, Ohio 43201

We have previously shown that in situ infrared monitoring of phospholipid monolayer films at the air/water interface revealed frequency shifts in both C-H stretching modes (2920 and 2850 cm<sup>-1</sup>) as the film is compressed. Re-examination of these conformation sensitive bands with higher spectral sensitivity yielded two distinct frequency shifts. These shifts suggest two phase transitions: from fluid disordered chains in the liquid expanded phase to more erect chains normal to the interface, to ordering of gauche rotomers in the solid condensed phase. The effects of compression and the presence of substrate ions and surface active proteins on the interfacial structure of the polar lipid headgroup were also studied by examination of the stretching vibrations between 1300-1000 cm<sup>-1</sup>. Possible interfacial structures are proposed and discussed.

**W-Pos167** RESOLUTION AND MEASUREMENT OF ADENINE AND GUANINE 8CH EXCHANGES IN DNA BY RAMAN OPTICAL MULTICHANNEL ANALYSIS. Renee Becka, Om Lamba and George J. Thomas, Jr., Div. of Cell Biol. and Biophys., School of Basic Life Sciences, Univ. of Missouri, Kansas City, MO 64110.

Deuterium exchange of 8C protons of adenine and guanine in nucleic acids is easily monitored by laser Raman spectrophotometry, and the average exchange rate ( $\langle k_A + k_G \rangle$ ) so determined can be exploited as a dynamic probe of the overall secondary structure of DNA or RNA (J. M. Benevides and G. J. Thomas, Jr., Biopolymers (1985) 24, 667-682). The present work describes a rapid Raman procedure, based upon optical multichannel analysis, which permits discrimination of the different 8CH exchange rates  $k_A$ , of adenine, and  $k_G$ , of guanine in a single experimental protocol. For this procedure, simultaneous measurements are made of the intensity decay (or frequency shift) in separately resolved Raman bands of A and G, each of which is sensitive only to 8C deuteration of its respective purine. Resolution of the rates  $k_A$  and  $k_G$  is demonstrated for nucleotide mixtures (5'dAMP + 5'dGMP), polynucleotides [poly(dA-dT).poly(dA-dT) and poly(dG-dC).poly(dG-dC)], and calf thymus DNA. We also show that the different exchange rates of G and A, in nucleotide mixtures and in DNA, may be well approximated by following the intensity decay of an exchange-sensitive, composite purine band (1482 cm<sup>-1</sup> Raman band) over a time domain which encompasses two distinct regimes, an initial exchange of G, and a subsequent slower exchange of A. The present work establishes an experimental basis for future study of purine-specific interactions which may be important in protein-nucleic acid binding and nucleic acid condensation (e.g. viral DNA packaging) reactions. (Supported by N.I.H.)

**W-Pos168** VIBRATIONAL CIRCULAR DICHROISM OF POLY(dG-dC): CALCULATIONS AND EXPERIMENTAL RESULTS, Miriam Gulotta, Roxanne Joseph, Dixie J. Goss, and Max Diem, Department of Chemistry, Hunter College, CUNY, New York, NY 10021.

The salt induced phase transition from right to left handed helicity of DNA polymers is well known. Although circular dichroism and Raman spectroscopy can be used to determine a conformation change, little is known about the details of the structural changes which accompany the B-Z transition in solution. Vibrational circular dichroism, in which the difference in absorption of left and right circularly polarized light in the infrared region is observed, has already been used in determining the secondary structure of polyamino acids and peptides. In DNA models, large IR signals due to carbonyl transition moments cause large bisignant couplets in VCD spectra. We have used salt to induce a B-Z transition in poly(dG-dC)poly(dG-dC) as well as in some smaller length GC oligonucleotides and have followed the transition using VCD spectroscopy. A theoretical framework for the interaction of dipoles in an  $n$ -mer has been developed and applied to systems consisting of between three and thirty interaction transitions has yielded spectral features which closely resemble observed VCD spectra. Using the theoretical model in conjunction with the experimental results, we can illustrate the structural path of the B-Z transition. Grant Support: NSF 86-07070 and 86-07934, NIH GM 28619, AHA-NYC Investigatorship (DJG), and PSC-CUNY Faculty Research Awards.

**W-Pos169** THE ROLE OF THE SOLVENT IN THE MODULATION OF THE d-d EXCITED STATE PROPERTIES OF NICKEL PORPHYRINS IN NONCOORDINATING SOLVENTS AS INVESTIGATED BY TRANSIENT RAMAN AND ABSORPTION SPECTROSCOPIES. Eric W. Findsen<sup>1,3</sup>, J. A. Shelton<sup>2</sup>, and M. R. Ondrias<sup>1</sup>.

<sup>1</sup>Department of Chemistry, University of New Mexico, Albuquerque, NM 87131, <sup>2</sup>Sandia National Laboratories, Albuquerque, NM 87185.

Permanent address: Department of Chemistry, University of Toledo, Toledo, OH 43606.

The modulation of the reactivity of porphyrins in biological systems by the environment is not well understood. In this report we present the results of an indepth study of the transient behavior of nickel protoporphyrin IX in several noncoordinating solvent systems. Using transient Raman spectroscopy we have compared spectra obtained at high and low photon densities and observed the effect of the solvent environment upon the reversible formation of nickel centered d-d excited state. Using transient Raman and absorption spectroscopies we have determined that the excited state electronic and vibrational properties of the porphyrin are very sensitive to the solvent environment. In contrast, the ground state Raman spectra of these systems are relatively insensitive to the solvent environment. The sensitivity of the d-d excited state to its immediate environment can be correlated to a solvent parameter termed  $E_1(30)$ , which is dependent upon both the inductive and dipolar characteristics of the solvent. We have determined that while both the porphyrin  $a_{1g}$  and  $a_{2u}$  orbitals are both affected, the  $a_{2g}$  orbital is much more sensitive to the solvent environment. This work performed at the University of New Mexico and Sandia National Laboratories. This work supported in part by the A.W.U. (to E.W.F.), NIH (GM33330 to M.R.O.), S.N.L. (to E.W.F. and M.R.O.), U.S. D.O.E. (DE-AC04-76DP00789 to J.A.S.) and the G.R.I. (5082-260-0767 to J.A.S.).

**W-Pos170** RAMAN STUDY OF THE C-D STRETCH AND C-H BENDING MODES OF THE NICOTINAMIDE ADENINE DINUCLEOTIDE (DEUTERATED REDUCED FORM) WHEN IT IS BOUND TO ENZYMES. H. Deng, D. Sloan, J. Burgner and R. Callender. Physics (H. D. & R. C) and Chemistry (D. S) Departments, City College of City University of New York, New York, NY 10031, and Department of biological Sciences (J.B), Purdue University, West Lafayette, IN47907.

It is well known that the oxidized and reduced forms of nicotinamide adenine dinucleotide ( $\text{NAD}^+/\text{NADH}$ ) are coenzymes of many dehydrogenases including lactate (LDH), malate (MDH) and liver alcohol dehydrogenases (LADH). These three enzymes catalyze the transfer of hydrogen (as a hydride ion) between the redox site of the coenzymes (A-side at C-4 position of the pyridine ring) and carbonyl carbon of their respective substrate in a direct and stereospecific manner. Using deuterated A-side NADD and sensitive difference Raman techniques developed in our lab, we have obtained the Raman spectra of NADD when it is bound to these enzymes we are then able to identify C-D bending and C-D stretching modes associated with these important A-side C-4 position hydrogen reaction coordinate. These modes are well characterized from all other vibrational modes of NADD as well as enzyme modes, and their shift from free NADD to bound NADD provides direct information about how this interaction coordinate is changed upon binding to the various enzymes. Based on these results, various models for the hydride transfer mechanism in these enzyme catalyzed reactions will be discussed.

**W-Pos171 FURTHER INVESTIGATION OF THE INFLUENCE OF TERTIARY STRUCTURE ON PROTEIN INFRARED SPECTRA.** J.F.Hunt, Department of Molecular Biophysics and Biochemistry, Yale University.

Previously, a transition dipole moment coupling model has been used to predict the occurrence of infrared absorption frequency shifts which derive from regular patterns in protein tertiary structure. In the current study, the validity and implications of this model are explored in greater depth:

First, the contribution of individual peptide backbone oscillators to the predicted delocalized molecular normal modes is examined when the model is applied to an isolated  $\alpha$ -helix; these eigenvector distributions are compared to those predicted by more rigorously correct computational models in order to assess the validity of the approximations inherent in the transition dipole moment coupling model.

Second, the sensitivity of the predictions of the model to variations in the input parameters is evaluated in the context of a close-packed helical bundle approximating the molecular geometry of the bacteriorhodopsin molecule. (The model has previously been used to explain the anomalously high amide I frequency of bacteriorhodopsin.) There are only three adjustable parameters in this model: the transition dipole moment intensity, its orientation relative to the atoms in the peptide bond, and the vibrational frequency of the unperturbed localized normal modes. Systematic variations in all three of these parameters over an appreciable range is shown not to alter the qualitative results of the calculations, i.e. the close apposition of  $\alpha$ -helices is predicted to cause a significant increase in the amide I frequency without an appreciable change in the amide II frequency.

Finally, the computational model is used to evaluate whether frequency shifts are predicted to occur in the infrared spectra of proteins containing other regular super-secondary structures.

**W-Pos172** CONTRIBUTIONS OF THE HYDROPHOBIC EFFECT TO THE STABILITY OF SPECIFIC PROTEIN-DNA COMPLEXES. Jeung Hoi Ha, Ruth Saecker Spolar, and M. Thomas Record, Jr., Departments of Chemistry and Biochemistry, University of Wisconsin, Madison, Wisconsin, 53706.

We find that one of the principal forces driving the site-specific binding of proteins to DNA is the hydrophobic effect. In the hydrophobic effect, nonpolar groups exposed to solvent are buried in the complex and water molecules of hydrophobic hydration on the protein are released. Reactions driven by the hydrophobic effect are characterized by a large, negative  $\Delta C_p^0$ . We observed a large, negative  $\Delta C_p^0$  for the interactions of RNA polymerase with a promoter, and for the interactions of lac repressor and EcoRI with their specific sites.

Equilibrium binding constants ( $K_{obs}$ ) were determined as a function of temperature by nitrocellulose filter binding assay. For the lac repressor-symmetric operator system,  $K_{obs}$  is a maximum near 20 °C and decreases at other temperatures. For the association process,  $\Delta C_p^0$  is -1.3 ( $\pm 0.3$ ) Kcal/mol•deg, corresponding to a burial of hydrophobic surface area of as much as 4000 Å<sup>2</sup> and a driving force of approximately -100 Kcal/mol. Preliminary results from studies of EcoRI binding to its specific site show a similar temperature dependence.

**W-Pos173** Charged Oligopeptide-Single Stranded Nucleic Acid Interactions as Models of the Electrostatic Component of Protein-Nucleic Acid Interactions. David Mascotti and Timothy M. Lohman, Department of Biochemistry and Biophysics, Texas A&M University, College Station, Texas 77843.

A significant component of the free energy of most protein-nucleic acid interactions is derived from the release of counterions from the nucleic acid upon formation of ionic interactions within the complex. The interpretation of the effects of varying salt concentration on these interactions has relied upon the use of positively charged oligopeptides as models of the electrostatic component of protein-duplex DNA complexes. We have begun to obtain such data for charged oligolysine-single stranded (ss) polynucleotide equilibria in order to facilitate interpretation of salt effects on protein-ss nucleic acid systems.

In these studies, we utilize a well-defined oligopeptide: (L-Lys)-(L-Trp)-(L-Lys)<sub>4</sub>-NH<sub>2</sub> (total charge of +6), as our model ligand. Amidation of the carboxy terminus has been included to obviate potential ambiguities due to the presence of a free carboxyl anion. We have used the quenching (Q) of the intrinsic tryptophan fluorescence to monitor the extent of binding by determining the relationship between Q and the fraction of bound oligopeptide. With this information, the equilibrium association constants of these oligopeptides to ss-polynucleotides have been determined as functions of monovalent salt concentration and type, pH, Mg<sup>++</sup> and temperature. With ss-RNA, log( $K_{obs}$ ) is a linear function of log[MX] over three orders of magnitude of  $K_{obs}$ . The log-log slope is dependent upon lattice type and pH and indicates that fewer than 6 (the peptide charge) monovalent cations are released upon binding.

(Supported by NIH GM39062)

**W-Pos174** ELECTROSTATIC CONTRIBUTIONS TO FILAMENTOUS PHAGE STRUCTURE. C.J. Marzec and L. A. Day, The Public Health Research Institute, 455 First Avenue, New York, New York, 10016

All filamentous bacteriophages (Ff, IK<sub>1</sub>, If<sub>1</sub>, Pf<sub>1</sub>, Pf<sub>3</sub>, Xf, etc.) consist of a circular, single stranded DNA molecule ensheathed by a protein coat made of several thousand subunits. The protein coats are similar in overall structure, but there are two types of helical symmetry and large differences in subunit amino acid sequence and in the nature of the DNA-protein interface. The nucleotide to subunit ratio, n/s, varies from 2.4 to 1.0. Each DNA is locally two-stranded, but not base paired, and the DNA structures are very different.<sup>1</sup> Site directed mutagenesis on the fd coat protein has demonstrated the essential role of electrostatics in the DNA-protein interaction; if one of four lysines near the C-terminus, the end nearest the DNA, is replaced by a neutral amino acid, the mutant phage are 4/3 longer, suggesting that more subunits and a more extended DNA structure compensate for the smaller number of neutralizing charges per subunit.<sup>2</sup>

We have prepared electrostatic models of the DNA-protein interactions. We treat the DNA as two helices of point charges of magnitude -e, and the protein as a 1-start or 5-start helix of point charges of value +ne, where n depends on the subunit. The potential distribution and the DNA-protein interaction energy are calculated analytically, via the linearized Poisson-Boltzmann equation, as a function of the DNA and protein helix parameters. In the most complex models, the space is divided into four regions, each with appropriate Debye-Hückel length and dielectric constant: a DNA cylinder, a small annular cylinder between the DNA and protein, the protein coat annular cylinder, and the solvent.

We find that the DNA-protein interaction is strongest for sets of helix parameters allowing spatial resonance between the DNA and protein helices. Strong resonances appear near the observed n/s values, suggesting that the viruses are tuned to local minima in electrostatic interaction energy. Also, we find that for a given set of helix parameters, the minimum of the total electrostatic energy does not generally occur when the DNA and protein charges are in exact local balance, implying that the simple idea of local charge neutralization may be too simple.

<sup>1</sup>Day, L.A., Marzec, C.J., Reisberg, S.A., and Casadevall, A. (1988) Ann. Rev. Biophys. Biophys. Chem. 17, 509-539.

<sup>2</sup>Hunter, G.J., Rowitch, D.H., and Perham, R.N. (1987) Nature 327, 252-254.

- W-Pos175 GENE 5 PROTEIN - SINGLE STRANDED DNA COMPLEX: COMPUTER MODELING STUDIES.** D. L. Hutchinson<sup>1</sup>, B. L. Barnett<sup>2</sup>, and A. M. Bobst<sup>1</sup>, <sup>1</sup>Department of Chemistry, University of Cincinnati, Cincinnati, OH 45221 and <sup>2</sup>Procter and Gamble Co., Miami Valley Research Laboratories, Cincinnati, OH 45239.

A toroidal complex consisting of eight dimers per turn is proposed for the extension of DNA from dimer to dimer using known bond length constraints, postulated amino acid - nucleic acid base interactions determined from NMR measurements, chemical modification studies, ionic strength dependent data, and results from electron micrographs. The binding channel has been dictated by these known parameters and the relative ease of geometrically fitting these constituents. This channel differs from that reported earlier by others. The computer modeling data suggest that the channel lies underneath the long arm "claw-like" extension (beta sheet) of the monomer, so that it rests inside the outer surface of the protein complex. An explanation is proposed for the two binding modes, n=4 (the predominant mode) and n=3, based on the weak binding interaction of Tyrosine 34. Also, the site of the immobilized nucleic acid base (on an ESR time scale) as reported from ESR studies (S-C. Kao, E. V. Bobst, G. T. Pauly, A. M. Bobst, *J. Biom. Struc. Dyn.* 3, 261 (1985)) is postulated as involving the fourth nucleotide of the nucleic acid binding site (from the 5'-end), and this particular base is stacked between Tyrosine 34 and Phenylalanine 73' (supported in part with NIH GM-27002).

- W-Pos176 <sup>1</sup>H NMR INVESTIGATION OF AVIAN RETROVIRUS NUCLEOCAPSID PROTEIN BINDING RNA OLIGO-NUCLEOTIDES.** Lisa M. Smith and Joyce E. Jentoft, Department of Biochemistry, Case Western Reserve University School of Medicine, 2119 Abington Road, Cleveland, OH 44106.

The avian myeloblastosis virus nucleocapsid protein (AMV pp12 or AMV NC) coats the RNA genome in the retrovirus, and is presumed to play a major role in the packaging of the RNA genome into the AMV virion. AMV NC binding of single-stranded RNA has been characterized by a fluorescence assay with poly(ethenoadenylic acid) (Jentoft, et al., *PNAS* in press). <sup>1</sup>H NMR spectra of AMV NC were analyzed to identify the resonances in the aromatic region. These identifications were used in further NMR studies to investigate the interactions between the protein and bound RNA oligonucleotides. No major changes in the chemical shifts of the aromatic resonances were observed upon nucleic acid binding indicating that the aromatic residues of the protein do not directly interact with bound nucleic acids. The spectral changes in both the aromatic and the aliphatic regions due to increasing bound RNA oligonucleotides will be discussed in detail. This data will also be discussed with regard to the structure of the protein in its liganded and unliganded states.

- W-Pos177 CHARACTERIZATION OF THE BINDING OF THE 7K PROTEIN FROM SULFOLOBUS SOLFATARICUS TO DNA.** Irene Zegar, James McAfee, John Hearn and John W. Shriver; Department of Medical Biochemistry and Department of Chemistry and Biochemistry, Southern Illinois University, Carbondale, Illinois, 62901

We have isolated a small DNA-binding protein from *Sulfolobus solfataricus*, a thermophilic archaebacteria which grows in thermal pools at 85 °C. The protein is expressed in large amounts as indicated by a yield of 40 mg of protein from 25 gm of packed cells. The molecular weight has been determined by HPLC to be approximately 7000 and appears to be monomeric as indicated by HPLC, ultracentrifugation and NMR studies. The 7k protein is most likely identical to Sso7d protein described by Grote et al (*Biochim. Biophys. Acta* 950 193 (1988)) and is thought to function as a histone-like protein, possibly stabilizing the DNA at the high growth temperature. We describe here the binding of the protein to nucleic acids monitored with fluorescence spectroscopy. The binding to double-stranded DNA (poly(dG-dC)) results in a maximum of 89% quenching of the intrinsic protein fluorescence in 0.01 M Na<sub>2</sub>HPO<sub>4</sub> (pH 7). The protein has a much higher affinity to double-stranded DNA than to single-stranded. The binding isotherm for binding to double-stranded poly(dG-dC) was fit with the McGhee-von Hippel model and indicates a binding site size of approximately 11 base pairs with an intrinsic binding constant of  $1.4 \times 10^6 \text{ M}^{-1}$  and no apparent cooperativity. The binding is highly salt and ionic strength dependent. The magnitude of the quenching is reduced to nearly zero in the presence of 0.1 M NaCl, whereas KCl has much less effect.

**W-Pos178** ROTATIONAL DIFFUSION OF NUCLEOSOME CORE PARTICLES MEASURED USING THE DECAY OF THE FLUORESCENCE ANISOTROPY. Louis J. Libertini and Enoch W. Small, Department of Biochemistry and Biophysics, Oregon State University, Corvallis, Oregon 97331.

In order for the biological functioning of chromatin to occur -- transcription, replication, or repair -- it must be necessary to disrupt the nucleosome structure and free the DNA, at least in a transient manner. For this reason a number of laboratories, including our own, have been investigating conformational changes that isolated nucleosomes undergo in solution, on the theory that such transitions may be related to changes which occur in vivo. One very interesting transition occurs at very low ionic strength. A disagreement exists in the literature as to whether this transition results in a large or small change in the overall shape of the particle. We have bound ethidium bromide to the core particles at very low ratios (about 1.5 ethidium per core particle) and examined the fluorescence at moderate (10 mM) and very low ionic strengths (<0.1 mM). Distribution analyses of the fluorescence intensity decays indicate binding similar to that of ethidium intercalated into free DNA, although distribution widths indicate somewhat more homogeneous binding for the core particle. Anisotropy decays of the ethidium fluorescence indicate motion on three time scales. Very fast motions are indicated by a decrease in the apparent value of  $r_0$ . Intermediate flexing motions occur with correlation times in the range of about 10 to 20 ns, and rotational correlation times are clearly apparent in the range of hundreds of ns. The rotational correlation time of 135 ns recovered at 10 mM ionic strength is consistent with the known size and shape of the core particle. At the much lower ionic strength we recover a poorly resolved correlation time of about 377 ns. Such a correlation time could only arise from a large overall shape in the particle. Supported by NIH grant GM 25663.

**W-Pos179** STUDY OF INTERACTIONS BETWEEN MYELOPEROXIDASE AND NUCLEIC ACIDS BY SIZE-EXCLUSION HPLC. W. E. Boernke and F. J. Stevens, Nebraska Wesleyan University, Lincoln, NB 68504 and Argonne National Laboratory, Argonne, IL 60439

Myeloperoxidase (MPO, E.C. 1.11.1.7) is an enzyme characteristically found in azurophil granules of the cytoplasm of phagocytic cells. Murao et al. (Proc. Natl. Acad. Sci., USA 85:1232, 1988) have recently used a monoclonal antibody obtained following immunization of mice with heterogeneous chromatin proteins to identify an apparent nuclear protein as MPO. DNA binding properties of MPO had not been previously noted, and the physiological role of this binding is not yet determined. We used size-exclusion high-performance liquid chromatography to characterize the nucleic acid binding properties of MPO. In this method, changes in elution patterns exhibited by a mixture of reactants relative to the elution behavior of the constituents chromatographed individually provides a direct observation of interaction. MPO binds both double-stranded and single-stranded DNA; higher avidity is demonstrated for the single-stranded form. MPO also binds RNA of sufficient length; interaction was observed with genomic RNA obtained from plant viruses, but no interaction was found with short, heterogeneous mRNA or tRNA. Binding of MPO to nucleic acid is sensitive to salt concentration in the physiological range; binding is effectively eliminated at concentrations above 0.4 M. These results illustrate a potential role for size-exclusion HPLC, which allows direct visualization of interaction without chemical modification of either component, in studies of interaction between proteins and nucleic acid. (Work supported by the U. S. Department of Energy under Contract No. W-31-109-ENG-38.)

**W-Pos180** AMV NUCLEOCAPSID PROTEIN BINDING TO SINGLE STRANDED POLY (1,N<sup>6</sup>-ETHENOADENYLIC ACID). Josephine Seznik and Joyce E. Jentoft. Department of Biochemistry, Case Western Reserve University, Cleveland, OH 44106.

The major nucleocapsid (NC) protein of avian myeloblastosis virus bind to single stranded RNA, and is associated with genomic RNA within the virus capsid. Binding of NC to nucleic acids was monitored through the use of the fluorescent nucleic acid probe, poly (1,N<sup>6</sup>-ethenoadenylic acid). Poly (1,N<sup>6</sup>-ethenoadenylic acid) used in our studies was eluted in the void volume of a BioGel A-0.5m column and heated to 80°C before use to assure that the sample was single-stranded and of sufficient length to make end effects negligible. NC binds to poly (1,N<sup>6</sup>-ethenoadenylic acid) with a site size, n, of 5 ± 1, a K<sub>a</sub> of 1 × 10<sup>5</sup> M<sup>-1</sup>, and a cooperativity parameter, ω, of 20–35 at pH 5.6 in 80 mM NaCl (Jentoft, et al., PNAS, in press). These studies were extended to include the pH dependence of n, K<sub>a</sub>, and ω, and the salt dependence of these parameters at selected fixed pH values. These studies are designed to establish the fundamental biophysical properties of the binding between NC and nucleic acid.

**W-Pos181 RADIAL MASS DENSITY PROFILES, MASS PER UNIT LENGTH, AND NUCLEOTIDE/SUBUNIT RATIOS FOR FILAMENTOUS BACTERIOPHAGES FROM ELECTRON MICROSCOPY.** S.A. Reisberg, J.S. Wall, and L.A. Day, The Public Health Research Institute, 455 First Avenue, New York, N.Y., 10016, and Department of Biology, Brookhaven National Laboratory, Upton, N.Y., 11973

The structures of the filamentous phage fd, If1, IK<sub>E</sub>, Xf, Pf1, Pf3, and C2 were investigated by scanning transmission electron microscopy (STEM). Computational techniques were developed to analyze low dose micrographs of the curved filaments. Mass per unit length (MPUL), particle length and radial mass distribution were obtained for each phage system. Three principal algorithms were devised. The first assigns a centerline with subpixel accuracy to the gently curved images. Relevant pixels are sorted and assigned to bins according to their perpendicular distance from this centerline by a second algorithm. A third algorithm reconstructs the radial density from the intensity profile formed from averaging the binned pixel data. Total particle length is obtained by computing the centerline length along the entire particle contour. The MPUL of a particle segment is calculated from total scattering intensity of that segment divided by the included centerline length. Calibration to absolute mass is by comparison with tobacco mosaic virus (TMV) included as an internal mass standard.

The total number of protein subunits, the axial rise per DNA base, *h*, and the stoichiometric ratio of DNA nucleotides to protein subunits, *n/s*, are calculated from the data. The *n/s* ratios of all of the viruses but Pf1 were found to be non-integer. An example of important differences is a comparison between fd and IK<sub>E</sub> which have identical coat protein symmetry and significant sequence homology; our STEM data show that IK<sub>E</sub> has *h* =  $2.99 \pm 0.05$  Å and *n/s* =  $2.16 \pm 0.16$ , but that fd has *h* =  $2.72 \pm 0.06$  Å and *n/s* =  $2.41 \pm 0.11$ . These values imply different DNA structures even for these otherwise similar phage.

The radial mass density profiles obtained were similar for all of the phage. The phage were found to be highly dense in their central DNA containing region and to have a mass shoulder at about 15-20 Å with a gradual mass falloff at higher radii. The particle radius, defined by the radial cutoff that includes 95% of the mass, is about 34 Å for all of the phage.

**W-Pos182 Studies of the Monomer - Tetramer Equilibrium of a Mutant *E. coli* ssDNA-Binding Protein, SSB-1.** Włodzimierz Bujalowski and Timothy M. Lohman, Department of Biochemistry & Biophysics, Texas A&M University, College Station, TX. 77843, (Intr. by M. M. Ziegler).

The *E. coli* SSB protein is a stable homotetramer in solution; however the ssb-1 mutation (his to tyr 55) destabilizes this tetrameric structure with respect to monomers (Williams, K.R., et al. (1983), J. Biol. Chem., 259, 7214) and we have undertaken a quantitative study of this equilibrium. There is no change in the intensity of the intrinsic protein fluorescence upon the association of the SSB-1 monomers. The extent of tetramer formation was monitored by the change in intrinsic protein fluorescence anisotropy accompanying the association. Theoretical analysis of the different aggregation mechanisms, which allows us to distinguish among some mechanisms will be presented. A comparison of the experimental isotherms with simulations for the general monomer ↔ dimer ↔ tetramer association indicates that the formation of the SSB-1 tetramer from the monomers can be described with high accuracy as a one step association of the four monomers into tetramer, so that dimers are not a highly populated species. In our standard conditions (25 °C, pH 8.1) an apparent aggregation constant  $K = 2 \times 10^{18} \text{ M}^{-3}$  is obtained. There is a strong temperature dependence of the SSB-1 tetramer formation with  $\Delta H = -59 \pm 15 \text{ kcal/mol}$  (pH 8.1). Studies of the pH, monovalent ( $\text{NaCl}$ ) and divalent salt ( $\text{MgCl}_2$ ) effects on the monomer ↔ tetramer association indicate, no influence of  $[\text{NaCl}]$  up to 1 M; however the presence of  $\text{MgCl}_2$  at concentrations above ~ 20 mM attenuates the formation of SSB-1 tetramer.

(Supported by NIH GM 30498)

**W-Pos183 Negative Cooperativity Among ssDNA Binding Sites within the *E. coli* Single Strand Binding (SSB) Protein Tetramer.** Włodzimierz Bujalowski and Timothy M. Lohman, Department of Biochemistry & Biophysics, Texas A&M University, College Station, TX. 77843

We have examined the salt and temperature dependences of the equilibrium binding of the *E. coli* SSB tetramer to a series of oligodeoxythymidylates, dT(pT)<sub>N-1</sub>, with N=16, 28, 35, 56 and 70. Using a thermodynamically rigorous method (Lohman and Bujalowski, (1988), Biochemistry, 27, 2260), we determined stoichiometries of 4,2,2,1 and 1 per protein tetramer for N=16,28,35,56 and 70, respectively. Evidence will also be presented for the existence of a true negative cooperativity among the multiple ssDNA binding sites on the SSB tetramer. We have quantitatively analyzed the binding isotherms using a statistical thermodynamic ("square") model of the tetrameric protein to obtain the *intrinsic* binding constant,  $K_N$ , and the negative cooperativity constant,  $\sigma_N$ . For all oligonucleotides, we find that  $K_N$  decreases significantly with increasing monovalent salt concentration, indicating a large electrostatic component to the free energy of the interaction. There is a strong temperature dependence for the intrinsic binding of dT(pT)<sub>15</sub>, such that  $\Delta H = -26 \pm 3 \text{ kcal/mole}$  dT(pT)<sub>15</sub>. Negative cooperativity exists under all solution conditions tested and is independent of anion concentration and type; however,  $\sigma_{16}$  decreases with decreasing cation concentration. These data and the lack of a temperature dependence for  $\sigma_{16}$  suggest that the molecular basis for the negative cooperativity is predominantly electrostatic and may be due to the repulsion of regions of ssDNA that are required to bind in close proximity on an individual SSB tetramer. The negative cooperativity stabilizes the formation of the (SSB)<sub>35</sub> binding mode in which ssDNA interacts with only 2 subunits of the tetramer.

(Supported by NIH GM 30498).

**W-Pos184** AN ENZYMATIC PROBE OF DNA FLEXIBILITY VARIATION, Michael E. Hogan, Mark W. Roberson, Robert H. Austin

The goal of the analysis presented here is to determine if, in the absence of significant local variation of DNA secondary structure, DNaseI cleavage within a B form helix is determined by local variation in the bending flexibility, as defined physically, ie, base sequence dependent variation of the force constant for bending the helix. Our analysis shows that the same elastic strain model used successfully to predict relative binding constants for the 434 repressor can be used to predict the cutting pattern of DNaseI both qualitatively and quantitatively. Since the model only has three fixed parameters and a simple mathematical form we propose that in those instances where a helix must be bent or twisted at the binding site the elastic strain model we have developed provides a useful conceptual framework to evaluate the contribution of bending or twisting rigidity to the energetics of DNaseI specificity. Further, because of the significant correlation which we have detected between the pattern of DNaseI cleavage and the prediction of elastic strain theory, we also suggest that in the absence of significant local variation of the helix structure DNaseI can serve as an enzymatic probe of DNA flexibility variation.

**W-Pos185** MUTATIONS AFFECTING THE AUTOREGULATORY FUNCTION OF THE DNA PROTEIN. H. Eberle, W.-S. Zhu, G. Kampo and K. Madden. Dept. of Biophysics, University of Rochester School of Medicine, Rochester, NY 14642

The DNA protein of Escherichia coli is required for the initiation of chromosomal replication. It binds to a specific sequence, TTAT<sub>C</sub><sup>A</sup>CA<sub>C</sub><sup>A</sup>, called the DnaA Box. This sequence is found repeated 4 times in the essential origin of replication. It is also found between promoter 1 (P1) and promoter 2 (P2) of its own gene and in the 5' region of other E. coli genes. Its binding to the origin of replication is necessary as a prepriming step of replication initiation. The binding in the promoter region of genes is thought to be involved in the regulation of gene expression, and in the case of its own gene, it has been demonstrated to be autoregulatory.

We have isolated a phenotypic revertant of a dnaA508 temperature sensitive mutant that appears to be cold sensitive (grows poorly at 30°C) and to be overproduced. This mutant dnaA gene, which may have a defect in autoregulation, has been sequenced and mutations identified. The binding sequence between P1 and P2 remains unchanged. Also DnaA Box-oligonucleotide affinity chromatography reveals that this mutant protein binds to the DNA Box. The phenotype of this mutant protein is discussed in relation to other mutations found within the gene.

**W-Pos186** OPTICALLY DETECTED MAGNETIC RESONANCE (ODMR) OF p10, A SINGLE-STRANDED NUCLEIC ACID BINDING PROTEIN OF MURINE LEUKEMIA RETROVIRUSES. Jose R. Casas-Finet (1), August H. Maki (1), William J. Roberts (2), James I. Elliott (2), and Kenneth R. Williams (2). (1) Department of Chemistry, University of California, Davis, CA 95616 and (2) Department of Molecular Biophysics and Biochemistry, Yale University, New Haven, CT 06510. (Intr. by Mark G. McNamee)

p10 contains one putative Zn binding site per protein molecule, which is composed of Cys26, Cys29, Cys39 and His34. Based on previous ODMR results [Casas-Finet, J. R., Jhon, N.-I., and Maki, A. H. (1988) *Biochemistry* 27, 1172] the single Trp35 undergoes stacking interactions with nucleic acid bases upon binding of p10 to single-stranded polynucleotides. We have investigated the effect of added metal ions by ODMR characterization of a chemically synthesized peptide spanning the entire protein sequence (56 a. a.'s). Moderate wavelength dependence of the zero-field splittings (zfs) |DI-IE| and 2IEI with phosphorescence emission wavelength is consistent with partial exposure of the Trp chromophore to the solvent in the free protein. Specific effects induced upon association of p10 with poly(5-mercuri)uridylic acid are of larger magnitude in the presence of Zn<sup>2+</sup> rather than in the absence of Zn<sup>2+</sup> or when the 3 Cys residues have been chemically blocked, although all forms bind single-stranded lattices with high affinity. Only in the presence of metal ions does p10 exhibit a Trp phosphorescence lifetime under 10 ms when associated with poly(5-mercuri)U. In the absence of added metal ions the heavy atom-perturbed phosphorescence lifetime of Trp35 in the complex is greater than 60 ms. The phosphorescence red shift (3.2nm), lifetime reduction (21%), and reduction of the zfs |DI| parameter (40 MHz) are greater for the Trp35 residue upon binding p10 to poly(dT) in the presence of added metal ions than in the absence of metal. Addition of Cd<sup>2+</sup> or Co<sup>2+</sup> instead of Zn<sup>2+</sup> results in very similar effects induced in the Trp residue upon protein binding to single-stranded polynucleotides. (supported by NIH grant ES-02662)

**W-Pos187 CALMODULIN ANTAGONISTS AND CALCIUM-CALPAIN INTERACTIONS.** H. Hong, S.C. El-Saleh\*, and P. Johnson (Intr. by P.D. Sullivan). Department of Chemistry and College of Osteopathic Medicine, Ohio University, Athens, Ohio 45701, and \*Department of Physiology and Cell Biophysics, University of Cincinnati Medical School, Cincinnati, Ohio 45267.

The effects of calcium and calmodulin antagonists [W-7 (N-(6-aminobutyl)-5-chloro-1-naphthalenesulfonamide) and W-13 (N-(4-aminobutyl)-5-chloro-2-naphthalenesulfonamide)] on the fluorescence of TNS (toluidinyl-naphthalene-sulfonate) bound to the individual subunits (80K and 30K) of Ep-64-inhibited chicken gizzard calpain II have been investigated. The effect of CDZ (calmidazolium) on the intrinsic fluorescence of the two subunits has also been studied. As in the case of intact calpain II, the fluorescence intensities of TNS in both 80K and 30K solutions were found to be calcium dependent. A 10% increase in TNS fluorescence intensity was observed and the  $pCa_{50}$  values for both subunits were similar to that for intact calpain II. W-7 and W-13 have no effect on the fluorescence intensity of TNS bound to the subunits, in agreement with the results obtained for the intact calpain. At  $20\mu M$  CDZ, the intrinsic fluorescence of intact calpain II and the separated subunits were decreased between 30-50% whereas with calmodulin, no decrease was observed. In the absence of CDZ, the intrinsic fluorescence of calpain II decreased with  $Ca^{2+}$  concentration ( $pCa_{50} = 4.52$ ), whereas in the presence of CDZ, intrinsic fluorescence increased at higher  $Ca^{2+}$  concentrations ( $pCa_{50} = 3.9$ ). These results indicate that both of the subunits of calpain can bind calcium and calmodulin antagonists and that the effects of these compounds on the intact enzyme may be the result of binding events at both subunits.

**W-Pos188 STRUCTURAL STUDIES OF CALMODULIN COMPLEXED WITH MLCKI.** \*Heidorn, D.B., \*Rokop, S.E., \*Seeger, P.A., <sup>1</sup>Blumenthal, D.K., <sup>2</sup>Means, A.R., <sup>3</sup>Crespi, H., and \*Trehewella, J.

\*Life Sciences and Physics Divisions, Los Alamos National Laboratory, Los Alamos, NM 87545; <sup>1</sup>Dept. of Biochemistry, Health Center at Tyler, University of Texas, TX 75710; <sup>2</sup>Dept. of Cell Biology, Baylor College of Medicine, Houston, TX 77030; <sup>3</sup>Chemistry Division, Argonne National Laboratory, Argonne, IL.

Small angle X-ray and neutron scattering have been used to study the solution structures of calmodulin and of calmodulin complexed with the synthetic peptide MLCKI in the presence of  $Ca^{2+}$ . The sequence of MLCKI corresponds to the calmodulin binding domain of skeletal myosin light chain kinase<sup>1</sup>. The neutron scattering data were collected (using the new low Q neutron diffractometer at the Los Alamos Neutron Scattering Center) from samples of deuterated calmodulin complexed with hydrogenated MLCKI in solutions of five different percentage  $D_2O$  concentrations. The deuterated calmodulin was obtained using a bacterial expression system grown on a deuterated medium<sup>2</sup>. The data reveal details of the structures of each of the individual components in the complex.

<sup>1</sup>Blumenthal, D.K., Takio, K., Edelman, A.M., Charbonneau, H., Titani, K., Walsh, K.A., and Krebs, E.G. (1985) *Proc. Natl. Acad. Sci. USA* 82:3187.

<sup>2</sup>Seeholzer, S.H., Cohen, M., Putkey, J.A., and Means, A.R. (1986) *Proc. Natl. Acad. Sci. USA* 83:3634.

**W-Pos189 CALMODULIN STRUCTURE IN SOLUTION STUDIED BY SMALL ANGLE X-RAY SCATTERING.** Authors: M. Kataoka, D. Engelman, J. Head\* and B. Seaton\*, Dept. of Molecular Biophysics and Biochemistry, Yale University, and \*Dept. of Physiology, Boston University School of Medicine.

Small angle x-ray scattering measurements have been carried out on bovine brain calmodulin under various physiological conditions in order to follow changes in its structure in solution. From our measurements we obtain data on the average radius of gyration of the two principal domains as well as the radius of gyration of the structure as a whole. Changes in these parameters are observed when the ionic environment of the molecule is altered.

A Guinier plot of the scattering from calmodulin in solution is well approximated by two straight lines, which is the expected result for a dumbbell-shaped structure. Only data on the inner slope have previously been analyzed (1,2). In the absence of magnesium, the average radius of gyration of the domains is not changed significantly (less than 0.5 Å) by calcium binding, but the distance between the two domains increases, supporting the calcium induced elongation of the calmodulin that was previously reported (1). In the presence of magnesium and the absence of calcium, both the radius of gyration of a domain and the inter-domain distance decrease, suggesting a compaction of the molecule. Measurements are now underway to document the behavior in the presence of both calcium and magnesium.

1. B. Seaton et al. (1985) *Biochem.* 24, 6740.

2. D. Heidorn et al. (1988) *Biochem.* 27, 909.

**W-Pos190** SOLUTION STRUCTURE OF MOTILIN. Nikhat Khan, Astrid Graslund, Viktor Mutt, Anders Ehrenberg, and John Shriver. Department of Medical Biochemistry, Southern Illinois University, Carbondale, Illinois 62901; Department of Biophysics, University of Stockholm, S-106 91 Stockholm, Sweden; Department of Biochemistry II, Karolinska Institute, S-104 01 Stockholm, Sweden. We have initiated a study of the solution structure of the gastrointestinal hormone motilin using circular dichroism and two-dimensional NMR at 500 MHz. Motilin is a 22 residue peptide, with the amino terminus (Phe1-Gly8) containing largely hydrophobic residues and the carboxy terminus (Glu9-Gln22) containing predominantly hydrophilic residues. CD measurements clearly indicate the presence of secondary structure which is destroyed upon addition of 6M guanidine hydrochloride. In order to facilitate the <sup>1</sup>H NMR resonance assignments we have chosen to initially use hexafluoroisopropanol-d<sub>2</sub> (HFPA) to preferentially stabilize the formation of secondary structure. Addition of fluorinated alcohols up to 20% significantly increases the  $\alpha$ -helical content of the hormone. Between 20% and 40% HFPA, the conformational equilibrium of the sample is relatively unchanged. Significant changes occur in the <sup>1</sup>H NMR spectrum upon addition of HFPA, particularly in the regions of Tyr7-Glu9 and Gln11-Gln14. The fingerprint region expands significantly, facilitating sequential assignments. The assignment of all the <sup>1</sup>H resonances is now essentially complete. Short NH<sub>i</sub> - NH<sub>i+1</sub> NOE connectivities are observed from residues Ile4 to Gln14 and Glu15 to Gln22. Longer range NOE crosspeaks are observed from Leu10 to Gln14 and from Lys16 to Asn19, which indicate the location of the secondary structure indicated by the CD spectra.

**W-Pos191** PEPTIDE CONFORMATION IN SOLUTION: SUBSTANCE P, ITS FRAGMENTS, AND ANALOGS. James L. Weaver\*, David Covell\*, and Robert W. Williams\*. \*Department of Biochemistry, Uniformed Services University of the Health Sciences, Bethesda, MD 20814, and Department of Mathematical Biology, National Institutes of Health, Bethesda, MD 20892.

Substance P (SP) is an 11 amino acid neuropeptide with the sequence RPKPQQFFGLM-amide. C-terminal fragments of SP 4-11 and 5-11 are more active than the parent molecule, while fragments shorter than SP 6-11 are inactive [see "Substance P and Neurokinins" (Henry et al., eds.) Springer-Verlag]. Raman spectroscopy of SP and its fragments reveals a correlation between secondary structure and activity. Active SP and active fragments are characterized by 50-60% beta-strand, 25-35% reverse turn or bend, less than 7% helix, and 10% unfolded structure. These measurements suggest a beta turn structure. This form is found in normal saline solutions, in the presence of negatively charged lipid vesicles, and in methanol. Inactive SP and fragments are characterized by greater than 80% unfolded structure. These include SP 1-11-acid, and fragments 7-11, 8-11, and 9-11. Our energy minimization calculations of SP in a vacuum and in water yield a family of reverse turn structures that appear to be consistent with the Raman measurements of the active peptides. To measure unfolded structure in these peptides using Raman spectroscopy, it was necessary to characterize the Raman spectra of several other peptides unfolded in solution. These spectra were added to a data base of known structures used to estimate protein and peptide secondary structure.

**W-Pos192** EFFECT OF ELEVATED HYDROSTATIC PRESSURE ON THE CONFORMATIONAL STRUCTURE OF POLYPEPTIDES AND PROTEINS IN WATER

P.T.T. Wong, D. Carrier and H.H. Mantsch.  
National Research Council of Canada, Ottawa, K1A 0R6, CANADA

Polylysine and the *E. coli* methionine repressor protein are used to illustrate the effect of pressure on the structure of a polypeptide and a globular protein. The conformation-sensitive amide 1 regions in the infrared spectra of polylysine and the met repressor protein were monitored as a function of hydrostatic pressure. Under ambient conditions the conformation of polylysine is mainly random coil at pH 7.5 and mainly  $\beta$ -sheet at pH 11.9. As the external pressure increases the conformation of polylysine changes drastically. At pH 11.9 the conversion occurs within the range 1-2 kbar whereas much higher pressures (~ 9 kbar) are required at neutral pH. The pressure-induced conformational changes in polylysine are reversible and are completely recovered after external pressure is released. On the other hand, the *E. coli* methionine repressor protein undergoes a rearrangement of  $\alpha$ -helical segments into  $\beta$ -type structures over the pressure range 3 to 18 kbar. This pressure-induced formation of  $\beta$ -strands is completely reversible. However, after decompression the  $\beta$ -strands reconver to less ordered helical or random segments. Thus, hydrostatic pressure affects the solution structure of this protein in two different ways, a reversible pressure-induced aggregation via intermolecular hydrogen bonding leading to the formation of new  $\beta$ -type structures, and a pressure-induced irreversible change in intramolecular conformation.

**W-Pos193** CLUSTERS AND NETWORKS OF WATER MOLECULES AND MICROHETEROGENEITY OF SIDE CHAIN IN THE CRYSTAL STRUCTURES OF CRAMBIN AT ATOMIC RESOLUTION.

Martha M. Teeter and Nam H. Heo, Department of Chemistry, Boston College, Chestnut Hill, MA 02167  
 Hakon Hope, Department of Chemistry, University of California at Davis, Davis, CA 95617

The crystal structure of a hydrophobic protein crambin (4700 MW) at 140 K (0.83 Å) revealed almost all of the expected waters (87 out of 92 expected which were modeled as 133 water and 10 ethanol positions). Most of the fully occupied waters are located on the surface of the protein, extending water networks or forming clusters of pentagons, while those with partial occupancies are involved in several continuous network structures of water molecules as well as local alternative conformations of short network structures. Several additional 5-, 6-, and 7-membered rings were found in those network structures which are not seen in the structure of crambin at 300 K. Other secondary waters with fractional occupancies belong to one of the two major network structures modeled. Refinement was converged to a conventional R index of 12.4 % with anisotropic thermal parameters (PROLSQ) and the resulting model is being analyzed.

The microheterogeneity of the side chains of residues 22 (Pro/Ser) and 25 (Leu/Ile) may effect the disordered networks of waters in the surrounding solvent region. Recently, we have collected a 1.2 Å data set of a crystal grown with crambin purified by HPLC presumably to Ser22 and Ile25. The R index is 14.8% at the present stage of refinement. A 2Fo-Fc map shows unequivocal density for only Ser at residue 22 and an ordered Tyr29 which was conformationally disordered due to the heterogeneity of residue 22. Residue 25, however, still shows Leu/Ile disorder. The water networks around Ser22 is being analyzed and their network structures will be compared with those with mixed residues.

**W-Pos194** CALORIMETRIC STUDY OF DISSOLUTION OF SOLID COMPOUNDS THAT MIMIC INTERACTIONS FOUND IN PROTEINS

Kenneth P. Murphy and Stanley J. Gill

Department of Chemistry and Biochemistry  
 University of Colorado, Boulder, CO 80309

Direct measurement of the heat of dissolution under saturation conditions for three solid diketopiperazines (cyclo(Gly-Gly), cyclo(Ala-Gly), and cyclo(Ala-Ala)) as a function of temperature (20-40°C). Effects of solute aggregates such as dimers were determined from heats of dilution experiments. The standard state enthalpy in and heat capacity change for dissolution for these compounds at 25°C is given as follows: Gly-Gly, 28.3 kJ mol<sup>-1</sup>, -93 J K<sup>-1</sup> mol<sup>-1</sup>; Ala-Gly, 19.2 kJ mol<sup>-1</sup>, 36 J K<sup>-1</sup> mol<sup>-1</sup>; Ala-Ala, 14.5 kJ mol<sup>-1</sup>, 135 J K<sup>-1</sup> mol<sup>-1</sup>. These values scaled to unit of surface area or per amino acid residues and extrapolated to a reference state of 110°C, compare favorably to the enthalpies of denaturation of proteins (lysozyme, ribonuclease, and myoglobin) scaled either to buried area or buried residues extrapolated to 110°C. This energetic evidence supports the view that the unsolvated protein core region behaves as an intramolecular solid.

This work was supported by NSF grant CHE-8611408

**W-Pos195** SOLUTION CONFORMATION OF BETA AMINO ACIDS. CALCULATION OF THE CIRCULAR DICHROISM OF HELICAL POLY( $\alpha$ -ISOBUTYL L-ASPARTATE). Mark C. Manning<sup>a</sup>, J.M. Fernandez-Santib<sup>b</sup>, J. Puiggali<sup>b</sup>, J.A. Subirana<sup>b</sup>, and Robert W. Woody<sup>a</sup>, Department of Biochemistry, Colorado State University<sup>a</sup>, Fort Collins, CO 80523 USA and Unidad de Quimica Macromolecular, Escuela T.S. de Ingenieros Industriales<sup>b</sup>, Diagonal 647, 08028 Barcelona, SPAIN.

Polymers of  $\alpha$ -isobutyl L-aspartate (PAIBLA) have been prepared and purified. These are poly  $\beta$ -amino acids, containing one more methylene group in the backbone than polypeptides. Fiber diffraction data suggest several possible helical conformations, both left- and right-handed, possessing 3.25 or 4 residues per turn of the helix. Circular dichroism (CD) spectra have been obtained of chloroform solutions of PAIBLA. Spectra have been calculated for each of the possible helical structures, in order to ascertain which conformation is most consistent with the CD curves. Helices with 4 residues per turn are not predicted to yield CD spectra like those observed experimentally. Two structures remain which cannot be excluded by CD measurements, both possessing 3.25 turns per residue and a rise of 4.97 Å per turn. However, one is right-handed and the other is left-handed. Effects of ester side chain conformation and small variations in backbone torsional angles are being evaluated. These structures are also consistent with <sup>13</sup>C NMR and infrared spectroscopic studies. (This work was supported by NIH grant GM 22994 to R.W.W., CICYT grant PA86-0218-C03-03 to J.A.S., and a grant of free computer time from the Colorado State University Computer Center.)

**W-Pos196** INHOMOGENEOUS LINE BROADENING OF THE NEAR-INFRARED C-T BAND IN HEMOGLOBIN AND [Fe-Mn] HYBRID HEMOGLOBIN AT LOW TEMPERATURE. M.D. Chavez,<sup>1</sup> S. Courtney,<sup>2</sup> M.R. Chance,<sup>2</sup> B. Hoffman,<sup>3</sup> D. Kuila,<sup>3</sup> J. Nocek,<sup>3</sup> J.M. Friedman,<sup>2</sup> and M.R. Ondrias.<sup>1</sup>  
<sup>1</sup>Department of Chemistry, University of New Mexico, Albuquerque, NM 87131, <sup>2</sup>AT&T Bell Laboratories, Murray Hill, NJ 07974 and <sup>3</sup>Department of Chemistry, Northwestern University, Evanston, IL 60201.

We present the results of a detailed low temperature study of the near-infrared charge-transfer band at  $\approx 760$  nm in five-coordinate ferrous hemoglobins and [Fe-Mn] hybrid hemoglobins. Deoxyhemoglobin, at pH 8.0 and pH 6.0 + IHP, shows an increase in the extinction coefficient and a lineshape change of the C-T band as the temperature is lowered from 160°K to 8°K. For HbCO and HbO<sub>2</sub>, the positions and lineshapes of the C-T bands are quite similar; however, the net photolytic yields from HbCO and HbO<sub>2</sub> are dramatically different. While complete photolysis is easily achieved for HbCO, only a  $\approx 50\%$  yield is obtained from HbO<sub>2</sub> even at 8°K under intense illumination. Using a kinetic hole-burning technique, the position and inhomogeneous broadening of the C-T band in the photodissociated hemoglobins have been monitored as a function of the extent of ligand rebinding, allosteric effectors, and pH. Although both CO and O<sub>2</sub> rebinding produce kinetic hole-burning in the lineshape of the C-T band, the degree of kinetic hole-burning for HbCO is quite pH dependent, diminishing markedly at high pH. These results will be discussed within the context of the current theories of the functional dynamics of hemoglobin. (Supported by the NSF DMB-8604435 and MBRS 08139-12 and 1856000-642A1.)

**W-Pos197** A New Quaternary Structure of Human Hemoglobin. Francine R. Smith and Charles W. Carter, Jr., Department of Biochemistry and Nutrition, University of North Carolina at Chapel Hill, Chapel Hill, NC 27599

Recent thermodynamic studies using human hemoglobins with site-specific structural modifications have shown that the  $\alpha^1\beta^2$  contact region is the principal site of interactions which comprise the "cooperative free energy" [Ackers, G.K. and Smith, F.R. (1985) *Ann. Rev. Biochem.* **54**: 597]. One of these modifications, that of the mutant hemoglobin Ypsilanti ( $\beta$ 99 asp-tyr), produced unusual changes in the stability of the fully-ligated and unligated tetramers, resulting in a dramatically altered cooperative free energy.

We are studying the structural changes which occur in hemoglobin Ypsilanti using single crystal X-ray diffraction. The structure of the fully-ligated (carbon monoxy) form has been solved at low resolution using molecular replacement techniques, and the results show that the quaternary form of hemoglobin Ypsilanti is distinctly different from either unligated or fully-ligated normal human hemoglobin. This has not been observed for any other forms of human hemoglobin. These new structural results and their implications for the mechanism of cooperativity in hemoglobin will be discussed. Supported by a grant from the Jane Coffin Childs Memorial Fund for Medical Research.

**W-Pos198** Proteolytic Variants of Alkaline Phosphatase. Jan F. Chlebowski, S. Olafsdottir, R. Tyler-Cross and C.H. Roberts, Department of Biochemistry and Molecular Biophysics, Virginia Commonwealth University, Richmond, VA 23298-0614

The *E. coli* phosphatase is a dimeric Zn(II) metalloenzyme composed of chemically and topically identical subunits. The tightly bound metal ions are located in adjacent binding sites and are required for expression of phosphate monoesterase activity. The bound metal ions also confer a high degree of stability to the native enzyme so that it resists thermal and chemical denaturation and retains activity on treatment with proteases. The metal-free apoprotein is, in contrast, inactive and susceptible to proteolytic degradation. A family of truncated forms of the native enzyme have been prepared using limited proteolysis to cleave peptides of variable length from the amino terminus of the enzyme. Deletion of 1 or 9 amino acids from both subunits is without effect while deletion of 11 amino acids markedly alters the structural and functional properties of the enzyme as monitored by changes in the near and far UV circular dichroic spectra, thermal stability and enzymatic specific activity. Deletion of an additional 24 amino-terminal residues produces no further alterations, identifying the N-10, R-11 residues as critical to the maintenance of the native enzyme structure. Removal of the metal ions from the truncated enzyme, (A-12 alkaline phosphatase) results in an irreversibly inactivated apo form, which fails to recover the structure or function of the native state on exposure to metal ions. Thus, the N-10, R-11 locus, located at a position distant from the enzyme active site and forming minimal contacts with the flanking subunit, influences distant loci in the enzyme. Crystals of the A-12 enzyme suitable for structure determination have been obtained and work is in progress.

**W-Pos199 IDENTIFICATION OF AUTOLYTIC CLEAVAGE SITES IN THE REGULATORY SUBUNIT OF CALPAIN II: A COMPARISON OF PARTIAL AMINO TERMINAL SEQUENCES TO DEDUCED SEQUENCE FROM COMPLIMENTARY DNA.** P. McClelland, J.A. Lash and D.R. Hathaway. Department of Medicine, Indiana University School of Medicine, Indianapolis, IN 46223

Vascular smooth muscle contains large amounts of a  $\text{Ca}^{2+}$ -activated thiol protease (calpain II). This enzyme is a heterodimer consisting of catalytic ( $M_r = 75,000$ ) and regulatory ( $M_r = 30,000$ ) subunits. Vascular calpain II is a proenzyme that is activated in the presence of  $\text{Ca}^{2+}$  by intramolecular autolysis of the regulatory subunit. Autolysis occurs in steps, generating fragments of 28.5 kDa, 27 kDa, 23 kDa and 18 kDa. The amino terminus of the 30 kDa regulatory subunit was blocked but successive subfragments, separated by SDS-PAGE and electroblotted onto PVDF paper, were found to have unique amino termini when subjected to gas-phase protein sequencing. In order to determine both the amino and carboxy sides of the peptide bonds hydrolyzed (ie. the cleavage sites), a full length copy of the cDNA encoding the regulatory subunit of calpain II was cloned from a λgt 10 cDNA library prepared from bovine aortic smooth muscle. The 1.4 kb insert isolated contained one major internal Eco RI restriction site yielding fragments of 0.5 and 0.9 kb. Sequencing of the two major cDNA fragments indicated a total of 263 amino acids with a high degree of homology to the previously reported sequence of porcine kidney calpain II regulatory subunit. Moreover, comparison of subfragment amino terminal sequences to the deduced sequence identified the following cleavage sites:

|          |                 |
|----------|-----------------|
| 30 kDa   | blocked         |
| 28.5 kDa | F - L —↓— K - G |
| 27 kDa   | L - G —↓— N - V |
| 23 kDa   | L - G —↓— G - V |
| 18 kDa   | I - E —↓— A - N |

Our studies show that: 1) autolysis of the regulatory subunit of calpain II occurs in discreet steps with successive cuts from the amino terminus of the subunit and 2) several unique peptide bonds are cleaved in the process with the sequence, L - G —↓— X - V, appearing at 2/4 cleavage sites. Thus, both primary and secondary structural factors must play important roles in determining specificity of calpain II.

**W-Pos200 INVESTIGATIONS OF THE STRUCTURE OF THE ADHESIVE POLYPHENOLIC PROTEIN FROM THE COMMON BLUE MUSSEL, *M. EDULIS* AND ITS INTERACTIONS WITH BIOMEMBRANES.**

Mark W. Trumbore and Leo G. Herbette. Depts. of Radiology, Medicine, and Biochemistry, and the Biomolecular Structure Analysis Center, Univ. of Conn. Health Center, Farmington, CT 06032.

The polyphenolic protein is an extremely potent naturally occurring adhesive produced by *M. edulis*. The adhesive is extremely stable and is very resistant to chemical and enzymatic degradation. The native adhesive has a molecular weight of 110,000 and consists of repeats of a 10 amino acid consensus sequence: ala-lys-pro-ser-tyr-3hydroxypro-4hydroxypro-thr-dopa-lys. To understand the mechanism of adhesion in this molecule, we have begun to study the structure of a short, 50 amino acid (5 decapeptide repeat) synthetic analog of the adhesive both in solution and in solid state. By trapping the adhesive between dipalmitoylphosphatidylcholine bilayers we were able to produce a solid state matrix in which to investigate the distribution of the adhesive, its conformation, and its interactions with biomembranes by x-ray diffraction. Our results have shown that the adhesive is restricted to the interbilayer water space with little or no perturbation of the hydrophobic interior of the bilayers. The trapped adhesive increases the electron density over a region of  $\sim 5 \text{ \AA}$  within the interbilayer water space. Based on the calculated volume of the molecule this result indicates that the adhesive exhibits an extended conformation when sandwiched between lipid bilayers. These data are currently being refined and compared to radius of gyration values and conformation models obtained from x-ray solution scattering experiments. Supported by RJR Nabisco, Inc. and by the State of Conn. Dept. of Higher Education Cooperative High Technology Program with Biopolymers, Inc. of Farmington, CT.

**W-Pos201 THE ROLE OF METALS IN THE TERTIARY AND QUATERNARY STRUCTURE OF YEAST ARGINASE.** Susan M. Green. Dept. of Biochemistry, Georgetown University, Washington, D.C. 20007.

Yeast arginase, a trimer of identical subunits, is a metalloenzyme containing three tryptophans per subunit. The enzyme contains a weakly bound catalytic manganese as well as a tightly bound structural metal. Studies were undertaken to characterize the role of the metals in the maintenance of both the tertiary and quaternary structure of the protein. Removal of the catalytic manganese results in a slight decrease in the thermal stability of the enzyme ( $T_m$  of  $62^\circ\text{C}$  is reduced to  $54^\circ\text{C}$ ) shown by differential thermal melting experiments, but no change in the frictional properties as evidenced by sedimentation studies. Fluorescence data demonstrate a 30% increase in the intensity of the steady-state spectrum without a change in the wavelength maximum of 335nm from the native spectrum, but resolution of the total time-resolved spectra into decay associated spectra (DAS) yielded almost no change in the shape of the DAS or the lifetimes of 0.1, 1.2, and 4.0ns. The two longer decay times were easily resolved, but the 0.1ns component is dominated by scattered excitation. Removal of the structural metal reduced the  $T_m$  to  $35^\circ\text{C}$ , and unfolding was demonstrated at  $30^\circ\text{C}$  by both analytical ultracentrifugation and difference absorption spectroscopy. Furthermore fluorescence results corroborate the metal-dependent unfolding. The intensity of the steady-state spectrum increased >100% with a redshift in wavelength maximum to 350nm. Both native DAS redshifted and became indistinguishable with the decay times increasing to 0.2, 1.8 and 5.4ns. These results demonstrate that the catalytic metal does not significantly alter the conformation of the protein, but removal of the structural metal causes unfolding. Also, manganese appears to quench by a static mechanism. The unfolding of arginase was further characterized by global analysis of fluorescence decay curves collected throughout the unfolding event. The analysis corroborates the shift to longer decay times. These data will be summarized in terms of the structural changes elicited by metal release.

**W-Pos202** **STRUCTURE OF THE ACTIVE COPPER SITES IN DOPAMINE  $\beta$ -HYDROXYLASE** W. E. Blumberg, AT&T Bell Laboratories, Murray Hill, NJ 07974, L. Powers, Dept. of Chemistry and Biochemistry, Utah State Univ., Logan, UT 84322-0300, P. R. Desai and J. J. Villafranca, Dept. of Chemistry, Pennsylvania State Univ., University Park, PA 16802, and J. H. Freedman, Dept. Molecular Pharmacology, Albert Einstein College of Medicine, Bronx, NY 10461.

X-ray absorption spectroscopy has been used to investigate the local environment of the copper sites in bovine dopamine  $\beta$ -hydroxylase which catalyzes the conversion of dopamine to norepinephrine in the adrenal medulla and noradrenergic nerve cells. The soluble form of the enzyme is a tetrameric glycoprotein monooxygenase containing eight type 2 or non-blue copper atoms per tetramer. The marked similarity of the x-ray absorption edge features of the oxidized and ascorbate reduced forms of the enzyme with those of Cu[imidazole]<sub>4</sub>, suggests that the ligation and geometry are very similar. Furthermore, this similarity is also true for the EXAFS data. Analysis data shows only nitrogen (or oxygen) ligation for both forms: four nitrogens at an average distance of  $1.97 \pm 0.02$  Å for the oxidized and  $2.05 \pm 0.02$  Å for the ascorbate reduced form. Although a change of ligation on reduction cannot be ruled out, the ligand types are restricted to those providing nitrogen or oxygen ligands. These results agree with those reported by Scott et al. (1988) Biochem. 27, 5411, for the oxidized enzyme. However, they differ significantly from the two or three nitrogen (or oxygen) ligands at 1.93 Å and one sulfur ligand at 2.30 Å these authors report for the reduced enzyme. Supported in part by NIH Grant GM29139.

**W-Pos203** **THE LIPOCALIN MODEL FOR OROSOMUCOID STRUCTURE—SUPPORT FROM MONOCLONAL ANTIBODIES (MAbs).** A. P. Villalobos, J. S. Ivancic, H. B. Halsall, Department of Chemistry, University of Cincinnati, Cincinnati, OH 45221-0172.

Orosomucoid (OMD) is divisible into CNBr (fragment) I (res 1-110) and CNBr II (res 112-183), with CNBr I containing all of the considerable (40%) carbohydrate content of this glycoprotein. The carbohydrate occludes about one-half of the surface area of OMD, however, which parts are screened will depend on the folded form of the protein core. It has been suggested (FASEB J. 1 (1987) 209-214) that OMD belongs to the  $\beta$ -lactoglobulin family, and would therefore consist of an antiparallel  $\beta$ -barrel. Such a structure would make OMD antigenically polarised, with predominant activity in CNBr II. We have been developing a library of MAbs against OMD (Fed. Proc. 45 (1986) 1574), and observe that 18 of 19 bind to CNBr II, in support of the concept of polarity and a lipocalin type of structure. The relative positions of epitopes has been assessed by simultaneous binding experiments monitored by size exclusion HPLC. The data indicate at least one main antigenic region in CNBr II, with the binding of 3 MAbs being mutually exclusive, while the remainder bind non exclusively in the presence of one of these three. It is likely that the small area exposed compared to the 600 Å<sup>2</sup> MAb footprint will only permit simultaneous binding of two or three MAbs.

**W-Pos204** **SEPARATION AND CHARACTERIZATION OF THE GENETIC VARIANTS OF HUMAN OROSOMUCOID.** Brian N. Stretcher, H. Brian Halsall, Department of Chemistry, University of Cincinnati, Cincinnati, OH 45221

A method whereby the genetic variants of orosomucoid can be separated has been developed. The method relies upon a single amino acid difference at position 149 between the two similar, yet distinct, orosomucoid gene products. The dominant gene product (GPI) has an arginine residue at this position, whereas the minor (approximately 25%) gene product (GPII) has a cysteine residue in the corresponding location. A sulfhydryl specific matrix, p-hydroxymercuribenzoate agarose (in 8M urea, 0.5M NaCl, 0.33M HOAc, pH 4.6) is used to remove the sulfhydryl containing GPII from GPI. GPII is then removed from the matrix by 0.1M cysteine. The unbound (GPI) and bound (GPII) fractions were cleaned-up by dialysis and gel permeation chromatography. Both products demonstrated reactivity with orosomucoid specific monoclonal antibodies. Analysis of the unbound fraction by SDS-PAGE showed homogeneous material with a molecular weight of 40,000 under both reducing and non-reducing conditions. Similar results were obtained for the bound fraction, except that under non-reducing conditions a significant band also appeared in the 80,000 dalton range. This behavior is characteristic of a disulfide linked dimer, which GPII might be expected to form under the conditions employed. Characterization of the fractions by CNBr cleavage and subsequent HPLC separation yielded cleavage patterns as predicted from literature amino acid sequences for the different gene products. It therefore appears that GPII can be separated in quantities substantial enough for further physical, chemical, and immunological studies.

**W-Pos205** INTERACTION OF A BIOLOGICALLY ACTIVE FLUORESCENT CALMODULIN WITH RAT LIVER NUCLEI.  
 Rama Kasturi and J. David Johnson. Department of Physiological Chemistry. The Ohio State University Medical Center Columbus, Ohio 43210

Rhodamine X-CaM is a biologically active fluorescent calmodulin (CaM) which undergoes an increase in its polarization with the calcium dependent binding of its target proteins (Mills et al. *Biochem.* 27, 991-996, 1988). We have used this change in fluorescence polarization to monitor calmodulin's interaction with rat liver nuclei. 50 nM of Rhodamine X-CaM was saturated with 300 µg of nuclei, indicating 0.166 picomoles of calmodulin receptors/µg of nuclear protein. Rhodamine X-CaM bound to its receptors in the nuclei half-maximally at pCa 6.4 (Hill coefficient = 1.5) in the absence of Mg<sup>++</sup> and at pCa 5.6 in the presence of 3 mM Mg<sup>++</sup>. Calmodulin antagonist drugs, calmidazolium and prenylamine, displaced Rhodamine X-CaM from its nuclear receptors with IC<sub>50</sub>'s of 100 nM and 15 µM respectively. Fluorescence microscopy and centrifugation studies confirmed that rhodamine X-CaM's fluorescence is associated with the nuclei (nuclear envelope, nuclear membrane and nucleolus) in the presence of Ca<sup>++</sup> but not in its absence (2mM EGTA) nor in the presence of calmodulin antagonist drugs. These studies elucidate the usefulness of Rhodamine X-CaM in the characterization of calmodulin's interaction with its receptors in subcellular components of the cell.

**W-Pos206** FIBER DIFFRACTION STUDIES OF CUCUMBER GREEN MOTTLE MOSAIC VIRUS AT 5Å RESOLUTION.  
 Sharon Lobert and Gerald Stubbs.

Dept. of Molecular Biology, Vanderbilt University, Nashville, TN 37235

Cucumber green mottle mosaic virus, watermelon strain (CGMMV-W) is a member of the tobamovirus group of plant viruses, of which tobacco mosaic virus (TMV) is the type member. These are rod-shaped helical viruses, with a single protein subunit, MW 17,500, that repeats in three turns of the viral helix. A single strand of RNA follows the helix at a radius of 40Å. The intact viruses can not be crystallized, so fiber diffraction methods have been used in structural studies. The structure of TMV has been determined at 2.9Å resolution. CGMMV-W coat protein has only 36% amino acid sequence homology with TMV, but the diffraction patterns and biological properties suggest that the two viruses have a high degree of structural similarity.

Fiber diffraction data are cylindrically averaged. The loss of information could be overcome by multi-dimensional isomorphous replacement, requiring a very large number of heavy-atom derivatives, but by assuming that the overlapping intensities are equal, it has been possible to make a 5Å electron density map of CGMMV-W using only two derivatives. A bundle of four  $\alpha$ -helices that dominates the protein structure is easily recognizable. The largest difference between TMV and CGMMV-W at this resolution is an increase of about 2Å in the distance between two of the helices, consistent with an increase in volume of predicted contacting amino acids. There is a .7Å increase in axial separation between subunits, which agrees with an increased volume of buried residues. Overall, correlation of amino acid volumes and structural parameters suggests that the very close intermolecular interactions observed in TMV will also be found in CGMMV-W.

**W-Pos207** UPPER AND LOWER BOUNDS ON THE NUMBER OF AMINO ACID RESIDUES AFFECTED BY EACH CARBOHYDRATE MOIETY IN PORCINE SUBMAXILLARY GLAND MUCIN. Noppawan Tanpipat and Wayne L. Mattice, Institute of Polymer Science, The University of Akron, Akron, Ohio 44325-3909.

Rotational isomeric state theory has been used to investigate the differences in conformations of glycosylated and unglycosylated porcine submaxillary gland mucin. The conformation dependent physical properties calculated are the dimensionless ratios  $\langle s^2 \rangle_0 / nl^2$  and  $\langle r^2 \rangle_0 / \langle s^2 \rangle_0$ , where  $\langle s^2 \rangle_0$  denotes the mean square unperturbed radius of gyration,  $\langle r^2 \rangle_0$  is the mean square unperturbed end-to-end distance, and n is the number of virtual bonds of length l. The amino acid sequence is that reported by Timpf et al., *J. Biol. Chem.* 263, 1081 (1988) for a fragment of 503 residues from apomucin. The experimental data that are the target of the calculations are those reported by Shogren et al., *Biopolymers* 25, 1505 (1986). The observed expansion of the protein core in response to glycosylation cannot be explained unless the values of  $\phi$  (the dihedral angle at the N-C<sup>α</sup> bond) and  $\psi$  (the dihedral angle at the C<sup>α</sup>-C bond) for at least five amino acid residues are significantly affected by each carbohydrate moiety. If the conformation of more than seven amino acid residues is affected, the molecule begins to depart from the observed result that  $\langle r^2 \rangle_0 / \langle s^2 \rangle_0 \sim 6$ . Therefore it is likely that 5-7 amino acid residues in the vicinity of each carbohydrate moiety have their values of  $\phi$  and  $\psi$  affected by glycosylation. This research was supported by a grant from the Cystic Fibrosis Foundation.

**W-Po208** SMALL ANGLE NEUTRON SCATTERING STUDIES OF THE DENSE CORES OF ISOLATED NEUROSECRETORY VESICLES. S. Krueger, National Institute of Standards and Technology, Gaithersburg, MD 20899; J. W. Lynn, University of Maryland, College Park, MD 20742; J. T. Russell and R. Nossal, National Institutes of Health, Bethesda, MD 20892.

Small angle neutron scattering was used to study the structure of the dense cores of intact neurosecretory vesicles (NSV) obtained from bovine pituitaries. The major constituents of the cores are neurophysin proteins and the neurohormones, oxytocin and vasopressin. Contrast variation techniques were used to minimize the scattering due to vesicle membranes and emphasize that due to the cores. By examining a suspension of NSV membranes along with the intact NSV, residual membrane scattering was eliminated. The resultant scattering is inconsistent with model calculations which assume that the vesicle cores consist of small, densely-packed particles or large, globular aggregates. Although a unique model cannot be determined, the data suggest that the core constituents form long aggregates which fold into compact structures. Results are compared with those of similar studies performed on purified neurophysins, neurophysins complexed with arginine-8 vasopressin, and NSV core lysates.